Live Learning Neuronal Networks: Plasticity of Bursts

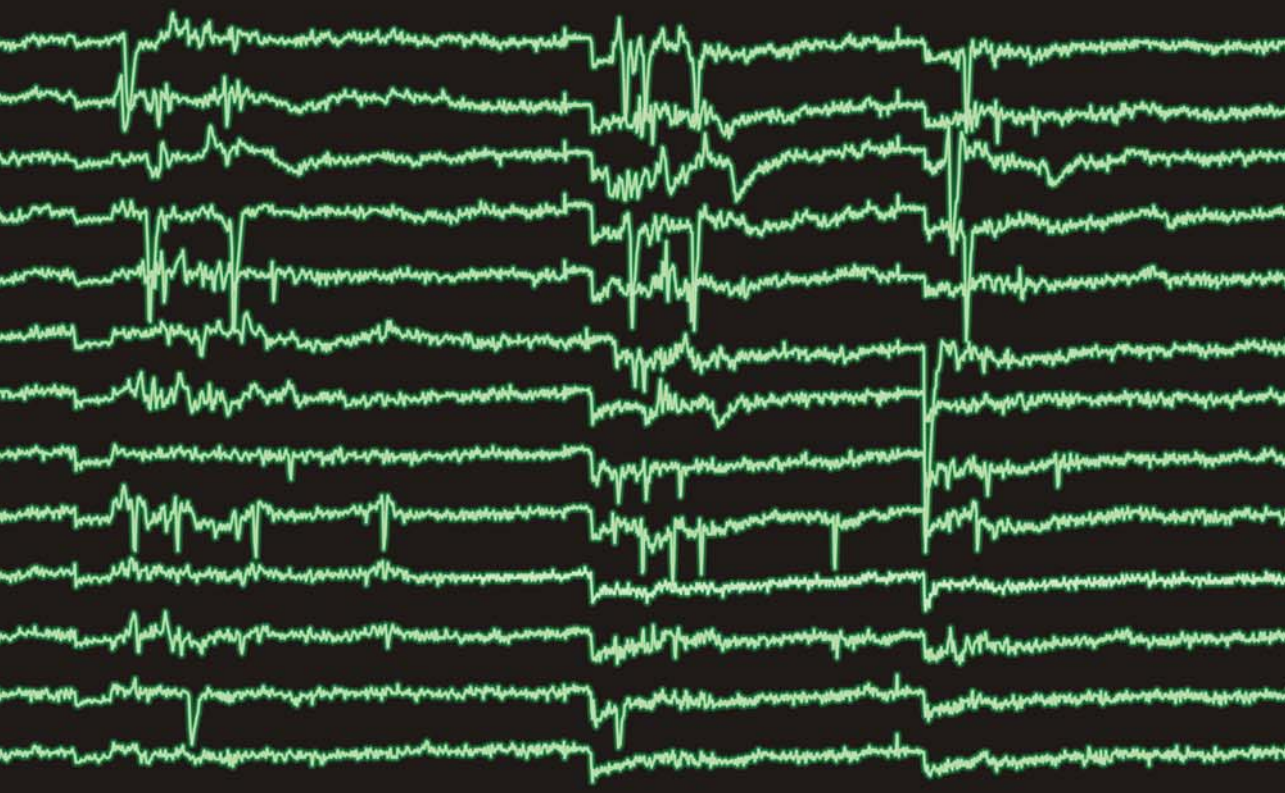

Jan Stegenga

LIVE LEARNING NEURONAL NETWORKS: PLASTICITY OF BURSTS

door

Jan Stegenga

Samenstelling Commissie

Voorzitter

Secretaris

T. Mouthaan	Universiteit Twente

Promotor

Prof. Dr. Ir. W.L.C. Rutten	Universiteit Twente

Promotor

Prof. Dr. E. Marani	Universiteit Twente

Leden

Dr. Ir. J. le Feber	Universiteit Twente
M. Giugliano, PhD	Universiteit Antwerpen
Dr. J. Van Pelt	Vrije Universiteit
Prof. Dr. Ir. C.H. Slump	Universiteit Twente
Prof. V. Subramaniam	Universiteit Twente

Paranimfen

Esther van der Heide

Remy Wiertz

Printed by

Gildeprint Drukkerijen BV, Enschede (www.gildeprint.nl)

ISBN 978-90-365-2767-5

LIVE LEARNING NEURONAL NETWORKS: PLASTICITY OF BURSTS

PROEFSCHRIFT

ter verkrijging van
de graad van doctor aan de Universiteit Twente,
op gezag van de rector magnificus,
prof.dr. H. Brinksma,
volgens besluit van het College voor Promoties
in het openbaar te verdedigen
op vrijdag 16 januari 2009, om 16.45 uur

door

Jan Stegenga

geboren op 19 april 1979
te Wijckel (Gaasterlân-Sleat)

Dit proefschrift is goedgekeurd door:

Prof. Dr. Ir. Wim L. C. Rutten
Prof. Dr. Enrico Marani

ISBN 978-90-365-2767-5

Contents

Chapter 1,

General Introduction

The nervous system makes it possible for humans and animals to interact with their environment. The incoming signals come from specialized neurons which are sensitive to a number of modalities, such as chemicals, light, heat and pressure. The outgoing signals are muscle contractions. Between sensory signals and actuary signals, a lot processing of information has to be performed. One of the most striking features of this processing is to recognize and memorize regularities in the environment, and change behaviour if necessary. Recognition, or learning and memorization, is the subject of several fields. On the highest level there is the psychology of behaviour (figure 1.1). It deals with the modification of behaviour in response to stimuli, rewards and punishments. It does not traditionally deal with the neurophysiologic aspect. However, psychological models have been very influential to the study of learning and memory on all levels. On the lowest levels, the field of neurophysiology studies the properties of the basic information processing unit of the nervous system; the neuron. Of particular interest in this field

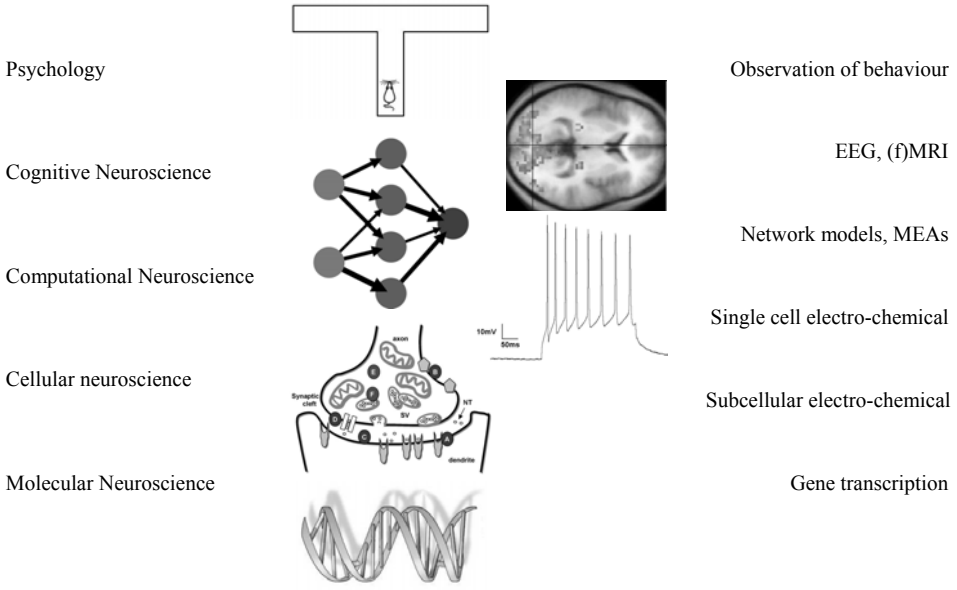

Figure 1.1. Studies of the brain at different levels. Due to advances in measurement systems, borders between areas are rapidly fading.

is the communication between two neurons, which is regulated by synapses.
Towards intermediate levels, models of neurons and synapses are used to study information processing on the scale of neuronal networks. *In-vivo* experiments at this level use non invasive techniques such as EEG and (f)MRI. In animal experiments, invasive techniques such as electrode implants are also used. Implanted electrodes have the advantage of being much more precise as to the spatial and temporal origin of the recorded activity. As an alternative to *in-vivo* experiments, primary cultures of dissociated neurons or organotypical slices can be used. Accurate measuring of activity is then possible, as well as observation through microscopes.

1.1 Learning and memory in psychology

In behavioural psychology, subjects are put in a controlled environment and their behaviour is studied. Stimuli consist of audiovisual or tactile signals. To alter behaviour in animals, they can be rewarded (food) or punished, or a survival instinct (reflex) can be triggered. The most well-known experiment is the association that Pavlov's dogs made between the sound of a bell and food after repeatedly ringing a bell when they were feeding. After a while, the dogs salivated to the sound of the bell alone. This is called classical conditioning; an already existing behaviour is associated with an otherwise neutral stimulus. The association could be severed by no longer ringing a bell during (or immediately before) feeding. Interestingly, no salivation occurred when the bell was rung after feeding. In other experiments, presenting the neutral stimulus after the natural response had an inhibitory effect. Therefore, causality and temporal proximity are important factors for the type and strength of an association.
Operant conditioning concentrates on the modification of behaviour under already existing conditions. Here, feedback of the performance in the form of reinforcement (reward) or punishment is applied. Feedback can be applied by a teacher (in the broadest sense), making operant conditioning applicable in practice. Operant conditioning also results in goal-directed learning, as a teacher applies feedback with a certain goal in mind.
Psychological studies of learning and memory did not end with the two forms of conditioning, but have since developed into a wide field with many close relations with cognitive neuroscience. Definitions of learning that are used slightly differ,

depending on the aspect that is studied. Two definitions that together cover the fundamentals are:

- The alteration of *behaviour* as a result of individual *experience*. When an organism can *perceive* and change its behaviour, it is said to learn. *(Encyclopedia Brittanica)*
- An organism is said to have learnt when it has increased its options for applying, to a *specific set of circumstances*, new or different behaviour which the organism believes will be to its *benefit*. *(Mike Willis Learning Services)*

Only the second definition explicitly mentions a goal, which is especially useful in experimental setups. In both definitions the environment plays an important role, as it is only though interaction with the environment that an organism gains experience.

1.2 Learning and memory in neuroscience

The brain can be divided into regions, each with a different (degree of) specialization. The hippocampus is of particular interest to the study of learning and memory, as it is shown to be involved in remembering spatial information [4-7]. A pivotal set of experiments was performed by Bliss and Lomo in 1973, in which they stimulated hippocampal neurons in anesthetized rabbits and recorded postsynaptic potentials in another neuron [8]. They showed that stimulation with trains of pulses called tetani (100 Hz; 1 s) resulted in an increase of the amplitude of postsynaptic potentials that could last as long as days. These cells, or rather their synapses, were capable of short- (minutes) and long-term (hours to days) memorization. The phenomenon was called Long Term Potentiation, or LTP. LTP was later found to be induced by two other protocols. In theta-burst stimulation, neurons are stimulated with short bursts of 4 or 5 pulses at 100 Hz, spaced approximately 200 ms apart [9]. The theta rhythm is observed in the EEG of the hippocampus during exploratory behaviour and retrieval of information. It was later shown that when the stimuli were locked to the natural theta oscillation, application of the stimuli at the peak of the oscillation resulted in LTP [6, 10]. Conversely, application of stimuli at the through of the oscillation resulted in LTD (Long Term Depression; the weakening of post synaptic potentials). The pairing of stimuli was the third approach found to elicit long lasting changes in synaptic efficacy [2, 3, 9, 11-13]. Upregulation could be achieved by stimulating the

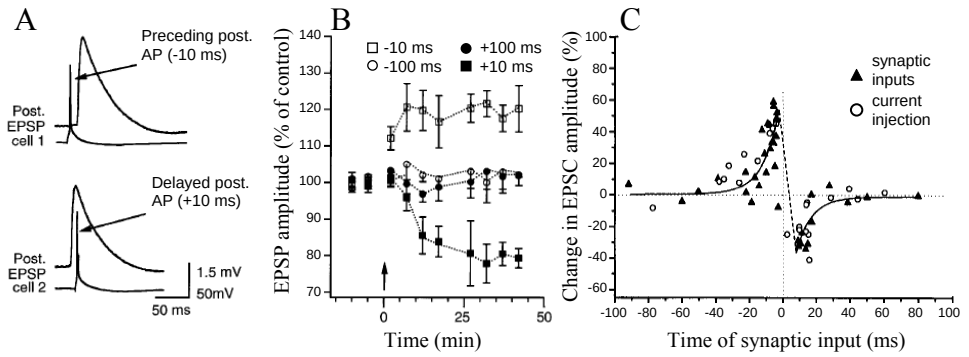

Figure 1.2. Spike timing dependent plasticity. A) Post-synaptic action potentials were triggered 10 ms before or after synaptic activation (EPSP onset). B) Differences between EPSP amplitude. For -10ms, long term potentiation occurred, while for +10ms long term depression was observed. Controls were obtained by using a time difference of ± 100 ms. (neocortical neurons [2]) C) EPSP change as a function of the time difference between AP and EPSP onset. (neurons from visual cortex [3]).

presynaptic neuron immediately before (0 to 20 ms) the postsynaptic neuron (figure 1.2). Downregulation would be induced by stimulating the postsynaptic neuron before the presynaptic neuron. There is no effect of these manipulations on other neuron pairs, therefore the modifications are synapse-specific. This mechanism was called spike-timing dependent plasticity (STDP). STDP, and also the mechanisms of LTP and LTD, support the well-known postulate of learning made by Donald O. Hebb in 1949 [14]:

"When an axon of cell A is near enough to excite cell B and repeatedly or persistently takes part in firing it, some growth process or metabolic change takes place in one or both such that A's efficiency, as one of the cells firing B, is increased."

Hebb's rule is prominently used because it links observations from the top-layers of investigation and the lower layers of neuroscience. It has spurred research into mechanisms that underlie this rule, but also into how this rule is used to form memory in networks of neurons. Generally speaking, finding (functional) connections that adhere to Hebb's rule (for example changed input-ouput functionality), is now equated to demonstrating that the network has the ability to learn and memorize [15]. More strictly, learning and memory involves some form of control by the experimenter over input-output relations [16, 17]. Useful (non-trivial) input-output relationships however, require a network of cells rather than a pair of cells.

1.3 Mechanisms behind synaptic plasticity

There are 2 main receptors that are involved in STDP; the AMPA and the NMDA receptor (figure 1.3). The AMPA receptor is permeable to K^+ and Na^+ when activated by glutamate, and provides normal transmission of action potentials. The triggering of STDP depends on the activation of NMDA receptors [9, 12]. The NMDA receptors are glutamate (the NMDA receptor is co-activated by glycine)-activated channels that pass Na^+, K^+ and Ca^{2+}, and which are blocked by Mg^{2+} at resting potential. When the post-synaptic dendrite becomes depolarized, either through persistent activation of the AMPA receptors or through dendritic action potentials, the Mg^{2+} block is released. The resulting influx of Ca^{2+} into the post synaptic cell triggers a multitude of second messenger systems [9]. One of these is the phosphorylation of AMPA receptors by Ca^{2+}-activated Calmodulin Kinase II (CaMKII), which results in a higher channel conductance. Another mechanism for

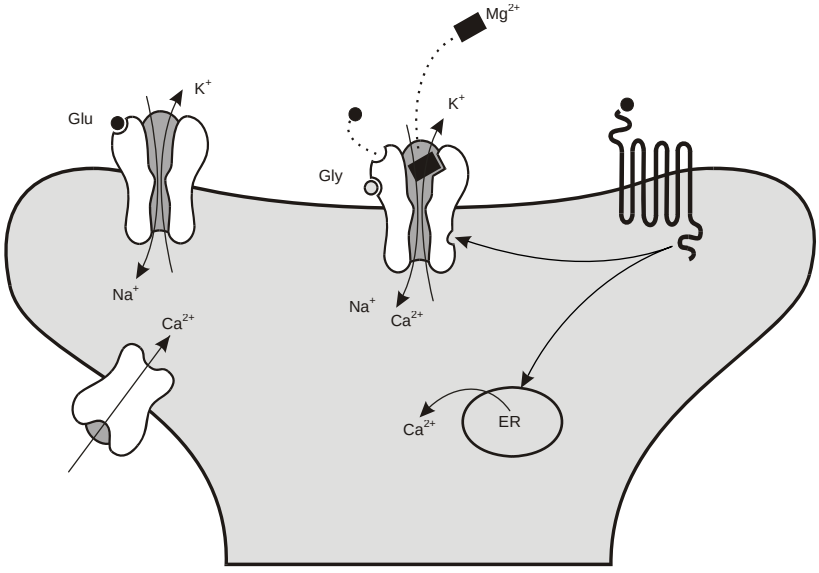

Figure 1.3. Schematic representation of the postsynaptic part of an excitatory synapse. The leftmost receptor (AMPA) governs normal transmission of action-potentials, depolarizing the membrane when glutamate binds to it. The middle receptor (NMDA), is activated by glutamate on the condition that the depolarization of the membrane is enough to clear the magnesium ion that normally blocks its channel. The metabotropic glutamate receptor (mGLUr) triggers second messenger systems that influence the NMDA channel conductance and the endoplasmic reticulum, causing both to increase the intracellular calcium concentration ($[Ca]_i$). Changes in $[Ca]_i$ are linked to changes in synaptic efficacy. The voltage dependent calcium channels (VDCC) amplify the increase of $[Ca]_i$ during depolarization, and are necessary for the maintenance of synaptic efficacy.

the cell to modulate the post synaptic depolarization is to increase or decrease the number of AMPA receptors. The more permanent the Ca^{2+}-concentration is increased, the more energy is expended for the potentiation. Therefore Ca^{2+} can also be released through other mechanisms, such as release from the Endoplasmic Reticulum (ER) or through influx by voltage-dependent calcium channels (VDCC's). By increasing the number (and types) of VDCCs, the Ca^{2+} can be increased on a more permanent basis, thus maintaining the potentiation for long periods of time (LTP) [18].
The presence of retrograde messengers, signalling the presynaptic cell to release more neurotransmitter have been hypothesized to play a role in LTP and LTD. One of the candidates was nitric-oxide. However, most phenomena can be explained by mechanisms taking place in the postsynaptic cell.

1.4 Why culture networks in-vitro?

Many of the results discussed so far have been achieved using patch-clamp methods either *in vivo*, or *in vitro*. Patch-clamp methods are intracellular, thus providing great detail also in the subthreshold regime, but impractical to measure

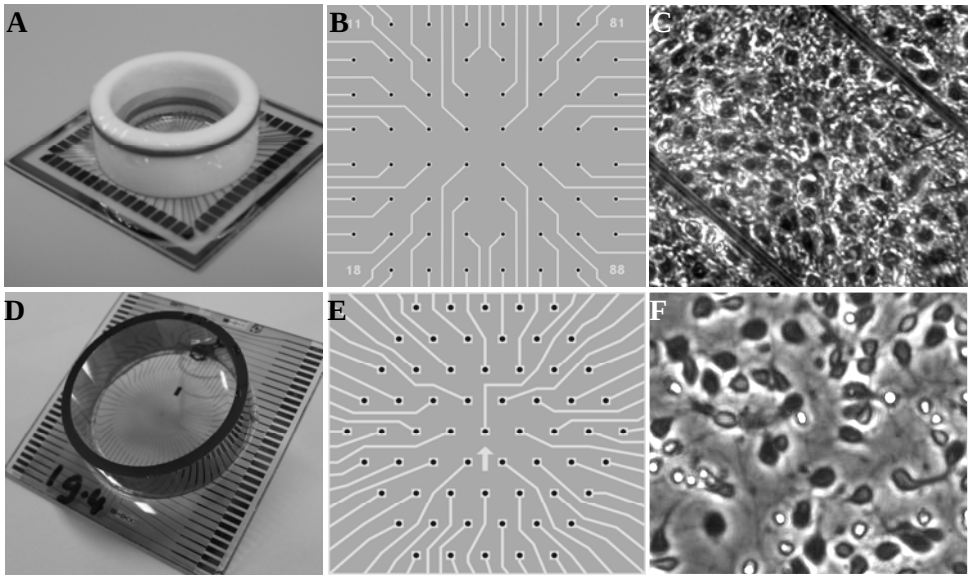

Figure 1.4. A) A Multi electrode array with sealing chamber produced by Multi-Channel Systems GmbH, Reutlingen, Germany B) Electrode layout of a MCSMEA. C) Phase contrast image of neurons cultured on a MEA. D-F) MEA produced at University of Twente, its electrode layout and image of a culture.

many neurons in parallel. The multi-electrode array (figure 1.4) has been developed to provide a platform to solve this. Some advantages of the MEA system are:

1. Networks can be isolated from activity of other regions. The brain is far too complex to study at once. *In vitro*, one can isolate one brain region, control the inputs that it receives, and study the output that it generates. The small networks grown on MEAs (100 to 100,000 neurons) provide an intermediate between single cell and two cell recordings used to study interactions between cells, and EEG-like methods used to study large networks and the intact brain.
2. Long term cell specific, extracellular recordings from many neurons are possible (Currently 60 electrodes). The neuron-electrode contacts are stable throughout the lifetime of the culture which can be several months. In contrast, patch-clamp recordings damage the neuron cell membrane which limits useful recording time to several hours and may alter processes based on the concentration of chemicals (as the intracellular fluid is slowly mixed with the pipette fluid).
3. Networks can be observed under a microscope. Neuronal cultures are kept essentially two dimensional, for the practical reason that substances needed for metabolism are transported by diffusion from the medium bath. For dissociated cultures, the layer of neurons and glial cells will be no more than 3 cells (15-30 um) thick [19]. For lower seeding densities one may be able to observe the network through normal phase-contrast microscopy. Otherwise, dyes can be used for imaging. Dyes are very versatile. For instance, it is possible to measure action potentials using voltage-dependent dyes, and calcium-dependent dyes can be used to track intracellular calcium concentration on a millisecond scale [20]. Being able to observe the culture makes it possible to make very precise lesions by laser.
4. Manipulations can be applied with more control. The effect of chemicals on survivability and activity cultures can be studied simply by adding it to bath solution. For instance, the local application of small amounts of picrotoxin, reducing the influence of inhibitory cells, through micropipettes has resulted in distinct changes in firing patterns [21].

Several drawbacks are:

1. The lack of afferent input to the network may lead to changes in network processing.
    a. The developmental aspect of this is that a certain accumulation of experiences is necessary for an organism to function normally. The brain is only hard-wired for the most basic of tasks, the rest it learns through interactions with the environment. The developmental aspect should be reflected in acute slices of brain tissue, but is not present in dissociated cultures.
    b. Another aspect is that no network region works entirely on its own. It receives chemical cues through the blood and from other brain regions it receives action-potential activity as well as chemical cues. These inputs are difficult to reproduce *in vitro*, but may be essential for proper functioning.
2. For dissociated networks; the lack of structure. Dissociated neurons grow into networks again *in vitro*, making it essentially randomly connected. This seriously hampers the translation of any findings made in dissociated cultures to *in vivo*.
3. Currently, only action potentials can be reliably measured. With patch-clamp methods, subthreshold activity can also be monitored. Due to the size of the recording electrodes in conventional MEA's and the limited seal between electrode and neuron however, this is impossible.

1.5 The in-vitro setup

In the late 1970's, lithographic methods were employed by the groups of Gross and Pine [22, 23] to produce what is now called a multi electrode array (MEA, figure 1.3). This made it possible to record action potentials from 60 neurons. Before the arrival of MEA's, action potentials were recorded using patch clamp methods. This limited the number of simultaneously recorded neurons to 3 or 4. The number of electrodes of MEAs is limited by the physical size of the contacts that connect the electrodes to the amplifiers. Miniaturization of the contacts may double the number of electrodes in the short future. The number of electrodes may become very much larger when the amplifiers and digitalization of signals is done on-chip [24]. MEAs can be used for recording tissue slices or dissociated neurons can be cultured on

them. Cultured networks have a longer lifetime and are better observable but in the process of dissociation the normal structure is lost.

Next to the amplifiers of the recording electrodes, the recording setup also has to provide the culture with everything it needs to survive. Figure 1.3A already shows the first step in this, a sterile, transparent cap that can be put over the culturing chamber in order to keep contaminations out. In our particular setup, the pre-amplifier stage of MCS provides means for heating the culture from below to a temperature that we set to 36˚C. Doing so caused evaporation of the medium which condensed to the cooler top of the MEA-cap and consequently the increase of salt concentrations in the medium. To prevent this, the top of the cap was also heated. The last step that we took to improve the maximum duration of measurement was to apply a flow of air/CO_2 mixture over the entire recording stage. This was necessary as the CO_2 dissolved in the medium would otherwise evaporate.

1.6 State of the art

Many aspects of cultured networks have been studied over the past years. Obviously, there are many structural changes during the development from a collection of dissociated neurons to intricately connected networks. The rules that govern outgrowth of neurons involve chemical gradients, but action potential activity is also involved [25]. It is interesting that during this time action potential activity too changes from isolated action potentials to highly correlated trains of action potentials [26]. Action potential activity is most likely initiated at the synapses where spontaneous release of neurotransmitter can occur. This activity spreads quickly through the culture in short network-wide bursts of action potentials (figure 1.5).

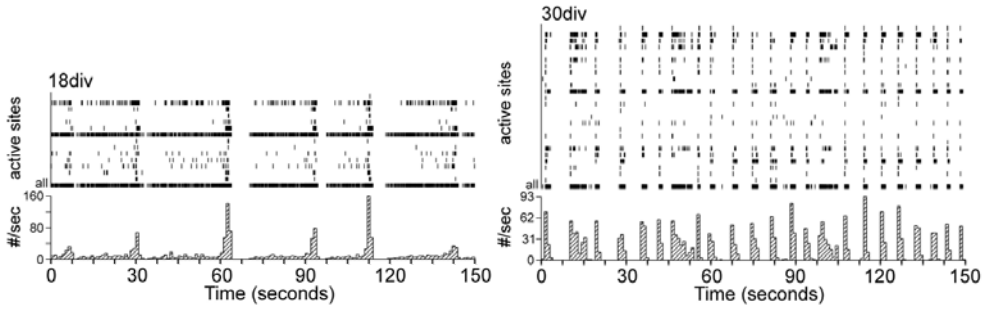

Figure 1.5. Simultaneous spike trains at 18 days *in vitro* (DIV) and 30 DIV. Top panels: Timing of spikes for each active recording site; 'all' denotes the aggregate of all electrodes. Lower panels: Aggregate spike rate determined in 1 second bins. During development more neurons become active and become entrained in bursts and the burst rate increases. What is not visible on this scale is that the peak firing rate also increases as the bursts shorten. Figures are modified from [1].

The bursting phenomenon is the hallmark of activity in dissociated cultures. It occurs in cultures from different brain regions (hippocampus, neocortex) and different species (mouse, cat, rat, locust) and persists for the entire lifetime of the culture. Many aspects of bursts have been investigated. Relatively simple analyses include inter burst intervals and burst sizes, burst initiation sites and their spread through the culture [27, 28]. Many groups now use analysis based on the time and electrode (place) of activity during bursts [19, 29-35]. It has been shown that synaptic transmission is more reliable when synapses are triggered by action potential trains instead of single spikes [36]. Combined also with the massively parallel input that every neuron receives during a network burst, it should not be surprising that bursts can have a stable structure. We have shown, based on a newly developed analysis of bursts, that in our cultures this structure progressively changes over a time-base of several hours during spontaneous development (Chapter 2).

Action potentials can also be triggered by applying electrical pulses to an electrode. This activity can spread in bursts, similar to spontaneous activity. Research into plasticity mechanisms in dissociated networks started with the application of tetani and observing whether LTP could be induced [37-40] (figure 1.6). Early results were positive, as a change in EPSPs was observed for more than 30 min after application of tetani to extracellular electrodes. At the same time, responses to test stimuli changed. This indicated that dissociated cultures could be influenced by external stimuli and appeared to pave the way for further investigations into learning and memory. Other algorithms used to induce changes to test stimuli (which were then ascribed to LTP) were 1) Tetani applied to 4-8 electrodes in

parallel, and 2) Tetani applied to 2 electrodes with a small shift of 10 ms. These stronger versions of known algorithms are testament to the fact that many groups have struggled with induction of plasticity. Our own experiments using these kinds of stimuli also revealed just exactly how difficult it is to induce and observe changes (Chapter 3).

The solution to this problem may lie in putting the network in a state which resembles the *in-vivo* state. This means that bursting behaviour should be prevented and dispersed activity promoted. This is possible by altering the chemical environment [39, 41-43], or by providing uncorrelated stimuli to many electrodes [44-46]. It is hypothesized that uncorrelated stimuli act to keep neurons in a state in which plasticity mechanisms are neither inactive nor overloaded (in contrast, overloading may occur during bursts). We observed that weaker stimuli were successful at inducing changes in networks that were brought in a more natural

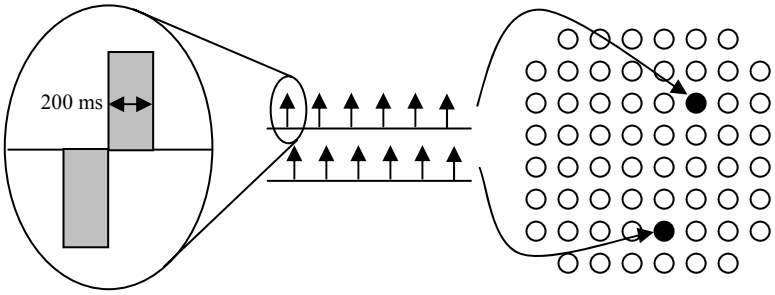

Figure 1.6. Principle of applying tetani. A single pulse train consists of a number of short balanced current pulses. Amplitudes range from 1 to 20 uA, depending on the electrode to neuron coupling. Tetanus trains are usually between 0.5 and 1 second long, and inter pulse intervals are smaller than 50 ms. Tetani are sometimes applied to several electrodes at the same time, or shifted in time by 0-20 ms.

state (Chapter 4).

Perhaps due to the difficulty of inducing plasticity, only one group has put forward and successfully implemented an algorithm to study learning in cultured networks. In their pivotal study, Shahaf *et al* took inspiration from theorems in behavioural psychology [17, 47]. In this theorem, an organism explores its options under the influence of a 'drive' (*e.g.* hunger). A stable state is reached when the drive disappears. They translated the drive to stimuli applied at a low rate, and observed that the response changed under its influence (figure 1.7). By terminating the drive when a desired response was observed, they were the first to include some form of feedback of the cultures' performance. The cultures were able to learn and memorize (in a broad sense), as the desired response would be reached faster in a repetition of the experiment. Initial investigations at replicating these results in our lab were unsuccessful [48]. In chapter 5 we present a slightly modified version of

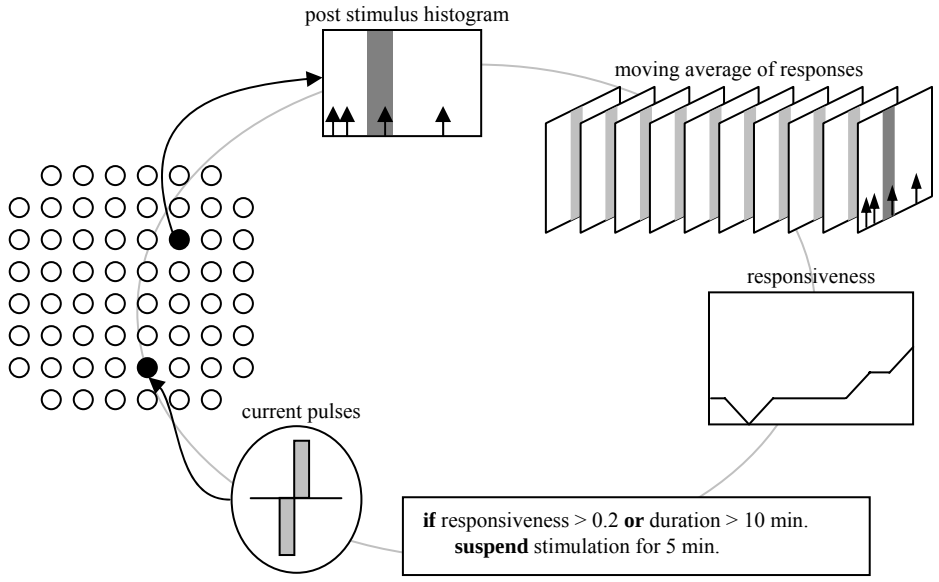

Figure 1.7. Conditional repetitive stimulation (CRS) algorithm. Current pulses were applied at a rate of 0.1 to 0.5 Hz. The post stimulus histogram of the evaluation electrode was then checked for the presence of spikes within the evaluation window. If there are more than 2 out of the last 10 responses that showed a spike in the evaluation window, stimulation was suspended for 5 minutes. The number of stimuli required to reach the criterion decreased.

this algorithm (and the culture selection process), which resulted in changes within bursts. Recently, another group has included feedback in their experiments to control a robots' movement [49]. The investigations so far have demonstrated that when feedback is used, single stimuli can alter the input-output relationships of networks.

1.7 Outline of this thesis

This thesis is based on a burst analysis method based on profiles of the instantaneous firing frequency which is introduced in chapter 2. The typical shapes and changes in shape of these profiles during development are treated. Also, a mathematical connection to widely used analyses based on electrode-electrode correlations of spike trains is made [15, 50, 51]. The stability of profiles and the level of detail provided by them, made analysis by burst and phase profiles an excellent candidate for further studies into plasticity and learning.
In chapter 3, profile analysis is applied to different paradigms of stimulation that should induce synaptic plasticity. Unexpectedly, changes of profile shapes in the

presence of stimuli did not exceed normal developmental changes. There were several possible explanations for this, most of which point at interference by network bursts. We explored a possible solution in chapter 4, where we show that background stimuli can be used to suppress bursts and induce an overall oscillation in the theta band (4-12 Hz) in the network. With a theta-rhythm in place, we further show that relatively weak tetani can induce changes in post stimulus histograms and profiles as well.

Chapter 5 deals with the change in profiles that accompanied training of a culture using the CRS algorithm. In these series of experiments the profiles changed significantly, with those profiles on the evaluation electrode changing more than other profiles. The stringent culture selection criteria and a number of changes we made to the original algorithm may be the cause that these experiments were successful, while others were not [48].

1.8 References

1. van Pelt, J., I. Vajda, P.S. Wolters, M.A. Corner, and G.J. Ramakers, *Dynamics and plasticity in developing neuronal networks in vitro.* Prog Brain Res, 2005. **147**: p. 173-88.
2. Markram, H., J. Lubke, M. Frotscher, and B. Sakmann, *Regulation of synaptic efficacy by coincidence of postsynaptic APs and EPSPs.* Science, 1997. **275**(5297): p. 213-5.
3. Zhang, L.I., H.W. Tao, C.E. Holt, W.A. Harris, and M. Poo, *A critical window for cooperation and competition among developing retinotectal synapses.* Nature, 1998. **395**(6697): p. 37-44.
4. Chrobak, J.J. and G. Buzsaki, *Gamma oscillations in the entorhinal cortex of the freely behaving rat.* J Neurosci, 1998. **18**(1): p. 388-98.
5. Hasselmo, M.E., C. Bodelon, and B.P. Wyble, *A proposed function for hippocampal theta rhythm: separate phases of encoding and retrieval enhance reversal of prior learning.* Neural Comput, 2002. **14**(4): p. 793-817.
6. Huerta, P.T. and J.E. Lisman, *Bidirectional synaptic plasticity induced by a single burst during cholinergic theta oscillation in CA1 in vitro.* Neuron, 1995. **15**(5): p. 1053-63.
7. Levy, W.B. and O. Steward, *Temporal contiguity requirements for long-term associative potentiation/depression in the hippocampus.* Neuroscience, 1983. **8**(4): p. 791-7.
8. Bliss, T.V. and T. Lomo, *Long-lasting potentiation of synaptic transmission in the dentate area of the anaesthetized rabbit following stimulation of the perforant path.* J Physiol, 1973. **232**(2): p. 331-56.
9. Raymond, C.R., *LTP forms 1, 2 and 3: different mechanisms for the "long" in long-term potentiation.* Trends Neurosci, 2007. **30**(4): p. 167-75.
10. Holscher, C., R. Anwyl, and M.J. Rowan, *Stimulation on the positive phase of hippocampal theta rhythm induces long-term potentiation that can Be depotentiated by stimulation on the negative phase in area CA1 in vivo.* J Neurosci, 1997. **17**(16): p. 6470-7.
11. Baras, D. and R. Meir, *Reinforcement learning, spike-time-dependent plasticity, and the BCM rule.* Neural Comput, 2007. **19**(8): p. 2245-79.
12. Bear, M.F. and R.C. Malenka, *Synaptic plasticity: LTP and LTD.* Curr Opin Neurobiol, 1994. **4**(3): p. 389-99.
13. Bi, G.Q. and M.M. Poo, *Synaptic modifications in cultured hippocampal neurons: dependence on spike timing, synaptic strength, and postsynaptic cell type.* J Neurosci, 1998. **18**(24): p. 10464-72.
14. Hebb, D.O., *The Organization of Behavior*. 1949, New York: John Wiley and Sons. 335.
15. Le Feber, J., W.L.C. Rutten, J. Stegenga, P.S. Wolters, G.J.A. Ramakers, and J. van Pelt, *Conditional firing probabilities in cultured neuronal networks: a stable underlying structure in widely varying spontaneous patterns.* J. Neural Eng., 2007. ***4***: p. 54-67.

16. Marom, S. and D. Eytan, *Learning in ex-vivo developing networks of cortical neurons.* Prog Brain Res, 2005. **147**: p. 189-99.
17. Marom, S. and G. Shahaf, *Development, learning and memory in large random networks of cortical neurons: lessons beyond anatomy.* Q Rev Biophys, 2002. **35**(1): p. 63-87.
18. Barria, A. and R. Malinow, *NMDA receptor subunit composition controls synaptic plasticity by regulating binding to CaMKII.* Neuron, 2005. **48**(2): p. 289-301.
19. Madhavan, R., Z.C. Chao, and S.M. Potter, *Plasticity of recurring spatiotemporal activity patterns in cortical networks.* Phys Biol, 2007. **4**(3): p. 181-93.
20. Berger, T., A. Borgdorff, S. Crochet, F.B. Neubauer, S. Lefort, B. Fauvet, I. Ferezou, A. Carleton, H.R. Luscher, and C.C. Petersen, *Combined voltage and calcium epifluorescence imaging in vitro and in vivo reveals subthreshold and suprathreshold dynamics of mouse barrel cortex.* J Neurophysiol, 2007. **97**(5): p. 3751-62.
21. Baruchi, I. and E. Ben-Jacob, *Towards neuro-memory-chip: imprinting multiple memories in cultured neural networks.* Phys Rev E Stat Nonlin Soft Matter Phys, 2007. **75**(5 Pt 1): p. 050901.
22. Gross, G.W., E. Rieske, G.W. Kreutzberg, and A. Meyer, *A new fixed-array multi-microelectrode system designed for long-term monitoring of extracellular single unit neuronal activity in vitro.* Neuroscience Letters, 1977. **6**(2-3): p. 101-105.
23. Pine, J., *Recording action potentials from cultured neurons with extracellular microcircuit electrodes.* Journal of Neuroscience Methods, 1980. **2**(1): p. 19-31.
24. Hafizovic, S., F. Heer, T. Ugniwenko, U. Frey, A. Blau, C. Ziegler, and A. Hierlemann, *A CMOS-based microelectrode array for interaction with neuronal cultures.* J Neurosci Methods, 2007. **164**(1): p. 93-106.
25. van Ooyen, A. and J. van Pelt, *Activity-dependent neurite outgrowth and neural network development.* Prog Brain Res, 1994. **102**: p. 245-59.
26. Kamioka, H., E. Maeda, Y. Jimbo, H.P. Robinson, and A. Kawana, *Spontaneous periodic synchronized bursting during formation of mature patterns of connections in cortical cultures.* Neurosci Lett, 1996. **206**(2-3): p. 109-12.
27. Feinerman, O., M. Segal, and E. Moses, *Identification and dynamics of spontaneous burst initiation zones in unidimensional neuronal cultures.* J Neurophysiol, 2007. **97**(4): p. 2937-48.
28. Ham, M.I., L.M. Bettencourt, F.D. McDaniel, and G.W. Gross, *Spontaneous coordinated activity in cultured networks: Analysis of multiple ignition sites, primary circuits, and burst phase delay distributions.* J Comput Neurosci, 2008. **24**(3): p. 346-57.
29. Baruchi, I. and E. Ben-Jacob, *Functional holography of recorded neuronal networks activity.* Neuroinformatics, 2004. **2**(3): p. 333-52.
30. Rolston, J.D., D.A. Wagenaar, and S.M. Potter, *Precisely timed spatiotemporal patterns of neural activity in dissociated cortical cultures.* Neuroscience, 2007. **148**(1): p. 294-303.
31. Beggs, J.M. and D. Plenz, *Neuronal avalanches are diverse and precise activity patterns that are stable for many hours in cortical slice cultures.* J Neurosci, 2004. **24**(22): p. 5216-29.
32. Eytan, D. and S. Marom, *Dynamics and effective topology underlying synchronization in networks of cortical neurons.* J Neurosci, 2006. **26**(33): p. 8465-76.
33. Segev, R., I. Baruchi, E. Hulata, and E. Ben-Jacob, *Hidden neuronal correlations in cultured networks.* Phys Rev Lett, 2004. **92**(11): p. 118102.
34. Stegenga, J., J. Le Feber, E. Marani, and W.C. Rutten, *Analysis of cultured neuronal networks using intraburst firing characteristics.* IEEE Trans Biomed Eng, 2008. **55**(4): p. 1382-90.
35. van Pelt, J., P.S. Wolters, M.A. Corner, W.L. Rutten, and G.J. Ramakers, *Long-term characterization of firing dynamics of spontaneous bursts in cultured neural networks.* IEEE Trans Biomed Eng, 2004. **51**(11): p. 2051-62.
36. Lisman, J.E., *Bursts as a unit of neural information: making unreliable synapses reliable.* Trends Neurosci, 1997. **20**(1): p. 38-43.
37. Jimbo, Y., H.P. Robinson, and A. Kawana, *Strengthening of synchronized activity by tetanic stimulation in cortical cultures: application of planar electrode arrays.* IEEE Trans Biomed Eng, 1998. **45**(11): p. 1297-304.
38. Jimbo, Y., T. Tateno, and H.P.C. Robinson, *Simultaneous induction of pathway specific potetiation and depression in networks of cortical neurons.* Biophys J, 1999. **76**(2): p. 670-678.
39. Maeda, E., Y. Kuroda, H.P. Robinson, and A. Kawana, *Modification of parallel activity elicited by propagating bursts in developing networks of rat cortical neurones.* Eur J Neurosci, 1998. **10**(2): p. 488-96.
40. Tateno, T. and Y. Jimbo, *Activity-dependent enhancement in the reliability of correlated spike timings in cultured cortical neurons.* Biol Cybern, 1999. **80**(1): p. 45-55.

41. Corner, M.A., R.E. Baker, and J. van Pelt, *Homeostatically regulated spontaneous neuronal discharges protect developing cerebral cortex networks from becoming hyperactive following prolonged blockade of excitatory synaptic receptors.* Brain Res, 2006. **1106**(1): p. 40-5.
42. Corner, M.A., J. van Pelt, P.S. Wolters, R.E. Baker, and R.H. Nuytinck, *Physiological effects of sustained blockade of excitatory synaptic transmission on spontaneously active developing neuronal networks--an inquiry into the reciprocal linkage between intrinsic biorhythms and neuroplasticity in early ontogeny.* Neurosci Biobehav Rev, 2002. **26**(2): p. 127-85.
43. Gross, G.W., B.K. Rhoades, H.M. Azzazy, and M.C. Wu, *The use of neuronal networks on multielectrode arrays as biosensors.* Biosens Bioelectron, 1995. **10**(6-7): p. 553-67.
44. Bakkum, D.J., Z.C. Chao, and S.M. Potter, *Spatio-temporal electrical stimuli shape behavior of an embodied cortical network in a goal-directed learning task.* J Neural Eng, 2008. **5**(3): p. 310-323.
45. Madhavan, R., Z.C. Chao, and S.M. Potter. *Artificial background sensory input aids functional plasticity in cultured cortical networks*. in *6th international meeting on substrate-integrated micro electrode arrays*. 2008. Reutlingen, Germany: BIOPRO Baden-Würtemberg GmbH.
46. Wagenaar, D.A., R. Madhavan, J. Pine, and S.M. Potter, *Controlling bursting in cortical cultures with closed-loop multi-electrode stimulation.* J Neurosci, 2005. **25**(3): p. 680-8.
47. Shahaf, G. and S. Marom, *Learning in networks of cortical neurons.* J Neurosci, 2001. **21**(22): p. 8782-8.
48. van Staveren, G.W., J.R. Buitenweg, E. Marani, and W.L.C. Rutten. *The effect of training on neuronal networks: can they learn?* in *2nd international IEEE EMBS conference on neural engineering*. 2005. Arlington, VA.
49. Bakkum, D.J., Z.C. Chao, and S.M. Potter, *Long-term activity-dependent plasticity of action potential propagation delay and amplitude in cortical networks.* PLoS ONE, 2008. **3**(5): p. e2088.
50. Aertsen, A.M.H.J. and G.L. Gerstein, *Evaluation of neuronal connectivity: Sensitivity of cross-correlation.* Brain Research, 1985. **340**(2): p. 341-354.
51. Castellone, P., W.L.C. Rutten, and E. Marani. *Cross-interval histogram analysis of neuronal activity on multi-electrode arrays*. in *IEEE EMBS Conference on Neural Engineering*. 2003. Capri Island, Italy.

Chapter 2,

Analysis of cultured neuronal networks using intra-burst firing characteristics

Abstract

It is an open question whether neuronal networks, cultured on multielectrode arrays, retain any capability to usefully process information (learning and memory). A necessary prerequisite for learning is that stimulation can induce lasting changes in the network. To observe these changes, one needs a method to describe the network in sufficient detail, while stable in normal circumstances. We analyzed the spontaneous bursting activity that is encountered in dissociated cultures of rat neocortical cells. Burst profiles (BPs) were made by estimating the instantaneous array-wide firing frequency. The shape of the BPs was found to be stable on a time scale of hours. Spatiotemporal detail is provided by analyzing the instantaneous firing frequency per electrode. The resulting phase profiles (PPs) were estimated by aligning BPs to their peak spiking rate over a period of 15 min. The PPs reveal a stable spatiotemporal pattern of activity during bursts over a period of several hours, making them useful for plasticity and learning studies. We also show that PPs can be used to estimate conditional firing probabilities. Doing so, yields an approach in which network bursting behavior and functional connectivity can be studied.

Stegenga J., le Feber J., Marani E. and Rutten W.L.C.

(published in: *IEEE Trans Biomed Eng*, vol. 55, pp. 1382-90, 2008.)

2.1 Introduction

The culturing of neurons on microelectrode arrays (MEAs) offers the possibility to study the patterns of action potentials generated by relatively small, single-layered networks of neurons. It has been shown that individual cultured neurons retain many properties of their *in vivo* counterparts [1, 2], it is hoped that some properties of networks of neurons are also retained. Learning and memory are two key properties of a neuronal network. There are several studies that suggest a learning behavior in networks cultured on MEAs [3-7], others speak of induced plasticity [8-11]. The difference is that one can only speak of learning when some sort of improvement in the response can be observed (i.e., goal-directed behavior), while plasticity merely requires the observation of changes induced by stimulation. Most studies use a stimulus-response test before and after the experiment in order to reveal the changes in a network after applying their learning or plasticity inducing algorithms [3, 4, 6, 7, 9]. These stimulus-response tests are relatively easy to conduct and can be repeated several times to enable statistical evaluation. However, it has been shown that responses to stimuli change over time [10]. This limits the number of responses that are allowed to be averaged and (therefore) also the amount of detail that can be extracted from these responses. In fact, the changing of responses suggests that the test stimuli themselves are inducing changes in the network. Several groups focus their attention to changes that may occur in the spontaneous activity before and after an experiment [8, 10, 12]. In order to distinguish changes in activity after learning experiments from the activity before, normal development should be known. In this view, it is important to know the timescale at which the chosen parameters change during normal development, because the spontaneous activity can change over several timescales (from minutes to days). The parameters should be stable over the duration of an experiment (usually several hours) to be useful for analyzing changes induced by stimulation, yet be sensitive enough to pick up the induced changes. Spontaneous activity is dominated by network bursts—periods in which the spiking activity is very high compared to the nominal level. Bursts are present throughout the cultures' measured lifetime, starting at four to seven days in vitro (DIV) and lasting for the entire culturing period [13, 14]. The appearance and structure of bursts change with age [13, 15-19]. Due to the fact that the spatiotemporal structure of bursts changes

with age but appears to be quite stable over a period of hours [7, 13], parameters extracted from bursts should have a natural timescale of no change during which it is possible to observe changes due to stimulation algorithms. In a detailed study, Van Pelt *et al.* [13] reported on the bursting behavior during the development of cultures (from 7 DIV to 49 DIV). They show that bursts change significantly during development by analyzing the array-wide spiking rate (AWSR) in intervals of 10 ms. The AWSR is a summation of action potentials over all electrodes. Their main finding was that the AWSR during bursts has long rise and long fall times in early development, which changes to very sharp and intense profiles after about 25 DIV ([13], Fig. 9). They also show that activity during bursts is electrode specific, such that neurons have a preferred phase during which they are most active. These and other changes in AWSR during development coincide with changes in synaptic connections [11, 20-27], suggesting that network bursts carry information about the networks' connectivity. Provided that network bursts are selectively sensitive to (changes in) synaptic connectivity, a network state for experiments that aim to induce synaptic changes can be derived from them. Network burst parameters have already been used in various studies involving plasticity. In 1998, Meada *et al.* [11] reported an effect after tetanisation (stimulation in trains with an interstimulation interval of 50 ms, lasting 1 s) in burst frequency and the number of spikes in bursts. However, the effect was observed for only 20 min (due to recording length). Also, changes in these coarse parameters require a large change in network connectivity because they are unlikely to change when a limited number of connections is altered. Indeed, Wagenaar *et al.* [28, 29] carried out similar experiments and found no significant changes in either responses to test stimuli or in spontaneous bursts (burst frequency and AWSR rise and fall times).

Time Development and Composition of Network Bursts

The analysis presented in this paper starts by considering the AWSR during network bursts in detail. A burst profile (BP) was calculated by smoothing the train of action potentials by Gaussian filtering. The BPs were examined over a period of several days to show that bursts change their morphology and reveal short-term stability. Next, the network bursts were analyzed in the spatiotemporal domain (i.e., per recording site). The rationale for doing so was the limited amount of detail that the BPs offer because they were calculated from the AWSR, which includes only temporal information. The obtained electrode-specific profiles were called

phase profiles (PPs) because they show the electrode's contribution at times relative to the time of maximum network synchrony. It has been suggested in several studies that there is an order in which sites become active during bursts. Beggs and Plenz [30] classified network bursts in coronal slices of rat cortex using the temporal order of firing. They showed that multiple spatiotemporal burst patterns are present at any time and suggest that these patterns form the basis for memory. Using a different approach, Baruchi and Ben-Jacob [31] showed that dissociated cultures of cortical neurons exhibit network bursts with a very similar structure. A spatiotemporal pattern during network bursts was also observed by Van Pelt *et al.* [13], even though no attempt was made to classify the bursts. The latter result may indicate that there is a dominant pattern present. In this study, we first confirmed the presence of a dominant pattern, and then calculated PPs by aligning several bursts without classification. PPs describe network bursting activity and, thus, form an indirect measure of the synaptic connectivity. In support of this view, we show that PPs can be used to estimate conditional firing probabilities (CFPs). The functional connectivity found by methods such as cross-correlation analysis [32] and conditional firing probabilities [33], can thus be connected to PPs. How PPs and CFPs are mathematically related is described in the Appendix.

2.2 Materials and methods

Cell Cultures

Cortical neurons were obtained from either newborn or E18 Wistar rats by trituration and chemical dissociation using trypsin. The cells were plated at a concentration of 1 million cells per ml (Romijn's R12 medium [34]) and allowed to adhere for 2 h. MEAs were coated with polyethylene-imine (PEI) to increase adhesion. The nonadhering cells were removed by refreshing medium, and 600 ml of R12 medium was added. The resulting monolayer had a density of about 5000 cells/mm. The medium was entirely changed twice per week. The cultures were stored in an incubator at 37 ˚C, at a CO_2 concentration of 5% and near 100% humidity. During measurements, the cultures were covered with a lid and tightly sealed with parafilm. Cultures were allowed to settle for 20 min before the start of measurement.

Measurement Setup

60-Channel Recordings: We used the MC1060BC preamplifier and FA60s filter amplifier (both MultiChannelSystems GmbH, Reutlingen, Germany) to prepare the signals for analog-to-digital conversion. Amplification was 1000 times in a range from 100 Hz to 6000 Hz. A 6024E data-acquisition card (National Instruments, Austin, TX) was used to record all 60 channels at 16 kHz. Custom-made Labview (National Instruments, Austin, TX) programs were used to control data acquisition and applied a threshold detection scheme with the objective of data reduction. The actual detection of action potentials was performed offline. During the experiments, the temperature was controlled at 36.0 ˚C, using a TC01 (multichannel systems) temperature controller. Noise levels were typically 3 to 5 µV. The MEAs had 60 titanium-nitride electrodes of 10 µm in diameter, spaced 100 µm apart in a square grid [see figure 2.1B].

16-Channel Recordings: Recordings before June 1, 2005, were made using MEAs manufactured at the University of Twente (referred to as UTMEAs). These had 61 gold electrodes and were 12 µm in diameter and spaced 80 µm apart in a hexagonal configuration [figure 2.1A]. After coating with platinum black, the noise levels were typically 7 µV. The area surrounding the electrode area was coated with Silastic 734, which increased the useful lifespan of the MEAs. The setup used a custom-made 16-channel amplifier, with an amplification of 230 in a range of 300 Hz to 6 kHz. A PCI-6023E data-acquisition card (National Instruments, Austin, TX) sampled the signals at 12500 Hz. The temperature was controlled at 36.0 ˚C.

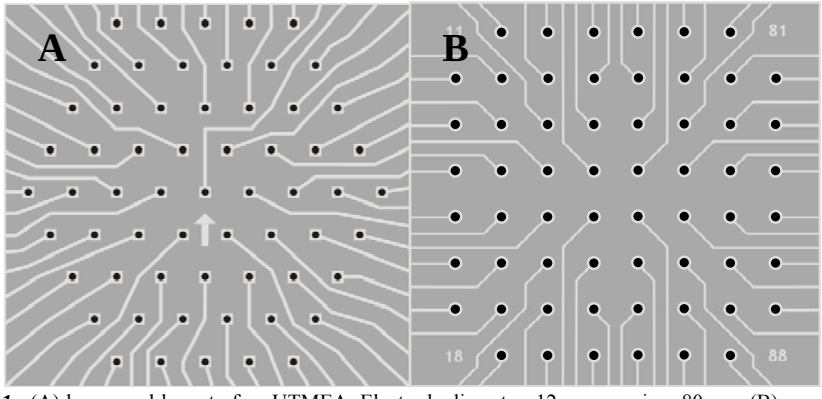

Figure 2.1. (A) hexagonal layout of an UTMEA. Electrode diameter: 12 µm; spacing: 80 µm. (B) square layout of an MCSMEA. Electrode diameter: 10 µm; spacing: 100 µm.

Table 2.1. Overview of the dataset in terms of MEA-type, number of measurements and number of cultures. The number of preparations of 1 day-old rats and the number of E18 preparations is given between the parentheses.

	UTMEA		*MCSMEA*	
	sessions	cultures	sessions	cultures
Single day	3	3 (3/0)	25	9 (9/0)
Multiple day	-	-	41	4 (3/1)

Experiments The experiments can be subdivided into two categories: 1) single-day measurement sessions, typically lasting 2 h, used to assess stability on a timescale of minutes to hours and 2) sets of measurements (i.e. multiple days), used to assess developmental changes as well as stability. Each set of measurements consists of at least five measurement sessions of a single culture (Table 2.1).

Data Processing

Spike detection Online preprocessing consisted of detecting threshold crossings and storing 10 ms of data for each candidate action potential. The threshold level was set at 5.5 times the estimated rms noise level of the electrode, which was continuously monitored. Detections were validated offline using the algorithm described in [35], as this was found to be a fast and reliable method. We required that no more than four detections occurred on the same sample in order to suppress synchronous artifacts picked up from external sources. In a heavily bursting culture, this requirement resulted in less than 0.1% data loss, while still being effective in detecting and removing these artifacts.

Network burst detection We refer to bursts as network bursts when the total firing rate, as determined in 10-ms bins, exceeded a threshold. The threshold was set at two spikes for each electrode that was considered active (spike rate 0.1 Hz). Whenever a bin exceeded the threshold, a BP was calculated in order to estimate the time at which the peak AWSR occurred (t_c). Once found, BPs and PPs were calculated from t_c-300 ms to t_c+300. Threshold crossings were treated in order of size, and overlap between profiles was prevented by setting all bins from t_c-600 to t_c+600 ms to zero. The influence of bin width and threshold combinations were tested, but led to comparable results between natural limits of: 1) high threshold-small bin width combinations that lead to missed events and 2) a low threshold-large bin width combinations that lead to false detections, and 3) bin widths that exceed inter burst intervals.

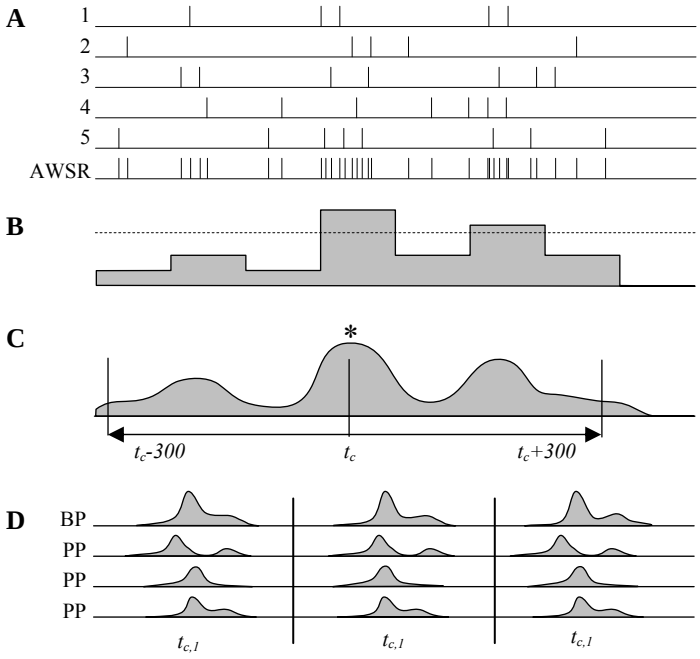

Figure 2.2. Calculation of burst profiles. (A) action potentials across all electrodes are added to make the AWSR. (B) The AWSR is binned and compared with a threshold. (C) Whenever the number of spikes per bin crosses a threshold, a profile is calculated by convoluting the AWSR spike train with a Gaussian (* denotes the burst peak). (D) The dataset is a series of burst profiles (BP) and phase profiles (PP).

Calculation of profiles A BP is an estimation of the instantaneous array-wide spiking rate (AWSR). To this end, all spike occurrences in a burst are taken together and convolved with a Gaussian probability density function (figure 2.2), with a standard deviation (SD) of 5 ms. This was wide enough to provide a smooth result near the maximum AWSR, and small enough so as not to obscure important details of the AWSR. A smooth graph near the maximum AWSR was important for aligning and comparing profiles. The profiles were 600 ms wide, large enough to capture the relevant features in most cases. Exceptions to the above were very young cultures in which bursts were typically longer and the maximum AWSR was lower. In these cases, a wider SD would have led to better results, but a changing SD would make comparing profiles with each other less direct; therefore, we used a fixed SD and a fixed profile width. The number of spikes that were recorded per electrode per burst was relatively small, when compared to the number of spikes in the AWSR. Therefore, more averaging was required to obtain a useful estimation of PPs. Averaging over multiple bursts, aligned to their peak AWSR was found to yield stable PPs. Averaging over a small amount of time (i.e., 15 min) was justified by the results of cluster analysis (as will be seen).

Comparing profiles We used the correlation coefficient to quantify changes between profiles. For two discrete time BPs, $A=\{a_1,a_2,\ldots a_K\}$ and $B=\{b_1,b_2,\ldots b_K\}$, the correlation coefficient is defined as:

$$C(A,B)=\frac{\sigma_{AB}}{\sigma_A\sigma_B}=\frac{\sum(a_k-\mu_A)(b_k-\mu_B)}{\left(\sum(a_k-\mu_A)^2\right)^{0.5}\left(\sum(b_k-\mu_B)^2\right)^{0.5}} \tag{2.1}$$

where the summations are over the discrete time parameter k, and μ is the average firing rate within one burst. The correlation coefficient is sensitive to changes in shape, but insensitive to changes in magnitude (i.e., total number of spikes per burst).

Convolution estimates of CFPs Relationships between single-electrode firing patterns were calculated using (2.9) from the Appendix

$$CFP_{ij}(\tau)=J\int_{t_m} f_i(t_m-\tau)f_j(t_m)dt_m \tag{2.2}$$

where $f_i(t)$ represents the PP of electrode i, scaled to unit area and J is a firing rate dependent scaling factor. As is explained in the Appendix, the outcome of convolving phase profiles yields an estimation of the conditional firing probability (CFP). We have used the algorithm described by Segev *et al.* [36] to check whether there are discernible differences between bursts. Shortly, the distance (i.e., dissimilarity) between bursts was calculated based on cross correlations between electrode firing patterns. The dendrogram clustering method used these distances to assign bursts to one of five classes.

1.3 Results

General progress and burst types

The earliest electrical activity was recorded at 6 DIV and consisted of apparently uncorrelated activity on a small set of electrodes. Network bursts were regularly observed from about 7 DIV and were present for the entire observed period (max. 61 DIV). Early network bursts generally recruited few electrodes, lasted for

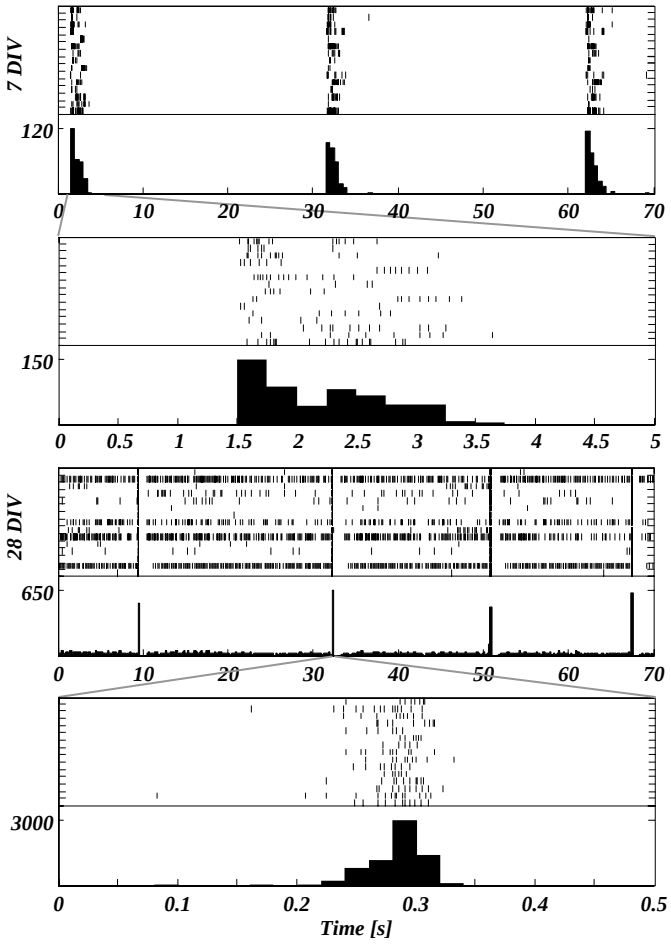

Figure 2.3. Activity at two different stages of development (7, 28 DIV). The top traces show the spike times of 15 electrodes, the bottom traces show the AWSR in bins of 0.5, 0.2, 0.5, 0.02 s respectively. At 7 DIV bursts are wide, sometimes lasting several seconds. At 28 DIV, the bursts have shortened dramatically.

seconds, and did not reach very high spike rates (Figure 2.3). At this stage in development, new sites were recruited; the network bursts shortened and became more intense. Around 9 DIV, the network bursts were intense enough to be automatically detected using the settings described in Section II and continued to be intense enough for the entire observed period. We checked for the influence of burst detection parameters and found that a large disparity existed between network bursts and false detections. We used the algorithm described by Segev *et al.* [36] to check whether there were discernible differences between bursts. In about one-third of all measurements, a second class was present with, on average, 15% bursts assigned to it.

However, an evolving burst pattern may also introduce a second class. We have used the following rules to categorize our measurements (Table 2.2): 1) There was

Table 2.2. Percentage of measurements assigned to one of three categories, tabulated per culture. Note that there is an obvious difference between cultures. The number of measurements per culture is denoted by N.

culture	N	Dominant (%)	ordered (%)	Unordered (%)
I	59	98.31	1.69	0.00
II	13	100.00	0.00	0.00
III	15	53.33	26.67	20.00
IV	19	78.95	10.53	10.53
V	10	40.00	40.00	20.00
VI	39	71.79	28.21	0.00
VII	7	85.71	0.00	14.29
VIII	8	50.00	37.50	12.50
IX	7	71.43	28.57	0.00
X	3	100.00	0.00	0.00
All	180	80.00	15.00	5.00

one or a strong (>95% of bursts belonging to 1 class) dominant burst type. This was the case in 80% of all measurements. 2) There was a significant (>5% and >2 bursts in the second class) second class, but the occurrences were in temporal order (suggesting a single, changing burst type). The degree of temporal ordering was quantified by calculating the number of alternations between bursts of the main class and second class. We compared this number to the theoretical value (threshold = mean - standard deviation, $\mu=N_2\cdot(N_1+N_2)^{-1}$, $\sigma=\mu\cdot(N_1+N_2)^{-0.5}$, where N_i denotes the number of bursts assigned to class i) of a randomly ordered sequence of the same size. In 75% of the remaining measurements (i.e., 15% in total), a temporal ordering was found. 3) There was a significant (>5% and >2 bursts in the second class) second class without temporal ordering. When this is the case, there were (at least) two different burst patterns contributing significantly. We have encountered this situation in only 5% of all measurements. Considering the large

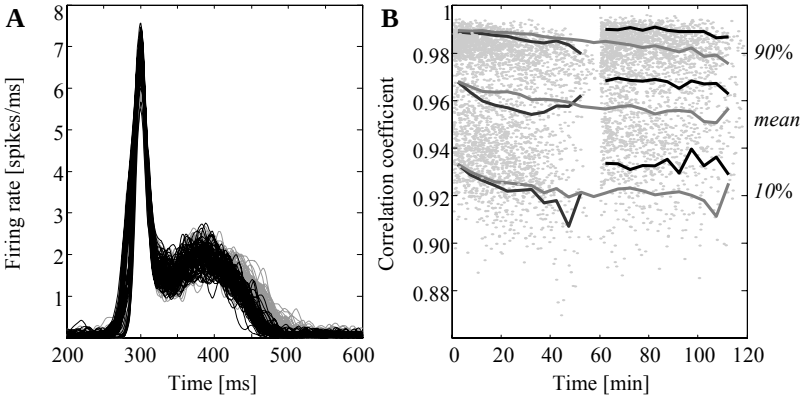

Figure 2.4. (A) All burst profiles during a two hour measurement at 14 DIV. Profiles from the first hour are shown in gray (N=81), those from the 2nd hour are shown in black (N=74). Only the non-zero part is plotted. (B) Correlation coefficients between burst profiles shown in (A). The dots show individual correlation coefficients between burst profiles in the first hour (0-60) and between bursts in the second hour (60-120). Lines show 5 minute average, 10% boundary and 90% boundary. Average slope is -0.007 per hour.

quantity of measurements that fit in the first and second category, we interpreted our measurements as the development through time of a single burst pattern. We accepted the occasional presence of burst types expressed in parallel as a minor disturbance, as even in the 5% of measurements when this is the case, only 18% of bursts were assigned to a second class.

Burst profiles

Figure 2.4 shows an example of all BPs during a 2-h measurement. BPs in thefirst hour (gray) were slightly wider than the profiles in the second hour of measurement (black). There was little variation in the general shape of the BPs from one burst to the other on a scale of ~10 ms. Also, the number of spikes, as indicated by the area underneath the graphs, and the peak firing rate appear to be well preserved over these 2 h of measurement. The correlation between individual bursts was extremely high, averaging 0.96 and a 10% lower boundary of 0.9. In addition to this, we found only a small negative slope in the average correlation. On a scale of days, figure 2.5 shows an example of the changes that BPs went through during maturation of the cultures. The BPs, averaged over 30 min for clarity, showed progressive small changes within a single measurement and larger changes between measurements. Several features of BPs in general are illustrated,

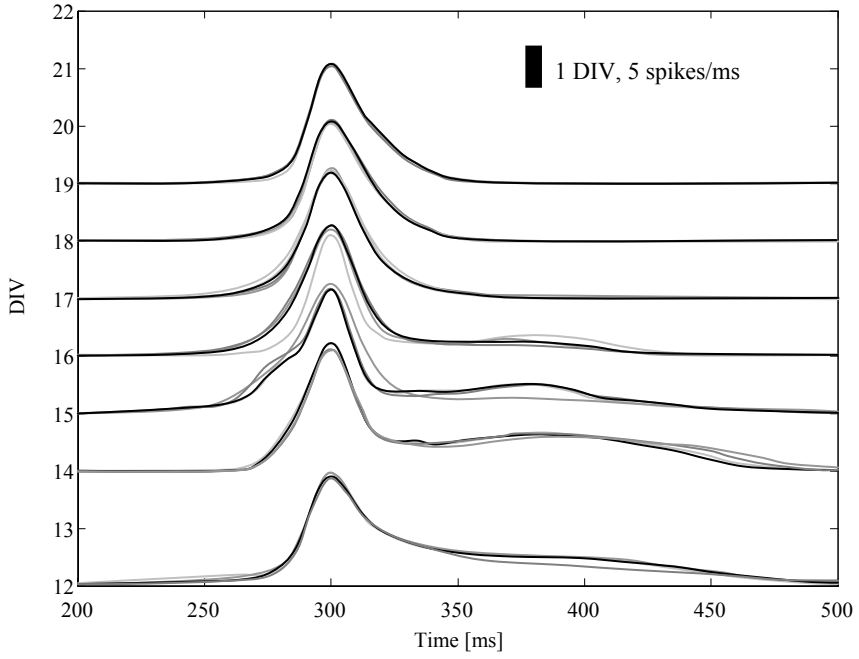

Figure 2.5. The development of burst profiles over several days in vitro (DIV). One division equals 1 day in vitro (DIV) and also 5 spikes per millisecond.

such as a long tail, a distinct second mode, and differences in rising and falling phases. We calculated the correlation coefficients between BPs for all cultures that we recorded from. For continuous recordings, we calculated the average correlation coefficient as a function of time difference binned in 15 min. Figure 2.6A displays the average of these intra measurement correlations for all cultures. Similarly, the correlation coefficients between BPs measured on subsequent days (inter measurement correlations) are displayed in figure 2.6B.We calculated the average decrease of correlation as a function of time for each culture and for all cultures in total. The influence of differences in the first day of measurement (9–12 DIV; 2.6B) was considered negligible.

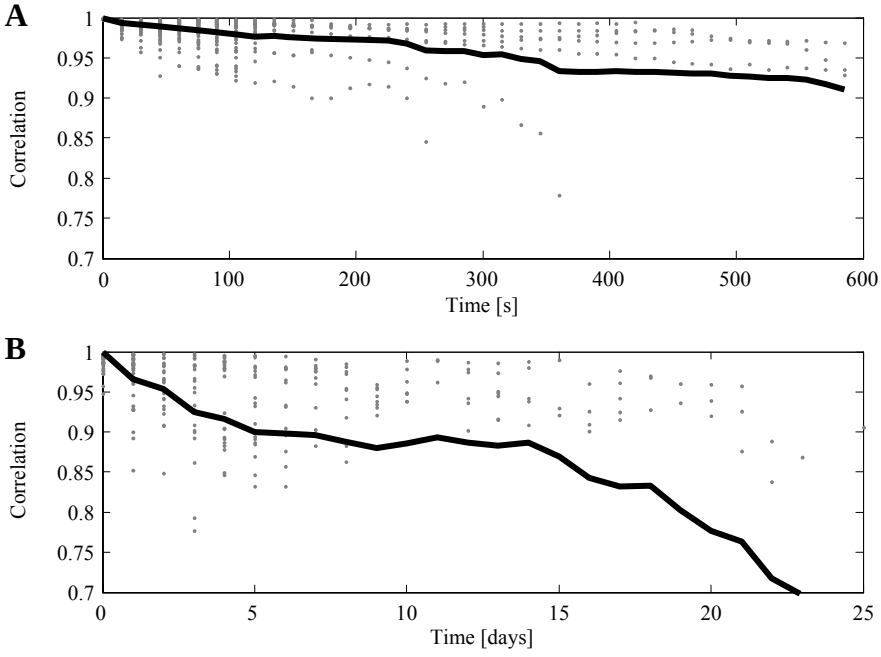

Figure 2.6. Correlation coefficients between burst profiles. (A) Intra measurement correlations. Each data point is a 15 minute average per culture. (B) Inter measurement correlations. Data points are average correlation coefficients between two sessions. Zero time indicates the first day of measurement and differs per culture (9-12 DIV). In both graphs profiles were averaged over 15 min before calculation to decrease computational load. The interpolating graphs are calculated by taking the mean slope per bin/day, with (0,1) as starting point.

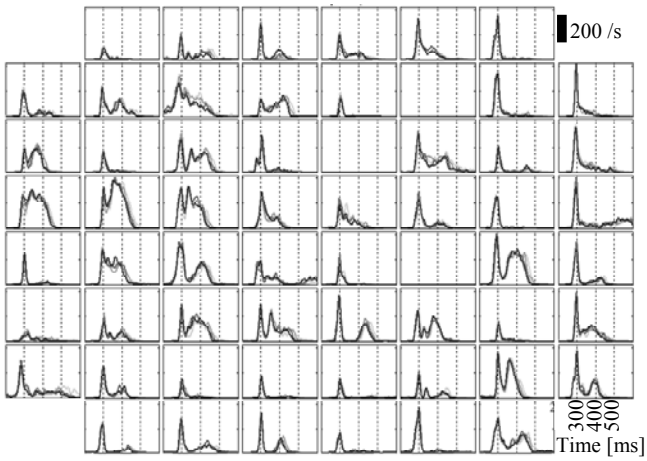

Figure 2.7. Example of the stability of phase profiles for all electrodes in a 2 hour measurement at 14 DIV (same data as in figure 4). Graph locations correspond to MEA layout. Each graph shows 4 phase profiles, each of which is an average over 30 minutes (42, 39, 32 and 32 bursts respectively). The maximum AWSR is set at 300 ms.

Phase profiles

A BP is essentially a global descriptive parameter and, thus, is unlikely to reveal changes between few pairs of electrodes. A phase profile can reveal more detailed information about individual electrodes. As figure 2.7 shows, the electrodes fired in a nonrandom order during a burst. Some were active as early as 100 ms before the main peak was reached, while others showed activity in the latter part of a burst. Most, if not all, active electrodes had a peak in their activity around the time of

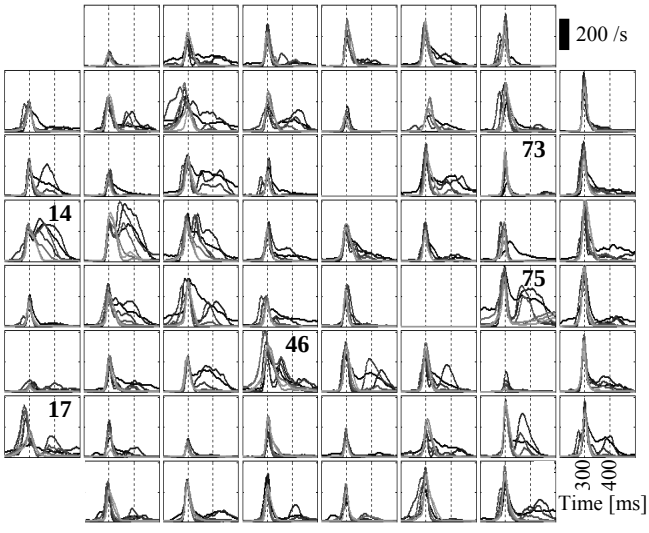

Figure 2.8. Phase profiles of a single culture measured 7 times in a span of 8 days. The corresponding burst profiles are shown in figure 5. Graph locations correspond to MEA layout. The AWSR peaks were set at 300 ms.

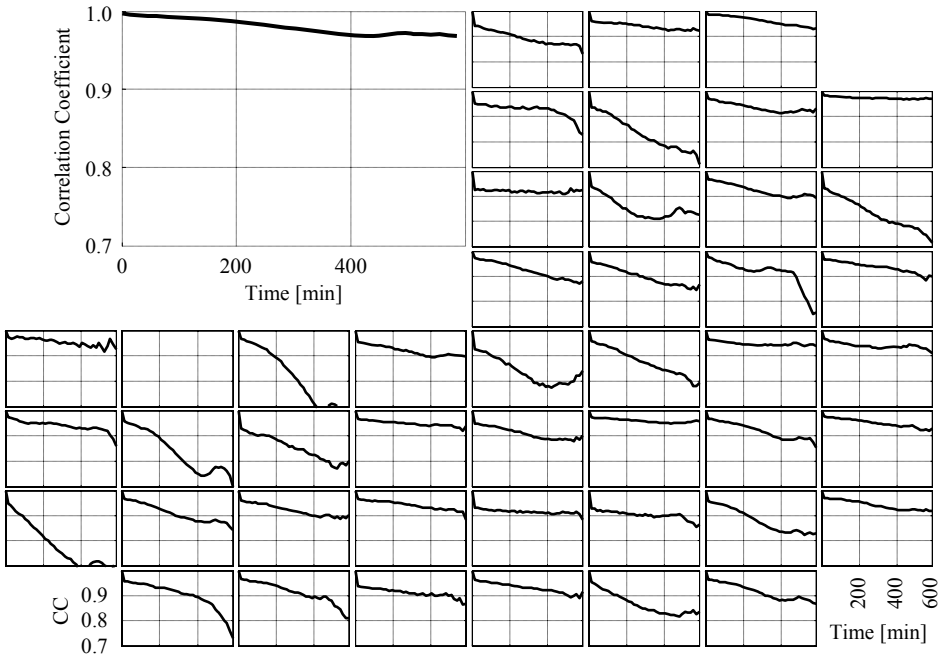

Figure 2.9. Stability phase profiles within a 10 hour continuous measurement. Phase profiles were averaged over 15 minutes before calculating correlations. Graph locations correspond to MEA layout. The inset shows the correlation coefficients between burst profiles.

maximum AWSR (*i.e.*, 300 ms). These observations are consistent with the observations already reported in [13] and [37]. In general, the profiles were too complex to be captured with a small number of descriptive parameters. The PPs showed progressions that resemble those of the BPs.

Fig. 8 shows PPs averaged per DIV, for several consecutive DIV. There was a clear trend, in BPs (corresponding BPs are shown in figure 2.5) and PPs, toward a single peak in the firing rate. A number of different progressive changes could be observed. For example, electrode 73 contributed very little in early recordings, but increased its number of elicited spikes during each measurement, eventually reaching a firing rate that was more than three times that found in early recordings. Electrode 14 started out with a dominant late phase of firing, which was completely absent in the late recordings. A bimodal firing pattern could be discerned in many electrodes (*e.g.*, 75) at some time during the development of this culture. Electrode 17 had, in most measurements, a single mode of firing. The latency at which the maximum firing rate at electrode 17 was achieved changed during development. For most of the measurements, electrode 17 was early to fire. The stability of PPs from burst to burst was less pronounced than that of BPs. Part of the difference

could possibly be explained by the relatively small amount of spikes per electrode per burst. To compensate for this, we averaged PPs over 15 min. The very small negative slope observed in the correlation coefficient between BPs indicated that bursts could be considered stable over such small periods (figure. 2.4). It can be seen in figure 2.9 that correlation coefficients dropped at different rates, depending on the electrode. Correlation coefficients were generally higher, and had a lower slope, when the number of spikes elicited per electrode per burst was large. The inset in figure 2.9 shows that the correlation coefficients between BPs decrease with time approximately as a weighted average of the correlation coefficients between PPs. Some electrodes clearly showed an increased rate of change during some periods, while others showed a more constant rate of change. The latter indicated changes that affected the network as a whole; the first indicated that the role of a neuron within the network could change. For comparison, the correlation coefficients of the culture shown in figure 2.8 are shown in figure 2.10. Here, also very different rates are observed, depending on electrode.

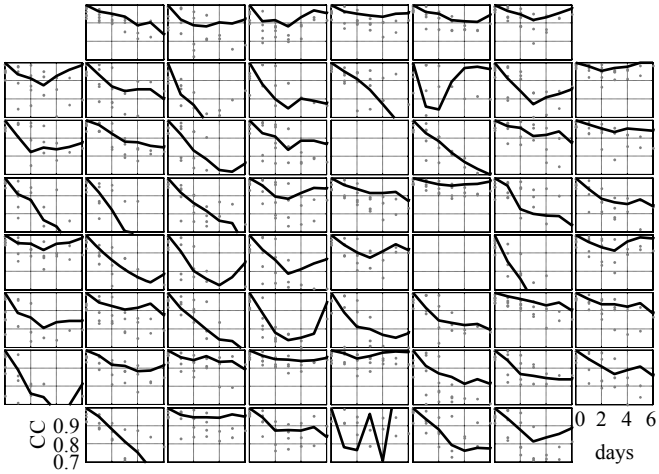

Figure 2.10. Correlation coefficients as a function of time, calculated over several measurement sessions of a single culture. Same data as in figures 5, 7 and 8. Dots show individual correlation coefficients. The interpolating graphs are calculated by taking the mean slope per bin/day, with (0,1) as starting point.

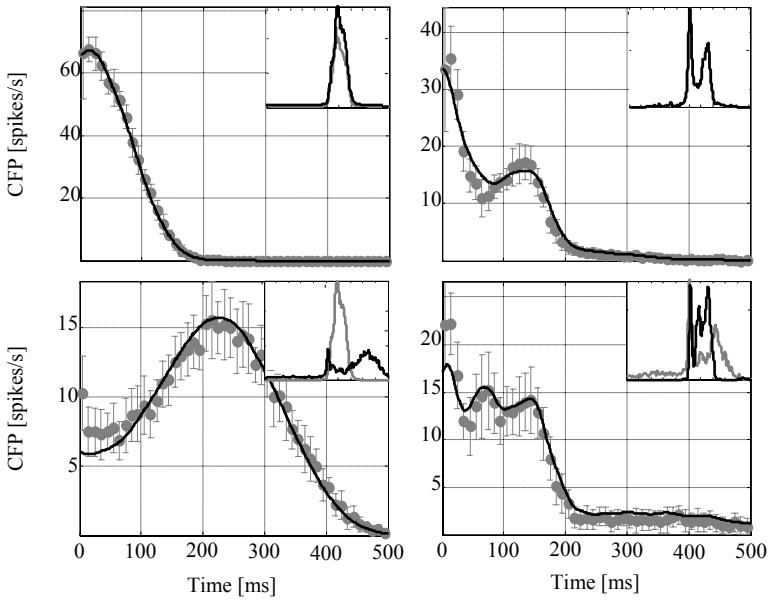

Figure 2.11. Examples of conditional firing probabilities (CFPs) calculated by the direct method and the convolution method, based on 1 hour of data measured at 14 DIV. Filled circles and standard deviations show the CFP calculated by equation (3), lines show the result of convolving the phase profiles. The insets show the phase profiles of the electrodes under consideration from 500 ms before to 500 ms after the burst peak.

Conditional firing probabilities

Figure 2.11 shows four examples of CFPs, as calculated by direct estimation [33] and by convolving PPs (Appendix). The convolution estimations of the CFPs follow the general shape of the direct estimate, often within the boundaries of one standard deviation. One limitation of the convolution estimate is that it cannot map refractory periods or discontinuities due to the continuous nature of the convolution and the smoothing applied when calculating the PPs. The estimation was more accurate when using small standard deviations in the filtering procedure of calculating the phase profiles.

2.4 Discussion

At any time during the period that we measured, there was either one, or one strongly dominant type of burst expressed by the culture. This contradicts several other findings, which reported a large diversity in bursts [19, 30, 36]. One difference is that we use a chemically defined medium [13, 34], whereas groups observing burst diversity all use 5% horse serum in their culture medium [19, 36].

Promoting glial cells this way has a noticeable influence on the network activity [38, 39], and may well lead to differences in bursting behavior. The apparent discrepancy may also be explained by differences in culture age. We measured cultures predominantly in the maturation phase, up to 21 DIV [5, 7, 13, 17, 22, 40], while other studies report on cultures which were considered mature, beyond 21 DIV . The apparent absence of diversity in bursts may have a profound impact on the information processing capabilities of a net work. Beggs and Plenz [30] conclude from brain slice recordings that the diversity of bursts is such that, should bursts be used to process information, the transfer of information is optimal. In this respect, our cultures would be unable to process any information, at least during the maturation phase. Since the cultures are randomly plated and have not received any external (electrical) stimuli since plating, one can assume that structure and activity have been shaped using self-generated signals [18]. Thus, the lack of structure and inputs may well contribute to the absence of burst diversity in the cultures during the maturation phase. The observation that BPs show very little variation from one burst to the next, and change their shape over a time scale of several hours has previously been made by Van Pelt *et al.* [13], but was never quantified. The correlations coefficients between bursts and those between PPs show that the variation in profile shape is very low. Some variation between bursts is reduced by Gaussian filtering, but the standard deviation used (5 ms) is very small compared to the length of a burst and the relevant features of the burst are still captured. The correlation coefficient as a measure to compare profiles is certainly biased to some extent. The correlation coefficient is more sensitive to changes in the main peak, where the firing rate is high, and less sensitive to any of the smaller, but nevertheless important, features. Bias is noticeable because many changes exclude the main peak, and their influence on the correlation coefficient depends on the size of the changed features relative to the peak size. Both BPs and PPs alter shape in an incremental way. This suggests that plasticity mechanisms are responsible for these changes, rather than random variations. Apart from synaptogenesis, which occurs mainly up to 18 DIV, modifications of synaptic efficacy occur when connected neurons spike within 20 ms of each other [41]. During network bursts, most electrodes spike in a period of about 100 ms and, thus, massive reinforcements of synaptic efficacies can be expected. These reinforcements help to preserve burst structure when there are no large changes in input and/or structure. It is known that during the third week in vitro, there is a period in which large numbers of synapses are pruned [42, 43]. In [13], large

changes in BPs are observed around this period, only to stabilize again afterwards. We have not observed changes of such magnitude, possibly due to less and/or slower pruning of synapses. We found that CFPs can be estimated from PPs via convolution which, combined with the stability found by both methods, suggests that functional connectivity and burst structure are expressions of the same underlying physical network structure. In view of multiple burst types reported by several researchers [14, 30, 36], it is necessary to first discriminate between different types of bursts (e.g., using the method described in [36]), and then calculate the PPs and CFPs, such that functional connectivity for each burst type is revealed.

2.5 Appendix

The phase profiles (PPs) can be used to construct electrode-to-electrode relationships by considering all combinations of two PPs and convolving these. The PPs are firing probabilities of the stereotypical activity during bursts. We will show that convolving two PPs yields the CFP of one electrode to another. These CFPs, in turn, define a network of (generalized or functional) connections in terms of strength and latency. We start with deriving the CFP, which describes the probability that neuron *j* fires at time $t+\tau$ when neuron *i* fires at *t*. We can describe the two spike trains by a summation of Dirac pulses (figure 2.2)

$$v_i(t) = \sum_{k=1}^{K} \delta(t - t_k) \tag{2.3}$$

$$v_j(t) = \sum_{m=1}^{M} \delta(t - t_m) \tag{2.4}$$

where t_k denotes the time at which neuron *i* fires its k^{th} action potential and similarly for neuron *j*. The CFP counts all occurrences that t_m-t_k that equals a certain delay τ, divided by the number of action potentials *K* elicited by neuron *i*:

$$CFP_{ij}(\tau) = \frac{1}{K} \sum_{k=1}^{K} \sum_{m=1}^{M} \delta(\tau - (t_m - t_k)) \tag{2.5}$$

Formula (2.5) is the direct estimate of the CFP, and is implemented in discrete form by Le Feber *et al.* [33]. The estimation accuracy increases when the number of action potentials in both time series (*K* and *M*) is large. It also implies that the relationship between *i* and *j* does not change with time, and that both time series are stationary. In a culture that exhibits bursting, a large fraction of the action potentials occurs during network bursts (it is regularly observed that 80% of spikes

are within bursts). The stereotypical firing pattern during bursts is described by the PPs. With proper scaling, the phase profiles can be interpreted as probability density functions (PDFs) of eliciting a single spike during a burst. In other words, t_k is a random variable with a distribution function $f_i(t)$ given by the normalized PP of neuron *i*. The conditional probability density function is given by:

$$f_{j|i}(\tau) = \int_{t_k}\int_{t_m} \delta(\tau - t_m + t_k) f_{i,j}(t_k, t_m) dt_k dt_m \qquad (2.6)$$

We will approximate the joint probability density function $f_{i,j}$ by

$$f_{i,j}(t_k, t_m) \cong f_i(t_k) f_j(t_m) \qquad (2.7)$$

This approximation is valid for the case where each neuron elicits one spike. Multiple spikes may be elicited on *j* in response to a single spike in *i* (all during bursts). This is accounted for by a scaling factor J ($\approx M/K$), thereby implicitly assuming that spikes elicited by *j* are randomly drawn from f_j. The CFP can then be expressed as:

$$CFP_{ij}(\tau) = J \cdot f_{j|i}(\tau) = J \int_{t_k}\int_{t_m} \delta(\tau - t_m + t_k) f_i(t_k) f_j(t_m) dt_k dt_m \qquad (2.8)$$

One integral can now be eliminated using the sifting property of the Dirac function

$$CFP_{ij}(\tau) = J \int_{t_m} f_i(t_m - \tau) f_j(t_m) dt_m \qquad (2.9)$$

Equation (2.9) constitutes a convolution between the phase profiles of electrodes *i* and *j*. The convolution estimate of the CFP in (2.9) and the direct estimation in (2.5) yield similar curves (figure 2.11). The main difference is that the direct method uses mainly averaging over time, while the convolution method uses interpolation (Gaussian filtering) as well as averaging over bursts (i.e., time). Consider also that not all action potentials occur in bursts; we expect that the CFP is better estimated directly from its definition. However, PPs are primarily meant to show contributions of single electrodes to network bursts.

2.6 References

1. Giugliano, M., et al., *Single-neuron discharge properties and network activity in dissociated cultures of neocortex.* J Neurophysiol, 2004. **92**(2): p. 977-96.
2. Rauch, A., et al., *Neocortical pyramidal cells respond as integrate-and-fire neurons to in vivo-like input currents.* J Neurophysiol, 2003. **90**(3): p. 1598-612.

3. Eytan, D., N. Brenner, and S. Marom, *Selective adaptation in networks of cortical neurons.* J Neurosci, 2003. **23**(28): p. 9349-56.
4. Marom, S. and D. Eytan, *Learning in ex-vivo developing networks of cortical neurons.* Prog Brain Res, 2005. **147**: p. 189-99.
5. Marom, S. and G. Shahaf, *Development, learning and memory in large random networks of cortical neurons: lessons beyond anatomy.* Q Rev Biophys, 2002. **35**(1): p. 63-87.
6. Ruaro, M.E., P. Bonifazi, and V. Torre, *Toward the neurocomputer: image processing and pattern recognition with neuronal cultures.* IEEE Trans Biomed Eng, 2005. **52**(3): p. 371-83.
7. Shahaf, G. and S. Marom, *Learning in networks of cortical neurons.* J Neurosci, 2001. **21**(22): p. 8782-8.
8. Jimbo, Y., H.P. Robinson, and A. Kawana, *Strengthening of synchronized activity by tetanic stimulation in cortical cultures: application of planar electrode arrays.* IEEE Trans Biomed Eng, 1998. **45**(11): p. 1297-304.
9. Jimbo, Y., T. Tateno, and H.P.C. Robinson, *Simultaneous induction of pathway specific potetiation and depression in networks of cortical neurons.* Biophys J, 1999. **76**(2): p. 670-678.
10. Madhavan, R., Z.C. Chao, and S.M. Potter, *Spontaneous bursts are better indicators of tetanus-induced plasticity than responses to probe stimuli*, in *2nd international IEEE EMBS conference on neural engineering*. 2005: Arlington, VA.
11. Maeda, E., et al., *Modification of parallel activity elicited by propagating bursts in developing networks of rat cortical neurones.* Eur J Neurosci, 1998. **10**(2): p. 488-96.
12. Chao, Z.C., et al., *Effects of random external background stimulation on network synaptic stability after tetanization.* neuroinformatics, 2005: p. 263-280.
13. van Pelt, J., et al., *Long-term characterization of firing dynamics of spontaneous bursts in cultured neural networks.* IEEE Trans Biomed Eng, 2004. **51**(11): p. 2051-62.
14. Wagenaar, D.A., et al., *Controlling bursting in cortical cultures with closed-loop multi-electrode stimulation.* J Neurosci, 2005. **25**(3): p. 680-8.
15. Chiappalone, M., et al., *Dissociated cortical networks show spontaneously correlated activity patterns during in vitro development.* Brain Res, 2006. **1093**(1): p. 41-53.
16. Ikegaya, Y., et al., *Synfire chains and cortical songs: temporal modules of cortical activity.* Science, 2004. **304**(5670): p. 559-64.
17. Van Pelt, J., et al., *Longterm stability and developmental changes in spontaneous network burst firing patterns in dissociated rat cerebral cortex cell cultures on multielectrode arrays.* Neurosci Lett, 2004. **361**(1-3): p. 86-9.
18. van Pelt, J., et al., *Dynamics and plasticity in developing neuronal networks in vitro.* Prog Brain Res, 2005. **147**: p. 173-88.
19. Wagenaar, D.A., J. Pine, and S.M. Potter, *An extremely rich repertoire of bursting patterns during the development of cortical cultures.* BMC Neurosci, 2006. **7**: p. 11.
20. Corner, M.A., et al., *Physiological effects of sustained blockade of excitatory synaptic transmission on spontaneously active developing neuronal networks--an inquiry into the reciprocal linkage between intrinsic biorhythms and neuroplasticity in early ontogeny.* Neurosci Biobehav Rev, 2002. **26**(2): p. 127-85.
21. Ichikawa, M., et al., *Formation and maturation of synapses in primary cultures of rat cerebral cortical cells: an electron microscopic study.* Neurosci Res, 1993. **16**(2): p. 95-103.
22. Kamioka, H., et al., *Spontaneous periodic synchronized bursting during formation of mature patterns of connections in cortical cultures.* Neurosci Lett, 1996. **206**(2-3): p. 109-12.
23. Kiddie, G., et al., *Biologically plausible models of neurite outgrowth.* Prog Brain Res, 2005. **147**: p. 67-80.
24. Neuhoff, H., J. Roeper, and M. Schweizer, *Activity-dependent formation of perforated synapses in cultured hippocampal neurons.* Eur J Neurosci, 1999. **11**(12): p. 4241-50.

25. van Ooyen, A. and J. van Pelt, *Activity-dependent neurite outgrowth and neural network development.* Prog Brain Res, 1994. **102**: p. 245-59.
26. Van Ooyen, A., J. Van Pelt, and M.A. Corner, *Implications of activity dependent neurite outgrowth for neuronal morphology and network development.* J Theor Biol, 1995. **172**(1): p. 63-82.
27. van Oss, C. and A. van Ooyen, *Effects of inhibition on neural network development through activity-dependent neurite outgrowth.* J Theor Biol, 1997. **185**(2): p. 263-80.
28. Wagenaar, D.A., J. Pine, and S.M. Potter, *Searching for plasticity in dissociated cortical cultures on multi-electrode arrays.* Journal of negative results in biomedicine, 2006. **5**(16).
29. Wagenaar, D.A., J. Pine, and S.M. Potter, *Searching for plasticity in dissociated cortical cultures on multi-electrode arrays.* Journal of negative results in biomedicine, 2007. **6**(3).
30. Beggs, J.M. and D. Plenz, *Neuronal avalanches are diverse and precise activity patterns that are stable for many hours in cortical slice cultures.* J Neurosci, 2004. **24**(22): p. 5216-29.
31. Baruchi, I. and E. Ben-Jacob, *Functional holography of recorded neuronal networks activity.* Neuroinformatics, 2004. **2**(3): p. 333-52.
32. Melssen, W.J. and W.J. Epping, *Detection and estimation of neural connectivity based on crosscorrelation analysis.* Biol Cybern, 1987. **57**(6): p. 403-14.
33. Le Feber, J., et al., *Conditional firing probabilities in cultured neuronal networks: a stable underlying structure in widely varying spontaneous patterns.* J. Neural Eng., 2007. ***4***: p. 54-67.
34. Romijn, H.J., F. van Huizen, and P.S. Wolters, *Towards an improved serum-free, chemically defined medium for long-term culturing of cerebral cortex tissue.* Neurosci Biobehav Rev, 1984. **8**(3): p. 301-34.
35. Wagenaar, D.A., T.B. DeMarse, and S.M. Potter. *MeaBench: A toolset for multi-electrode data acquisition and online analysis*. in *2nd international IEEE EMBS conference on neural engineering*. 2005. Arlington, VA.
36. Segev, R., et al., *Hidden neuronal correlations in cultured networks.* Phys Rev Lett, 2004. **92**(11): p. 118102.
37. Eytan, D. and S. Marom, *Dynamics and effective topology underlying synchronization in networks of cortical neurons.* J Neurosci, 2006. **26**(33): p. 8465-76.
38. Brewer, G.J., M.D. Boehler, and B.C. Wheeler. *Added astroglia promote greater synapse density and higher activity*. in *5th International Meeting on Substrate-Integrated Micro Electrode Arrays*. 2006. Reutlingen, Germany: BioPro.
39. Nam, Y., et al., *Patterning to enhance activity of cultured neuronal networks.* IEE Proc Nanobiotechnol, 2004. **151**(3): p. 109-15.
40. Watanabe, S., et al., *Development of low magnesium-induced spontaneous synchronized bursting and GABAergic modulation in cultured rat neocortical neurons.* Neurosci Lett, 1996. **210**(1): p. 41-4.
41. Zhang, L.I., et al., *A critical window for cooperation and competition among developing retinotectal synapses.* Nature, 1998. **395**(6697): p. 37-44.
42. Ramakers, G.J., et al., *Activity-dependent plasticity of inhibitory and excitatory amino acid transmitter systems in cultured rat cerebral cortex.* Int J Dev Neurosci, 1994. **12**(7): p. 611-21.
43. van Huizen, F., H.J. Romijn, and A.M. Habets, *Synaptogenesis in rat cerebral cortex cultures is affected during chronic blockade of spontaneous bioelectric activity by tetrodotoxin.* Brain Res, 1985. **351**(1): p. 67-80.

Chapter 3,

Robustness of spontaneous burst profiles in electrically stimulated neuronal cultures

Abstract

In previous studies, the effect of electrical stimulation on dissociated networks of neurons has been investigated using global measures of spontaneous activity (*e.g.* burst rate). Due to the inconclusive results of these studies we proposed that more localized measures of activity be used for analysis. To this end, we developed an analysis of network bursts through firing rate profiles. These were calculated for summed activity, yielding burst profiles (BPs), and for each electrode, yielding phase profiles (PPs). Here, we applied this analysis to quantify the effect of electrical stimulation on networks cultured on multi electrode arrays. The stimuli were either single pulses or pulse trains, delivered to 1 or 2 electrodes. Stimuli on the second electrode were delayed by 10 ms. Differences in BP and PP shape in spontaneous recordings before and after stimulation were quantified. This confirmed that the PPs were location specific and were easier to influence than BPs, probably due to interactions within sub-networks. Overall, spontaneous network bursts were extremely robust despite these stimuli, as the profiles did not change shape significantly when compared to ongoing spontaneous changes. We suggest that the large number of spikes in network bursts interfered with external induction of plasticity processes.

Stegenga J., Marani E. and Rutten W.L.C.

(submitted to: *Journal of Neural Engineering*)

3.1 Introduction

Networks of neurons cultured on multi- electrode arrays (MEAs) are a valuable tool for understanding the behaviour of neurons within a network of cells. MEAs allow measurement of action potentials and selective stimulation of up to 60 neurons. Many studies have been devoted to mapping the development of spontaneous firings neurons under normal culturing conditions [8-15]. These studies have revealed a development of the physical structure that parallels basic stages in *in-vivo* development, such as the development of synapses [18]. The spiking activity follows the structural development and, in the absence of external stimuli, the spiking activity patterns act to reinforce structural development [10].
The spiking activity in dissociated neural networks typically consists of bursts, short (50ms to 1s) periods in which most neurons spike, separated by periods (1s to 10m) of low frequency spiking activity of few neurons. The normal development of these bursts has been studied extensively [8, 10, 12, 14, 15, 19]. The general finding is that bursts have a structure that is stable over several hours, while changing over the course of days. Besides general parameters, such as inter burst intervals (IBIs), maximum firing rate or number of action potentials (APs) per burst, the spatio-temporal structure of bursts is now subject of scrutiny [7, 8, 14, 20]. We investigated the possibility of changing the spatio-temporal structure of spontaneous bursts through electrical stimulation. Through the reciprocal relationship between activity and connectivity, this amounts to the preservation of new or modified synaptic connections. The stimuli are required to drive the network away from its initial state to another (stable) state. The effort required to do that is unknown, but several forms of stimulation that modify the electrical activity of (groups of) neurons are reported on in literature. Table 3.1 shows several such studies on dissociated neuronal cultures.

From *in-vivo* experiments, a well known form of stimulation is the application of short trains of stimuli at a high frequency (e.g. 150 stimuli at 20 Hz [21]). These trains, or tetani, were used by Bliss *et al* [21] in 1973, where they resulted in a long-lasting (hours to days) increase in synaptic efficacy, known as long term potentiation (LTP). Markram *et al* did experiments using paired stimulation of two

Table 3.1. Overview of studies on changes in network activity by electrical stimulation. Tetani are bursts of stimuli (trains), usually 0.5 to 1 seconds long, with an inter-train-interval (ITI) of 1 to 20 seconds. A volley is like a train, except that a different electrode is stimulated with each pulse. Note that all studies are on cortical neurons obtained from rats, except Ruaro *et al*, who used hippocampal neurons. (*: bipolar stimulation)

study	Number of electrodes	Stimulus parameters	Evaluated Aspect	Effect
Maeda [1]	5	Tetani: 20 /s, 20x; ITI 10-15 s, 5-10x	Burst rate and burst size, both spontaneous and elicited by test stimuli.	Increase in burst rate and spikes per burst. Both spontaneous and as elicited by test stimuli.
Jimbo [2]	1 or 8	Tetani: 20 /s, 11x; ITI 5 s, 10x	Whole cell voltage clamped recordings.	Increase in EPSC currents.
Jimbo [3]	1	Tetani: 20 /s, 20x; ITI 5 s, 10x	Number and timing of spikes elicited per neuron in response to test stimuli.	Increase or decrease of EPSC's and number of elicited spikes depending on pathway.
Tateno [4]	1 or 2	Tetani: 20 /s, 10x; ITI 5 s, 20x	Reliability of APs after test stimuli, time between test stimuli and first spike.	Shortening of latency and reduction of jitter of first spike in some neurons. Increase of effect from 1 to 2 electrodes.
Shahaf [5]	2*	Single Pulse, ISI, 1-3 s, 10 max	Increase in number of spikes on 1 evaluation electrode, within a window of 40-60 ms after stimulus.	Increase in spikes elicited in window.
Wagenaar [6]	5-10	Volleys: 500 /s, 10x; IVI 5s, 17 min	Burst size, IBI, spikes in bursts per unit time.	None found
	1 or 8	Tetani: 20 /s, 20; ITI 2 s, 20x	Responses to test stimuli, 10-50 ms or 100-500 ms after test stimuli	None found
	2	Tetani: 20 /s, 20; ITI 6 s, 150 x, shift 5 ms	Responses to test stimuli, 10-50 ms after test stimuli.	Increase in number of spikes elicited by leading electrode; decrease for following electrode.
Madhavan [7]	2	Tetanus: 20 /s, 18000x (15 min), shift 10 ms	Spontaneous expression rate of burst types (BT).	Generation of new BT's, increase or decrease (elimination) in expression rate of BT's.
Ruaro [16]	15	Tetani: 250 /s, 100x ITI: 2 s, 40x	Responses to test stimuli, both per electrode and summed. In particular, number of spikes within 50 ms after stimulus are used.	Increase in setFR between 1 and 50 ms. Increase in GFR between 10 and 90 ms.
Chao [17]	2	Tetanus: 20 /s, 18000x (15 min), shift 10 ms	Center of Activity Trajectory (CAT) of evoked activity 0 – 100 ms after test stimuli on 6 electrode sites.	CAT's change significantly on some of the test electrodes.

monosynaptically connected neurons in cortical slice cultures and found long lasting (≥ 30 min) changes in synaptic efficacy, dependent on the latency between stimuli [22]. This is referred to as spike timing dependent plasticity (STDP). Both LTP and STDP require pre- and postsynaptic activity, and their mechanisms may overlap. We used tetani and paired stimuli, as well as paired tetani and single pulses. This way we had variations in both the temporal and spatial domain. Table 3.1 shows that most studies use tetani applied to one or more electrodes simultaneously; that paired tetani are only used by Wagenaar *et al* and that the application of paired single pulse stimuli is new to dissociated neuronal networks.

Responses to test stimuli have been used in most studies to demonstrate changes in the network (table 3.1). Test stimuli are preferred by many because much of the statistical fluctuations that spontaneous activity is subject to can be circumvented by averaging over many stimuli. However, there is some controversy as to whether test stimuli can have long term effects on network activity of their own [23, 24]. In this study we evaluated the network activity by means of firing-rate profiles of the activity during spontaneous bursts (analogous to smoothed firing rate histograms in evoked activity). Next to a profile of the array-wide spiking rate, a *burst profile* (BP), we also calculated the per-electrode spiking rate profile; the *phase profiles* (PPs). We have shown previously that in spontaneous recordings, both BP and PP shapes were stable over several hours. We also observed quite complex shapes of PPs, even in 1 culture during 1 hour of recording [19]. We chose therefore to measure changes in general shape (using the mean squared value of the difference between two profiles), rather than specific parameters such as rise or fall times. Specific parameters have the disadvantage of having a limited physiological range over which they can vary. This may result in the saturation of the observed parameter or (consequently) insensitivity if it should be near the extreme of the range. The general shape of PPs in particular, can alter in a multitude of ways, thus partially protecting against saturation.

Previously used measures of spontaneous activity were burst rate and number of spikes per burst [1, 6] (also table 3.1), and the expression rate of burst types [7]. Mostly, these measures were global in nature, although Van Pelt *et al* do report on electrode specific contributions, but only in a single experiment [25]. The PPs are electrode specific as well. The stability of PPs during spontaneous development [19] made them a good candidate for evaluating the effects of stimulation, as global parameters proved difficult to change in other studies [6]. We hypothesized that since a PP represents the instantaneous spiking rate of a single neuron during a

burst, changing it may require mostly local changes to the network. It may therefore require less effort to change PPs than globally defined parameters (*e.g.* burst rate, BP).

3.2 Materials and methods

Cell cultures

Cortical neurons were obtained from either newborn or E18 Wistar rats by trituration and chemical dissociation using trypsin. The cells were plated at a concentration of 10^6 cells/ml, and allowed to adhere for 2 hours. MEAs were coated in advance with polyethylene-imine (PEI) to increase adhesion. The non-adhering cells were then removed by refreshing medium, and 600 µl of R12 medium [26] was added. The resulting monolayer had a density of ~2000 cells/mm^2 three days after plating. Two-thirds of the medium was changed twice a week. The cultures were stored in an incubator at 37 ºC, at a CO_2 concentration of 5 % and near 100% humidity.

Measurement setup

We used a MC1060BC setup and MEAs from MultiChannel Systems GmbH. The MEAs had 60 Titanium-Nitride electrodes in an 8x8 square grid without the corner electrodes. The inter-electrode distance was 100 µm, and the diameter of the electrodes was 10 µm. During measurements, the MEAs were sealed using a membrane cover, as described in [27]. The temperature was controlled at 36˚C and a CO_2-concentration of 5% was maintained. Custom made LabView (National Instruments, Austin, Tx) programs were made to control data-acquisition and trigger stimuli. Cultures were left to acclimatize in the measurement setup for 20 minutes before experiments were started.

Stimulation methods

In preparation for plasticity inducing measurements, cultures were probed on all 60 electrodes at a rate of 0.2 Hz to determine which electrodes and which amplitudes to use. All stimuli were biphasic, negative phase first, current pulses with duration of 200 µs per phase. The amplitudes were in the range of 8 to 20 µA. From these probing sessions we chose the electrodes which were most effective in increasing the array-wide spiking rate (AWSR) in the first 500 ms after stimulus. Measurements consisted of multiple stimulation sessions, interleaved with 1 hour

evaluation periods in which no stimulation was applied (figure 3.1). Stimulation electrodes differed between consecutive stimulation sessions, thus minimizing interaction between sessions. On average, there were 7.2 stimulation sessions per measurement; 2.8 of which were control (CTRL, no stimulation) experiments. Controls were always 1 hour in length. An hour was long enough for a possible increase in plasticity threshold due to previous stimulation to subside [28], and for accurately estimating profiles of the spontaneous bursts (section 3.2.4). Stimulation sessions were either 30 (N=84) or 60 (N=133) minutes in length, which is longer than the critical period for consolidation of LTP in hippocampal slices [29] and also longer than the period that stimulation was applied in any of the reports in table 1. In the following, the stimulation methods are described.

Single Electrode/Single Pulse (SESP). In stimulation by SESP, a single electrode was stimulated at a rate that triggered bursts with maximum probability and spontaneous bursts in between were minimized (range: 0.1 to 1 Hz). Van Pelt *et al* reported on preliminary results where low frequency single site stimulation was applied for 1 hour. They observed an increase in burst rate and shortening of both the rise and fall times [25]. Marom *et al* applied SESP for 2 and 10 minutes and observed changes in functional connectivity which was proportional to the duration of stimulation [5]. Figure 3.2 shows typical post stimulus histograms this and the other stimulation methods.

Single Electrode/Pulse Trains (SEPT). Tetanic stimulation to a single electrode was successfully used by Jimbo *et al* to induce changes in responses to test stimuli [2, 3]. In concordance, we used trains of 10 pulses at 20 Hz with an inter train interval (ITI) of 3 to 10 seconds. ITIs were adjusted to the maximum rate at which bursts could be induced. Wagenaar *et al* used 20 trains of 20 pulses at 20 Hz, but

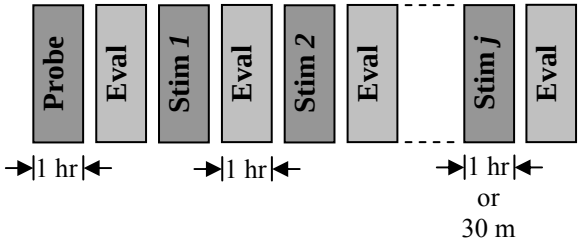

Figure 3.1. Time line of a measurement. After probing each electrode, evaluation (Eval) and stimulation sessions were alternated. Every measurement included at least one control (sham stimulation) session. Up to 10 stimulation sessions could be part of one continuous measurement.

found no significant effect in responses to test stimuli [6]. We used many more trains (360 to 1200 trains) in our experiments.

Paired Electrodes/Single Pulse (PESP). As the induction of LTP requires both presynaptic and postsynaptic activity, we paired two stimulus sites and allowed the responses to interact. *In-vivo*, it has been found that both increases and decreases in synaptic efficacies occur, depending on the time difference between the presynaptic and postsynaptic action potential [30]. In networks of dissociated neurons, PESP has not yet been used in other studies. Two electrodes that were active within bursts and regularly evoke bursts when stimulated were selected. The latency between stimuli was 10 ms while the ISI on one electrode was 2-5 s. The latency in the present study was selected in accordance with other studies, in which relations with this latency were (spontaneously) upregulated [11, 30].

Paired Electrodes/Pulse Train (PEPT). In stimulation by PEPT, tetanic stimulation was applied to two electrodes with a shift of 10 ms. This type of stimulation has

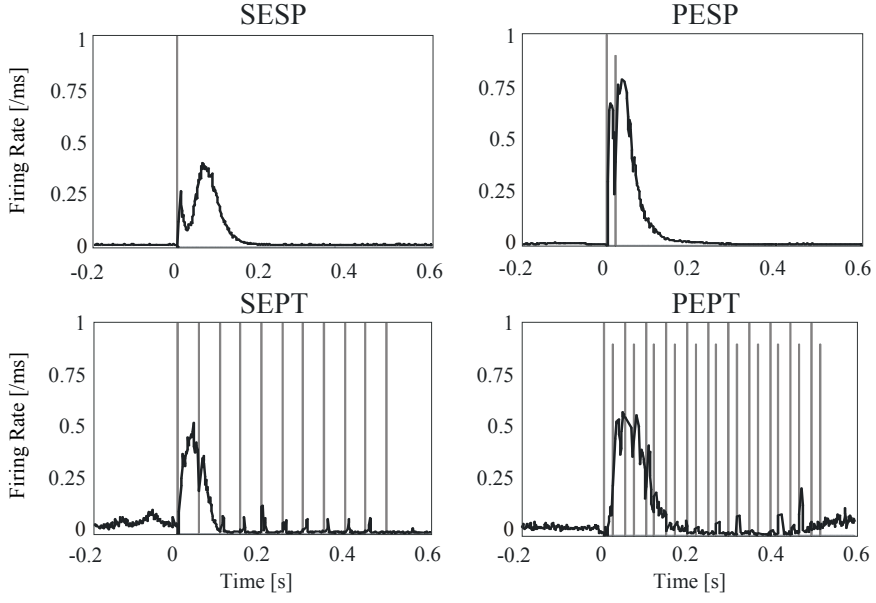

Figure 3.2. Peristimulus histograms. In each panel, the summed firing rate determined in 1 ms bins and averaged over all stimuli in one example experiment is shown. The SESP stimulation method shows most clearly an early response between 0 and 10 ms and a late response between 20 and 200 ms. The early response can contain spikes that are directly caused by stimulation and do not involve synaptic transmissions, the late response is characterized best as a triggered network burst. Only a single burst was triggered by each of the algorithms, but direct responses appear to be present throughout the trains.

been used by Wagenaar *et al* [6]. They found that responses (defined as the number of spikes between 10 and 50 ms) to test stimuli on the leading electrode were enhanced, while responses on the following electrode decreased. However, these changes were only observed in a medium with high concentration of Mg^{2+} (1.8 mM, enough to suppress spontaneous bursts). We used a prolonged stimulation sequence of 60 minutes instead of 3 minutes as Wagenaar *et al* used, in an attempt to compensate for the relatively low Mg^{2+} concentration of 0.68 mM in our medium.

Data processing

Spike detection. Online processing consisted of detecting threshold crossings and validating these by the algorithm described by [31]. The threshold level was set at 5.5 times the estimated RMS noise level of the electrode, which was continuously monitored.

Network Burst detection. Network bursts were detected whenever there were more than $2N$ spikes in a 100 ms bin, where N is the number of electrodes showing regular activity. An electrode was considered active if its average (calculated over at least 1 hour) firing rate exceeded 0.1 Hz. The calculation of active electrodes was for determining a reasonable threshold for network bursts only; all electrodes were considered in further analysis. Next, a burst profile was calculated in order to estimate the time at which the peak array-wide spiking rate (AWSR; activity summed over all electrodes) occurred (t_c). Once found, burst and phase profiles were calculated from t_c-LB ms to t_c+UB ms. The influence of both bin size and threshold were tested, but led to comparable results over a wide range. LB and UB were adjusted to include the whole burst by visual inspection. Minimal values were 100 ms and 300 ms respectively. Figure 3.3 clarifies the procedure for burst detection.

Calculation of burst profiles. A burst profile (BP) is an estimation of the instantaneous AWSR. To this end, all the spike-occurrences in a burst were taken together and convolved with a Gaussian, the width (standard deviation, SD) of which was adjusted such that a smooth graph near the maximum AWSR was obtained. A smooth graph was important for aligning (and comparing) bursts. The

SDs used for BPs ranged from 5 to 15 ms, which was small compared to the length of bursts. Examples of BPs can be seen in figure 3.6.

Calculation of phase profiles. Phase profiles (PPs) are estimations of the instantaneous firing rate of a single electrode and were calculated similarly to BPs. The standard deviation used for smoothing was set to 2 times the SD used for calculating BPs, or to 20 ms whichever was smaller. This has been done to partly compensate for the limited number of spikes per electrode. Examples of PPs can be seen in figure 3.7.

Averages of phase profiles. Whereas bursts generally encompassed enough spikes to make a smooth and reliable BP with a SD <10 ms, this was not the case for PPs. As done previously, the PPs were averaged in bins of 5 minutes by aligning burst to the main peak in the BP [19]. The averaging of profiles resulted in less noisy PPs, while retaining timing information which would be obscured by the use of large SDs during PP calculation. The criteria that were set for burst detection

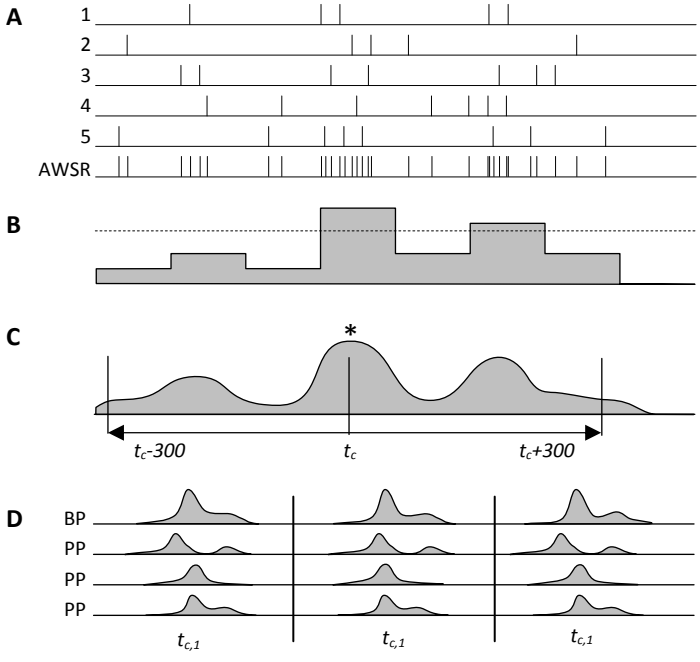

Figure 3.3. Calculation of burst profiles. (A) action potentials across all electrodes are added to make the AWSR. (B) The AWSR is binned and compared with a threshold. (C) Whenever the number of spikes per bin crosses a threshold, a profile is calculated by convoluting the AWSR spike train with a Gaussian (* denotes the burst peak). (D) The dataset is a series of burst profiles (BP) and phase profiles (PP).

ensured that all bursts could be considered network bursts, with contributions of at least half of the active electrodes and peak firing rates above 0.2 spikes/ms. The latter criterion was added to ensure a reasonable alignment of profiles. A detailed check for the presence of multiple burst types was not performed. If several types were present, the averaged profiles would be sensitive to the rates at which burst types occurred. We treated the averaged profiles in the same way as individual profiles.

Comparing profiles. We calculated the *within group* and the *between group* distances for both BPs and PPs, where the 2 groups refer to before or after stimulation. The distance measure we used was the average root mean square (RMS) of the difference between profiles. Let i denote the i-th burst, I the number of bursts and pp^b a phaseprofile, all in the before group, and mutatis mutandis for the after group. For a profile in the before group, the within (BB_i) and between (BA_i) distance measures are defined as:

$$BB_i = \frac{1}{I}\sum_{n=1}^{I} RMS\left(pp_i^b - pp_n^b\right) \tag{3.1}$$

$$BA_i = \frac{1}{J}\sum_{n=1}^{J} RMS\left(pp_i^b - pp_n^a\right) \tag{3.2}$$

Similarly for profiles in the after group we find:

$$AA_j = \frac{1}{J}\sum_{n=1}^{J} RMS\left(pp_j^a - pp_n^a\right) \tag{3.3}$$

$$AB_j = \frac{1}{I}\sum_{n=1}^{I} RMS\left(pp_j^a - pp_n^b\right) \tag{3.4}$$

The between group distances BA and AB were taken together and compared with the within group distances BB and AA which were also taken together. We tested whether the mean of the between group distances significantly exceeded the mean of the within group distances using single sided student-t tests. Since the total time span in the within groups is 1 hr, while it is 3 hrs for between group distances, a significantly changed profile can be due to either stimulation or normal development of connectivity. We therefore compared only sets of data, as we could not make inferences from individual experiments. In particular, we compared the ratio of significantly changed profiles for each of the 4 stimulation methods to the ratio of significantly changed profiles in the set of control measurements.

$$\text{decision ratio} = \frac{N(\text{significantly changed phase profiles})}{N(\text{active electrodes})} \tag{3.5}$$

On average, there were 20 active electrodes, yielding 20 *t*-tests. Therefore, a Bonferoni corrected significance level of α=0.0025 was used to protect against type 2 errors. The magnitudes of changes were also quantified. This required normalization of the distances to the RMS of the average profile to account for differences in firing rate (between electrodes, as well as cultures). The normalization is either to the before or after group, such that *AB* is normalized in the same way as *BB* and *BA* the same as *AA*:

$$nBB_i = \frac{BB_i}{RMS\left(\frac{1}{I}\sum_{n=1}^{I} pp_n^b\right)}, \tag{3.6}$$

$$nAA_i = \frac{AA_i}{RMS\left(\frac{1}{J}\sum_{n=1}^{J} pp_n^a\right)} \tag{3.7}$$

The average effect in one of the 4 stimulation methods could then be compared to the average effect found in the control experiments. For visualization, we scaled the normalized group distances such that the average within group distance was 1 (figure 3.7). As a check, we started out by comparing several global (derived from AWSR), shape specific parameters. These were the rise time, fall time, peak AWSR and burst size (figure 3.4).

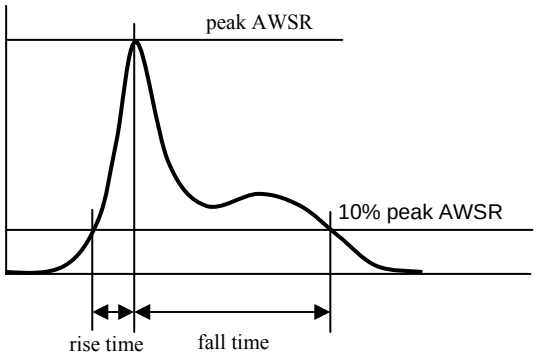

Figure 3.4. Example of a BP and several of the global parameters defined on it. The area of the profile gives the number of spikes within the burst.

Results

A total of 211 experiments were done on 14 cultures, with ages ranging from 7 to 75 DIV (table 3.2). Some examples of the responses elicited by the various stimulation methods were already shown in figure 3.2. Triggering bursts by stimuli was considered important, but the evoked bursts were not used for further analysis, as these are compromised by stimulation artefacts in 3 of the stimulation methods.

Table 3.2. Overview of experiments. Experiments in which there was insufficient response to stimulus, or in which the number of spikes per burst was very small, were excluded.

	$N_{Experiments}$	$N_{Cultures}$	DIV
CTRL	80	14	7 - 75
SESP	28	9	7 - 72
PESP	20	8	9 - 75
SEPT	38	7	9 - 72
PEPT	45	5	20-74

Our analysis started with several well-used global, shape specific, parameters (figures 3.3 and 3.5). For each stimulation method, these were tested for increase or decrease before and after stimulation by two tailed *t*-tests (α=0.05). A significant change was not found in any of the stimulation methods. A division in age groups, *i.e.* developing cultures (up to 21 DIV) and mature cultures (21 DIV and older), did

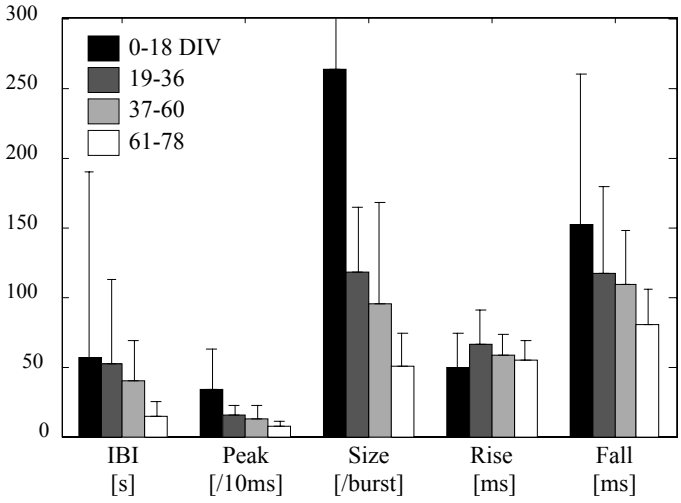

Figure 3.5. Age dependency of specific parameters of burst profiles. While the burst rate increased with age, the number of spikes and the peak intensity (shown as spikes per 10 ms) decreased. The rise times did not change much, but the fall times indicate that bursts became shorter with age. Bars show mean + standard error of mean.

not uncover any differences in plasticity (results not shown). Figure 3.5 shows the development of the specific parameters as a function of age. These are comparable to development in unstimulated cultures. This confirmed to us that the use of global (and specific) parameters may be limited.

A BP can be considered a global parameter, but was analysed in a non-specific manner. Thus, changes in peak firing rate, size and rise and fall times would all show in the analysis. A deviating example of an experiment in which both the BP and a number of PPs significantly changed is shown in figures 3.6 and 3.7. The BP shows a well defined and large peak, and the overall shape is clearly non-Gaussian. A peak of 1 (spikes per ms) can be achieved by ~25 action potentials in close succession, using a standard deviation of 10 ms. The burst profile changed such that its peak became more localized and its tail became prolonged. The normalized distances for the within-group (*AA* and *BB*) and between-group (*AB* and *BA*) show a clear increase.
The average PPs of the same experiment are shown in figure 3.7. It is easy to see noticeable changes, most of which towards a broadening of activity (e.g. 12, 31 and 87). Most changes occur after the burst centre, in the falling phase of the burst. The qualitative shape features of the phase profiles is preserved in most cases. Modulation of the total activity, i.e. scaling of the phase profile, regularly occurs on the stimulated electrode and here also on electrodes 62 and 68. Since so many PPs were changed, and these changes were correlated, the BP was also changed. However, experiments like the one shown in figures 3.6 and 3.7 were exceptional; there were many more cases in which only a few PPs were altered, and the BP

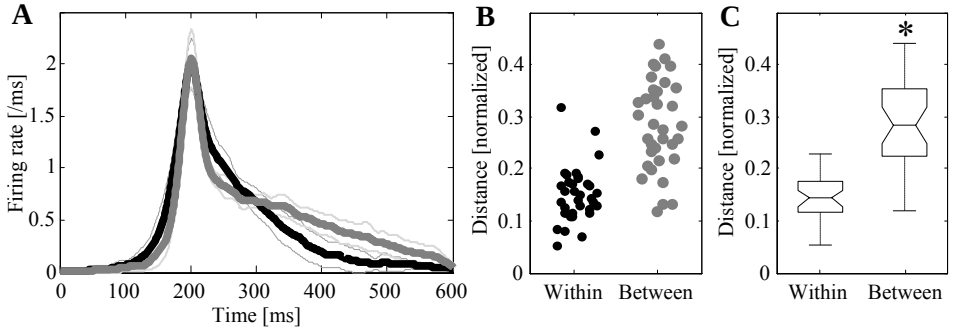

Figure 3.6. A) Average burst profiles before (black) and after stimulation. Thin lines show average plus or minus standard deviation. B) Normalized distances within group (*BB* and *AA*) and between groups (*AB* and *BA*). For burst profiles, an average within group distance of 0.1 to 0.2, corresponding to statistical fluctuation, is usually observed. C) Box plots of the distances in B. A single sided *t*-test showed a significant change ($p<0.0025$), indicating that the shape of the profile had changed.

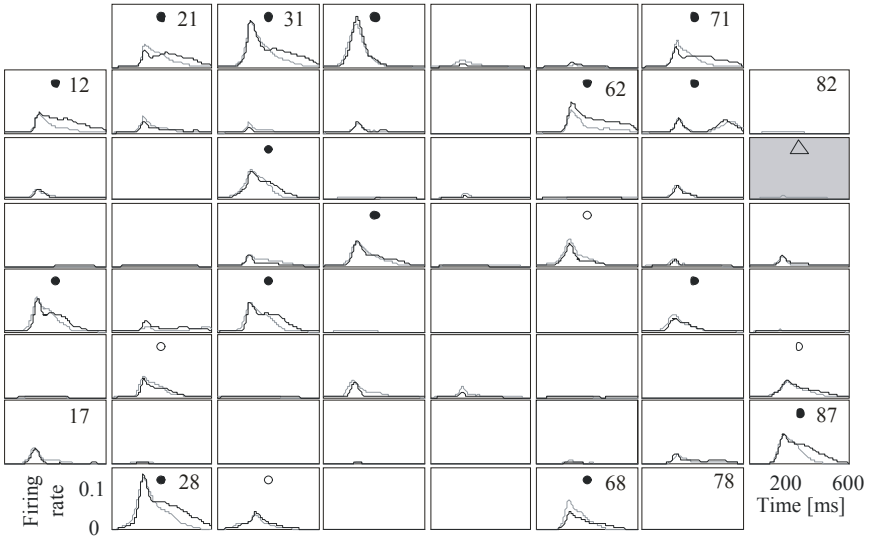

Figure 3.7. Changes in the phase profiles of the same experiment as in figure 1. Dots mark the electrodes that were tested (selected by contribution). Filled dots mark PPs that were significantly altered. For clarity, only the average PPs are shown. Stimulation was on the shaded electrode. Black lines represent PPs before stimulation and red after stimulation.

remained essentially the same.

Decision ratios

Stimulation at a single electrode can potentially affect firing patterns of neurons throughout the culture, as is exemplified by the profiles in figures 3.6 and 3.7, but see also [7]. Table 3 shows the decision ratios that were observed, grouped according to the various stimulation methods. An appreciable number of BP and PP changes were observed during control, indicating that normal development of bursts should be taken into account in this kind of experiment. SESP stimulation showed a low number of BP changes, while its number of PP changes was close that found in CTRL. PEPT stimulation however showed low numbers of BP and PP changes. The SEPT and PESP stimulation methods show an increased decision ratio on BPs, but only PESP stimulation also showed an increased decision ratio of PPs. Although the percentages are nearly the same, the number of phase profiles that were changed was much larger. In total, we found 66 BP changes out of 211 experiments and 1301 PP changes out of 3867 active electrodes.

Electrodes that were directly activated by stimulation may be more affected than others. Table 3.3 shows an apparently increased decision ratio for PPs on electrodes that were used for stimulation, even though the standard deviations for

these data are large. In total, we found 45 changed profiles on 123 stimulated electrodes. This translates into 36.5 ± 4% changed profiles on stimulated electrodes compared to 32.0 ± 0.1% changed PPs on non-stimulated electrodes. Again, a division in age groups did not alter the results. This may partly stem from the increases in standard deviations, as the number of experiments in a group goes down.

Table 3.3. Decision ratios (percentage ± standard deviation) for burst profiles (BP) and phase profiles (PP). Phase profiles were further subdivided in those that were used for stimulation and those that were not. *: significantly changed when compared to control measurements (two-sided t-test, $p<0.01$). #: significantly changed when compared to non stimulated profiles in same group.

	BP	**PP**		
		all	*Stim*	*Non-stim*
CTRL	30 ± 5	35 ± 1	-	-
SESP	21 ± 8*	35 ± 2	45 ± 15#	35 ± 2
SEPT	40 ± 11*	30 ± 2*	42 ± 14#	30 ± 2
PESP	46 ± 8*	44 ± 2*	46 ± 6	44 ± 2
PEPT	20 ± 6*	19 ± 1*	19 ± 6	19 ± 2

Distances

A clearer picture of induced changes may emerge from data on the (normalized) distance measures, summarized in figure 3.8. Distances in this figure were normalized to the RMS of the profile (either BP or PP) and then scaled such that the mean within group distance was unity. For the BPs, the distances show much the same as the decision ratios, with only PESP having a significantly ($p<0.001$) larger effect than normal development (CTRL). Of the PPs on non-stimulated electrodes, the effects of the single pulse stimulation methods were significantly above normal development, while those using pulse train stimuli were lower than CTRL. When compared to electrodes in the same stimulation method, the effect on stimulated electrodes increased for SEPT, PESP and PEPT stimulation. Perhaps not surprisingly, SESP did not show a difference between stimulated and non-stimulated electrodes. It appears that either pulse trains or pulse pairs were required for this, tentatively suggesting a change in the functional relationship between the two stimulated electrodes. Figure 8c shows an alternative division of phase profiles into those with a large contribution to a burst (>10%) and those with a small contribution. In all cases the large profiles were more plastic than the small profiles.

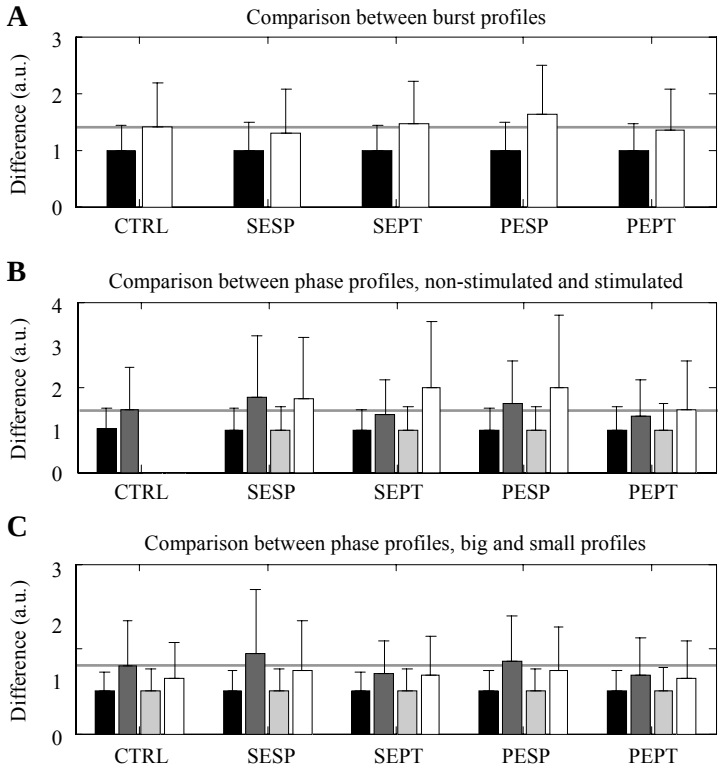

Figure 3.8. A) Differences in shape between burst profiles before (black) and after applying one of the stimulation paradigms. Differences were normalized to the before group. Bars show means + standard deviations. B) Differences in shape between phase profiles before and after applying one of the stimulation paradigms. Phase profiles were split into non-stimulated phase profiles (2 leading bars of each group) and phase profiles of electrodes used for stimulation. C) Same as B, but split into profiles with a large amount of spikes and those with a small amount of spikes.

3.4 Discussion

None of the stimulation methods had a measurable effect on one of the specific burst statistics (peak firing rate, rise and fall times). However, a ceiling effect may have been present in any one of these statistics, as the stimulation sessions were only separated by one hour. Such an effect did not appear to be prohibitive when considering general shapes of BPs and PPs, as distances increased throughout measurements. Of the 4 stimulation methods, PESP was most successful, even though the differences with normal development were small. Surprisingly, single pulse stimulation resulted in an increase in effect on non-stimulated PPs, while pulse train stimulation resulted in a decrease. As expected, the effect on PPs of stimulated electrodes was larger when two electrodes were stimulated. Large

profiles turned out to be more plastic than small profiles, which may stem from the fact that small profiles usually have a Gauassian-like appearance. BPs or PPs with a non-Gaussian appearance have more distinctive features, and may be easier to alter. All the changes that we observed were however small when compared to results reported by literature (table 3.1). We next provide several possible mechanisms to explain this apparent discrepancy and give our outlook on the applicability of the profile method in this kind of experiment.

Stabilizing effect of spontaneous activity

Lack of interaction with the outside world may be the cause that bursts, while transitory *in vivo*, persist *in vitro*. Bursting starts at about 7 DIV, and thus bursts have ample time to construct very strong pathways through activity-dependent outgrowth. Our stimulation methods triggered bursts, but the spatio-temporal structure of the triggered bursts is determined largely by the underlying connectivity. Successive stimuli (in one train) did evoke direct reactions, but were not able to alter the spatio-temporal structure of the triggered burst, probably due to the massive number of inputs received from other, not directly stimulated, neurons. Thus, it may be that the number and timing of spikes within bursts override any changes made by stimuli. This would implicate that the triggering of bursts by itself will not alter the activity patterns faster than spontaneous development, even when triggering bursts at a rate of up to 6 times the spontaneous rate, which we sometimes achieved.

Mg^{2+} concentration and NMDA receptor activity

Our findings apparently contradict the findings of Maeda *et al*, who found that both tetanic or single stimuli were effective in increasing network burst size and rate, as long as the stimuli evoked bursts [1]. However, in their study as well as in the studies of Jimbo *et al* and Tateno *et al*, the Mg^{2+} concentration, $[Mg^{2+}]$, was adjusted such that spontaneous bursting was either decreased or abolished (table 5). Maeda *et al* also report that without the elevated $[Mg^{2+}]$, their algorithm did not induce any changes in network activity. Wagenaar *et al* similarly found a significant change only when bursts were suppressed by an elevated Mg^{2+} concentration [6]. We note that in comparison with other plasticity studies, our $[Mg^{2+}]$ is rather low (table 4). The $[Mg^{2+}]$ is important for the proper working of

the NMDA-receptor which in turn plays a pivotal role in both LTP and LTD. It is known that in Mg^{2+}-free medium, the LTP mechanism is saturated already by low frequency spiking. In contrast, at physiological concentrations of Mg^{2+} (1 mM), the NMDA receptor controlling LTP is only unblocked by the applied tetani [32]. However, the latter results were obtained either *in-vivo* or in slice cultures which do not show bursting like in dissociated cultures. We have observed that partially blocking NMDA receptors resulted in a decrease in bursting intensity (peak firing rates, data not shown). Thus, it is likely that NMDA receptors are active during spontaneous bursts, disrupting any induced changes. Colina *et al* found that activation of NMDA receptors prior to LTP induction by theta burst stimulation, increased the threshold for inducing LTP [28]. Therefore, bursting cultures may have a higher threshold for plasticity. The minimal number of spontaneous bursts between stimuli ensured that NMDA channels were predominantly activated in response to stimuli. Also, the duration of stimulation sessions (60m) was longer than the period needed for consolidation of LTP [29].

Culturing density

Apart from an elevated [Mg^{2+}], most groups use cultures with lower cell densities than ours. Low-density cultures generally exhibit a lower burst rate and a lower number of spikes per burst, presumably due to fewer synaptic connections [15]. This implies that pathways in sparse cultures receive less reinforcement from bursts and/or have less competition from other pathways. External stimulation in sparse cultures may thus be more influential in sparse cultures than in dense cultures.

Stimulation methods

Stimuli triggered bursts with high probability. This suggests that there may already have been strong connections between stimulation electrodes and the rest of the network, and that further potentiation of these connections would either be impossible or undetectable. However, not only the directly stimulated pathways are subject to change, but also pathways that were active during evoked bursts, as shown in [5]. In addition, only Maeda *et al* explicitly state that they used electrodes for stimulation which had a ‘moderate local response’, while others report that triggering bursts was required for changes to occur [1, 5, 25]. We did not observe

Table 3.4. Details of experimental settings of several studies (see also table 1). This study used relatively dense cultures and low Mg^{2+} concentration. The possible influences of differences in experimental settings, all toward a lower intensity of bursting, are highlighted in the last column.

study	**$[Mg^{2+}]$ (mM)**	**Density ($/mm^2$)**	**Electrodes (um)**	**DIV**	**˚C**	**Burst modification**
Maeda [1]	0-2 (tuned)	10000 (clusters)	100/1000	7-42	20	Adjusted Mg^{2+}
Jimbo [2]	1-10 (tuned)	-	50/250 30/150	7-35	-	Adjusted Mg^{2+}
Jimbo [3]	1	Estimated from picture: 900	30/180 Divided by 500	30-50	-	Adjusted Mg^{2+} /Low density
Tateno [4]	1	Estimated from picture: 800	30/180 Divided by 500	40-50	20	Adjusted Mg^{2+} /Low density
Wagenaar [6]	0.8	2500	30/200	10-32	35	Adjusted Mg^{2+}
Shahaf [5]	-	Estimated from picture: 300	30/200	14-21	37	Low density
Madhavan [7]	-	3000	30/200	14-28	35	Suppression by tetanus itself
Ruaro [16]	0.8	8000	30/500	21-100	37	None
Chao [17]	-	7000	30/200	28-92	37	Suppression by tetanus itself
This study	0.68	2000	10/100 30/200	7-77	36	

graded responses, as bursts were evoked in an all or nothing fashion. Of the three studies in tables 3.1 and 3.4 that use similar $[Mg^{2+}]$ and culture densities equal to (or larger than) than ours, the stimulation methods were however quite different from ours. Ruaro *et al* stimulated 15 electrodes in parallel at a very high frequency, which induced many spikes and possibly activated STDP-mechanisms even before a burst was evoked. Chao *et al* and Madhavan *et al* used a single train of 15 minutes applied to 2 electrodes at a frequency of 20 Hz (yielding an aggregate frequency of 40 Hz). Applying stimulation continuously as apposed to short trains has been shown to reduce burst rate to as little as 5% of spontaneous levels [33]. Parallel, continuous inputs may thus be essential in overcoming the stabilizing influence of spontaneous activity.

Applicability of the profile method

We found many PP changes in our experiments, which can be seen as a confirmation that the analysis is sensitive to changes in the network. Furthermore, we found that PP changes occurred frequently in the absence of BP changes, thus supporting our initial assumption about locality of PPs. Even without the confirmation of a significant change in PPs, the analysis appears valid. However, the stability of profiles that was reported earlier was not found in control measurements in this study [14, 19]. The origin of this discrepancy may lie in slight differences in measurement setup. For instance, we switched to semi-permeable membranes for sealing cultures since our last study. A drawback of the method is that accurate comparison depends on the alignment of BPs. In this study we used the time of maximum firing frequency for this. For less intense bursting this may become problematic and other methods for alignment could be used. One could for example use the maximum in a cross correlation for alignment. Finally, all bursts, whether evoked or spontaneous, appear to follow the pathways that were created during development. Evoked burst would then merely serve to confirm the established connectivity rather than change it.

3.5 References

1. Maeda, E., Y. Kuroda, H.P. Robinson, and A. Kawana, *Modification of parallel activity elicited by propagating bursts in developing networks of rat cortical neurones.* Eur J Neurosci, 1998. **10**(2): p. 488-96.
2. Jimbo, Y., H.P. Robinson, and A. Kawana, *Strengthening of synchronized activity by tetanic stimulation in cortical cultures: application of planar electrode arrays.* IEEE Trans Biomed Eng, 1998. **45**(11): p. 1297-304.
3. Jimbo, Y., T. Tateno, and H.P.C. Robinson, *Simultaneous induction of pathway specific potetiation and depression in networks of cortical neurons.* Biophys J, 1999. **76**(2): p. 670-678.
4. Tateno, T. and Y. Jimbo, *Activity-dependent enhancement in the reliability of correlated spike timings in cultured cortical neurons.* Biol Cybern, 1999. **80**(1): p. 45-55.
5. Shahaf, G. and S. Marom, *Learning in networks of cortical neurons.* J Neurosci, 2001. **21**(22): p. 8782-8.
6. Wagenaar, D.A., J. Pine, and S.M. Potter, *Searching for plasticity in dissociated cortical cultures on multi-electrode arrays.* Journal of negative results in biomedicine, 2006. **5**(16).
7. Madhavan, R., Z.C. Chao, and S.M. Potter, *Plasticity of recurring spatiotemporal activity patterns in cortical networks.* Phys Biol, 2007. **4**(3): p. 181-93.
8. Eytan, D. and S. Marom, *Dynamics and effective topology underlying synchronization in networks of cortical neurons.* J Neurosci, 2006. **26**(33): p. 8465-76.
9. Jimbo, Y., A. Kawana, P. Parodi, and V. Torre, *The dynamics of a neuronal culture of dissociated cortical neurons of neonatal rats.* Biol Cybern, 2000. **83**(1): p. 1-20.
10. Kamioka, H., E. Maeda, Y. Jimbo, H.P. Robinson, and A. Kawana, *Spontaneous periodic synchronized bursting during formation of mature patterns of connections in cortical cultures.* Neurosci Lett, 1996. **206**(2-3): p. 109-12.

11. Le Feber, J., W.L.C. Rutten, J. Stegenga, P.S. Wolters, G.J.A. Ramakers, and J. van Pelt, *Conditional firing probabilities in cultured neuronal networks: a stable underlying structure in widely varying spontaneous patterns.* J. Neural Eng., 2007. ***4***: p. 54-67.
12. Maeda, E., H.P. Robinson, and A. Kawana, *The mechanisms of generation and propagation of synchronized bursting in developing networks of cortical neurons.* J Neurosci, 1995. **15**(10): p. 6834-45.
13. Segev, R., I. Baruchi, E. Hulata, and E. Ben-Jacob, *Hidden neuronal correlations in cultured networks.* Phys Rev Lett, 2004. **92**(11): p. 118102.
14. van Pelt, J., P.S. Wolters, M.A. Corner, W.L. Rutten, and G.J. Ramakers, *Long-term characterization of firing dynamics of spontaneous bursts in cultured neural networks.* IEEE Trans Biomed Eng, 2004. **51**(11): p. 2051-62.
15. Wagenaar, D.A., J. Pine, and S.M. Potter, *An extremely rich repertoire of bursting patterns during the development of cortical cultures.* BMC Neurosci, 2006. **7**: p. 11.
16. Ruaro, M.E., P. Bonifazi, and V. Torre, *Toward the neurocomputer: image processing and pattern recognition with neuronal cultures.* IEEE Trans Biomed Eng, 2005. **52**(3): p. 371-83.
17. Chao, Z.C., D.J. Bakkum, and S.M. Potter, *Region-specific network plasticity in simulated and living cortical networks: comparison of the center of activity trajectory (CAT) with other statistics.* J Neural Eng, 2007. **4**(3): p. 294-308.
18. Ichikawa, M., K. Muramoto, K. Kobayashi, M. Kawahara, and Y. Kuroda, *Formation and maturation of synapses in primary cultures of rat cerebral cortical cells: an electron microscopic study.* Neurosci Res, 1993. **16**(2): p. 95-103.
19. Stegenga, J., J. Le Feber, E. Marani, and W.C. Rutten, *Analysis of cultured neuronal networks using intraburst firing characteristics.* IEEE Trans Biomed Eng, 2008. **55**(4): p. 1382-90.
20. Beggs, J.M. and D. Plenz, *Neuronal avalanches are diverse and precise activity patterns that are stable for many hours in cortical slice cultures.* J Neurosci, 2004. **24**(22): p. 5216-29.
21. Bliss, T.V. and T. Lomo, *Long-lasting potentiation of synaptic transmission in the dentate area of the anaesthetized rabbit following stimulation of the perforant path.* J Physiol, 1973. **232**(2): p. 331-56.
22. Markram, H., J. Lubke, M. Frotscher, and B. Sakmann, *Regulation of synaptic efficacy by coincidence of postsynaptic APs and EPSPs.* Science, 1997. **275**(5297): p. 213-5.
23. Madhavan, R., Z.C. Chao, and S.M. Potter, *Spontaneous bursts are better indicators of tetanus-induced plasticity than responses to probe stimuli*, in *2nd international IEEE EMBS conference on neural engineering*. 2005: Arlington, VA.
24. Vajda, I., J. van Pelt, P. Wolters, M. Chiappalone, S. Martinoia, E. van Someren, and A. van Ooyen, *Low-frequency stimulation induces stable transitions in stereotypical activity in cortical networks.* Biophys J, 2008. **94**(12): p. 5028-39.
25. van Pelt, J., I. Vajda, P.S. Wolters, M.A. Corner, and G.J. Ramakers, *Dynamics and plasticity in developing neuronal networks in vitro.* Prog Brain Res, 2005. **147**: p. 173-88.
26. Romijn, H.J., F. van Huizen, and P.S. Wolters, *Towards an improved serum-free, chemically defined medium for long-term culturing of cerebral cortex tissue.* Neurosci Biobehav Rev, 1984. **8**(3): p. 301-34.
27. Potter, S.M. and T.B. DeMarse, *A new approach to neural cell culture for long-term studies.* J Neurosci Methods, 2001. **110**(1-2): p. 17-24.
28. Huang, Y.Y., A. Colino, D.K. Selig, and R.C. Malenka, *The influence of prior synaptic activity on the induction of long-term potentiation.* Science, 1992. **255**(5045): p. 730-3.
29. Colino, A., Y.Y. Huang, and R.C. Malenka, *Characterization of the integration time for the stabilization of long-term potentiation in area CA1 of the hippocampus.* J Neurosci, 1992. **12**(1): p. 180-7.
30. Zhang, L.I., H.W. Tao, C.E. Holt, W.A. Harris, and M. Poo, *A critical window for cooperation and competition among developing retinotectal synapses.* Nature, 1998. **395**(6697): p. 37-44.
31. Wagenaar, D.A., T.B. DeMarse, and S.M. Potter. *MeaBench: A toolset for multi-electrode data acquisition and online analysis*. in *2nd international IEEE EMBS conference on neural engineering*. 2005. Arlington, VA.
32. Coan, E.J., A.J. Irving, and G.L. Collingridge, *Low-frequency activation of the NMDA receptor system can prevent the induction of LTP.* Neurosci Lett, 1989. **105**(1-2): p. 205-10.
33. Wagenaar, D.A., R. Madhavan, J. Pine, and S.M. Potter, *Controlling bursting in cortical cultures with closed-loop multi-electrode stimulation.* J Neurosci, 2005. **25**(3): p. 680-8.

Chapter 4,

Theta stimulation in cultured neocortical networks

Abstract

The most striking and persistent activity pattern in cultures of dissociated neurons is network-wide bursting. Bursts have been shown to interfere with controlled activation of plasticity mechanisms and can be suppressed by applying stimuli at a sufficient rate. We used random background stimulation (RBS) to suppress bursts and modulated RBS with a frequency in theta range (4-12 Hz) to enhance the effect of tetani on network activity. From animal *in-vivo* research it is known that in hippocampus, theta rhythms in local EEG occur during learning tasks, *e.g.* exploratory behaviour. In addition, long term potentiation or long term depression can be induced in hippocampus by single short tetani, depending on the phase of theta at which the tetani were applied. We similarly applied short tetani (4 pulses, 200 Hz) to one electrode at the peak or trough of RBS. We compared results with two controls 1) 1 pulse applied at the zero-crossing of RBS, and 2) no RBS and no pulses. We show that tetani applied at the peak of RBS result in potentiation of post-stimulus histograms (PSTHs) compared to both controls. Conversely, tetani at the trough and single pulses at the zero-crossing of RBS (control 2) resulted in similar depression of PSTH when compared to no stimulation controls.
In addition to PSTHs, we analyzed (electrode specific) firing rate profiles within spontaneous bursts before and after theta stimulation. The results of profile analysis are in agreement to PSTH-analysis, with the largest changes found for tetani applied at the peak while tetani at the trough or pulses at the zero-crossing show no significant differences from no stimulation controls. This study suggests that plasticity mechanisms in culture may be differentially accessible by tetani through enforcing an oscillatory state.

Stegenga J., le Feber J., Marani E. and Rutten W.L.C.

(submitted to: *European Journal of Neuroscience*)

4.1 Introduction

Multi-electrode arrays (MEAs) offer a means to investigate memory and learning on the small-network scale. Cultures of dissociated neurons are widely used to create a monolayer of cells on the MEA surface. Such monolayers of neurons are easily accessible for recording and stimulation, and may facilitate learning and memory studies. However, it has been very hard to improve on earlier results on neural plasticity that were obtained either *in vivo* or on acute slice preparations *in vitro*, using cultures of dissociated neurons. The lack of a known network structure and a large variety in culturing methods increase the difficulty of achieving consistent results. There has been much debate on how bursts of action potentials, which are characteristic for networks of dissociated neurons, should be interpreted and/or handled [1-3]. Several views as to the origin of bursts exist. Most notably, bursts *in vitro* resemble the activity observed during early development of the nervous system [4-7]. Persistence of bursts throughout the lifetime of cultures may thus indicate a state of arrested development [8]. The slow progression of burst shapes during spontaneous development [1, 2, 9], which mimics the changes in physiological network structure, supports this view. Bursts *in vivo* usually subside as sensory neurons become active and the brain receives input. Thus, lack of afferent external input to cultures is another reason why bursts may be observed in cultures. The fact that bursts can be suppressed by random background stimulation (RBS) supports this second view [3]. A number of publications by the group headed by S. M. Potter indicate that plasticity mechanisms may be more accessible to strong stimuli when bursts are suppressed by RBS [10-12]. Given the density of action potential firings and the fact that spontaneous bursts readily activate NMDA receptors during bursts [8, 13], it is reasonable that at least part of the available plasticity mechanisms are regularly activated by bursts in a manner that is not under the experimenters control. In their studies, stimulus locations were fully randomized while inter-stimulus intervals (ISI) were fixed (*e.g.* 50 ms) [3, 12]. Even though this form of RBS may be useful for suppressing bursting activity, activity *in-vivo* (as measured by EEG) has an apparently random component with several more prominent rhythms. We emulated more biologically plausible activity patterns in culture; using stochastic RBS with approximately exponentially distributed inter-stimulus intervals. Moreover, since oscillations in the EEG are associated with certain computational tasks [15-17], we used semi-stochastic RBS

that has a certain rhythmic component. Doing so, may reveal new information processing properties of *in-vitro* networks.

Plasticity mechanisms are extensively researched in the hippocampus, which is known to be involved in storage of long term memories [18-22]. Of particular interest is the role of oscillation of large scale dendritic currents (measured by local EEG) in the theta band (4-12 Hz) [17, 20]. Theta oscillations are associated with behaviour that is related to learning (sniffing, exploring, rearing and attending to stimuli). It has also been shown that synaptic plasticity is greatly enhanced when theta oscillations are present, with a single stimulation burst resulting in significant changes in excitatory post-synaptic potentials (EPSPs). More specifically, applying a train of stimuli (4 pulses, 200 Hz) at 90˚ phase of the local theta oscillation resulted in long term potentiation (LTP) while the same train of stimuli applied at -90˚ resulted in long term depression (LTD) of EPSPs [20, 21]. Such trains of stimuli resemble the afferent signals generated *in-vivo* by pyramidal cells (e.g. by place-field specific pyramidal cells during exploration) [17]. Theta oscillations can be induced in the hippocampus through cholinergic activation, but is also supported by inputs from outside the hippocampus (*e.g.* the septum). The mechanism by which theta oscillations appear to control LTP and LTD however is not fully understood. A possible mechanism that has been put forward is a general oscillation of inhibitory neurons which modulates the excitability of post synaptic neurons and consequently modulate the direction of change through spike-timing dependent plasticity (STDP; Hebb's rule) [17].

Applying stochastic RBS modulated by a theta rhythm may serve two purposes. First, RBS suppresses bursts which would otherwise activate plasticity mechanisms. Second, theta oscillations in RBS may further modulate excitability in the culture, such that phase-locked trains of stimuli have effects that are phase specific.

4.2 Materials & Methods

Culturing

Cells were obtained from the cortices of newborn Wistar rats. Cells were dissociated mechanically by trituration and chemically by treatment with trypsin. The plating concentration was 1 million cells per ml, which resulted in a monolayer of cells with a density of ~2500 cells per mm^2 at 2 days *in vitro*. The center area of

Multi electrode arrays (Multichannel systems GmbH, Reutlingen, Germany) was covered with poly-ethyl-imine (PEI) to promote adhesion. Next, a drop of plating fluid was placed in the center of the MEA and cells were allowed to attach for 4 hours, after which the plating medium was washed and non-adhering cells were removed. Cultures were stored in an incubator at 37˚C, 5% CO_2 and near 100% humidity. Medium was replaced every 2 days. Standard 60 electrode MCS MEAs were used with electrodes spaced 200 µm apart and electrode diameters of 30 µm. In total, 8 different cultures were used, taken from 5 different platings. Culture ages range from 20 to 89 days *in vitro* DIV, but most (13/17 recording sessions) were performed between 20 and 35 DIV.

Experimental setup

Measurement setup. We built our measurement setup around a standard setup (1060BC preamplifier, STG1002 stimulus generator) by MCS (Multichannel Systems GmbH, Reutlingen, Germany). Data acquisition was done using a 6024E card by NI (National Instruments, Austin, TX), and controlled by custom LabView (NI) programs. During measurements, the MEAs were sealed using a semi-

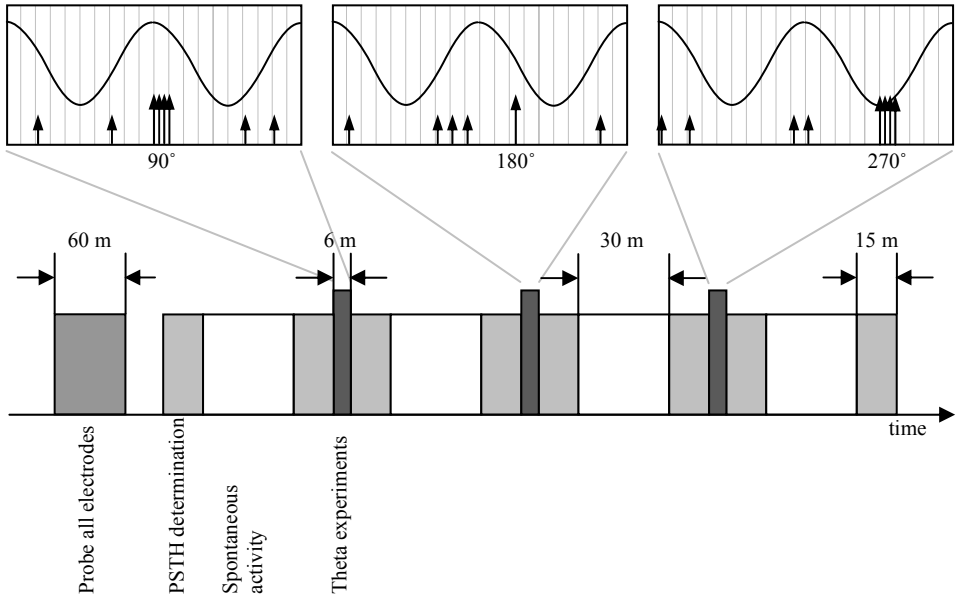

Figure 4.1. Timeline of a measurement. First, all electrodes were probed with stimuli of 3 different amplitudes. Based on the array-wide-PSTHs, a selection of 10-13 electrodes was made for further use. Next, evaluation periods were interleaved with theta stimulation. An evaluation period consisted of two probe sessions and 30 minutes of spontaneous recording. At least 3 different theta settings were used (90˚, 180˚ and 270˚; long arrows indicate tetani; see insets) in random order, sometimes extended with a control in which no theta was applied.

permeable membrane (MCS), and the temperature was controlled at 36˚C. Furthermore the CO_2-level surrounding the culture chamber was controlled and the culture chamber was heated from the top by a Peltier-element to prevent condensation of the medium. Cultures were left to acclimatize in the experimental setup for 30 minutes before recordings were started. Stimuli were always monopolar, biphasic (200 μs per phase) current pulses. During theta stimulation, the same pulse was used for all electrodes.

Protocol. All 60 electrodes were randomly probed 4 times with three different amplitudes (between 8 and 20 μA) at 5 second intervals, to determine the subset of electrodes to be used for theta stimulation. Ten to thirteen electrodes whose array-wide PSTH showed a peak larger than baseline activity were chosen for further use. A single stimulus amplitude for all electrodes was chosen for the entire duration of the measurement. Once chosen, the experiment comprised evaluation periods, interleaved with short periods of theta stimulation (figure 4.1). An evaluation period consisted of probing the subset of electrodes such that PSTH could be calculated, a period in which there was only spontaneous activity and again a probing sequence. Probing sequences involved the electrodes used for theta stimulation plus one electrode used for applying tetani. The probe sequences are fully randomized, using fixed amplitudes at 5 second intervals and repeated at least 15 times. During probing sessions and spontaneous recordings, spikes were detected using a threshold crossing algorithm and validated in real time using an algorithm described by Wagenaar *et al* [23]. During theta stimulation sessions, raw data of all 60 electrodes were saved. This was due to limitations in computer resources. The raw data files were analyzed offline in the same way as would otherwise have been done in real time.

Theta stimulation. Theta rhythm stimuli were generated in a probabilistic manner in both time and space. At every step of 20 ms, a decision was made to stimulate or not, by comparing a randomly generated number to a target stimulation rate (see also top panels in figure 1):

$$Stim(t) = \begin{cases} yes, & \bar{x}_t \le f_s(t) \\ no, & otherwise \end{cases} \qquad (4.1)$$

Where $\bar{x}_t$ is a value taken from a uniform distribution on the interval [0, 50], and the instantaneous target stimulation rate is given by:

$$f_s(t) = f_{av} + \Delta f \sin(2\pi f_\theta t) \quad (4.2)$$

Where f_{av} is the average stimulation frequency, Δf is the frequency deviation and f_θ is the theta modulation frequency. The average stimulation rate was set 10 Hz and the theta frequency was set to 4 Hz. The frequency deviation was set to 10 (or 8) Hz, such that the instantaneous frequency varied between 0 (2) and 20 (18) Hz. A steps size of 20 ms was chosen to allow uploads of electrode switching. An average frequency of 10 Hz was enough to significantly suppress bursting (results, but see also [3]). Peak stimulation frequencies of 20 Hz were well below the maximum of 50 Hz, such that a disproportionate number of inter stimulus intervals (ISI) of 20 ms was prevented. If f_s remained constant, the ISI would be negative exponentially distributed, indicating a generic random sequence of stimuli. The sequence of stimulation sites (10-13 sites) was also fully randomized. Consecutive stimuli on the same electrode were allowed.

Phase locked tetani. Tetani consisting of 4 pulses at a rate of 200 s^{-1} were applied at particular phases of the theta rhythm to one electrode which was not used for RBS. An experiment consisted of at least three theta stimulation sessions with phase locked tetani. Thirteen experiments additionally contained a sham session in which no stimuli at all were applied. The parameters used are summarized in table 4.1.

Table 4.1. Parameters used for several modes of theta stimulation. Note that at 180˚ theta only 1 pulse was applied. Together with no theta, 180˚ theta was used as a control. Tetani were repeated every 5 seconds. The last column lists the number of experiments with these settings.

Intervention	*Phase [˚]*	*Pulses*	*ITI [s]*	*N*
Theta 90˚	90	4	5	20
Theta 180˚	180	1	5	19
Theta -90˚ / 270˚	270	4	5	20
No theta	-	-	-	13

Note that 90˚ of theta corresponds to peak RBS firing rate (18 or 20 Hz), 180˚ corresponds to the average RBS rate of 10 Hz and 270˚ to the minimal RBS rate of 0-2 Hz (see figure 4.1). In addition, RBS was suspended from 40 ms before tetanus to 40 ms after tetanus, due to setup limitations. The number of pulses per tetanus were chosen in accordance to Huerta and Lisman [20], who found that 4 pulses (at 200 Hz) were enough to induce LTP or LTD of the same magnitude as traditional protocols. However, only very small effects were found for tetani with fewer

pulses. Subsequent groups used 4-5 pulses at either 200 or 400 Hz (400 Hz chosen to limit tetanus duration) [19, 21]. In view of this, delivering a single pulse at any phase is not expected to induce any connectivity changes. We phase-locked a single pulse to the zero-crossing of theta (*i.e.* 180˚), where no effects of tetani were expected either.

Analysis

Post stimulus histogram analysis. The network state was evaluated using post stimulus histograms made during evaluation periods. Electrode specific PSTH's were made of responses to stimuli to each electrode used for theta rhythm stimulation. A PSTH was calculated as the average histogram of activity between 0 to 500 ms after probe stimuli, using bins of 5 ms. The sum of all PSTHs to a particular stimulation electrode is the array-wide PSTH (awPSTH). The change in area of the PSTHs was taken as a measure for changes in network responses.

$$change = \frac{area\_after - area\_before}{area\_before} \tag{4.3}$$

Where before and after are with respect to one of the applied interventions. A threshold PSTH area of 10 spikes was set to decrease numeric fluctuations caused by division by a small number. Coincidentally, this also vastly reduced the number of PSTH's that merely contained direct responses. A histogram of changes was made to visualize the aggregate results of the applied interventions. The effectiveness of an intervention was calculated using:

$$\sum \text{distribution}(i) \cdot \text{change}(i) \tag{4.4}$$

or:

$$\frac{\sum \text{distribution}(\text{change} > 20\%)}{\sum \text{distribution}(\text{change} < -20\%)} \tag{4.5}$$

Where *distribution* is the normalized histogram of changes. Equation 4 describes the average change. Equation 4.5 calculates the ratio of potentiated versus depressed PSTH's, using a threshold of 20% in accordance to Chiappalone *et al* [24].

Burst profile analysis. In addition to PSTHs, bursts during spontaneous sessions were analyzed using a method introduced earlier [1]. Shortly, the array wide spiking rate was calculated by convolving the spike-train with a Gaussian. Whenever the resulting signal crossed a threshold, a part of the signal centered to the first peak after threshold crossing was selected. Spiking rates of individual electrodes were calculated, also by convolving spike-trains with a Gaussian. Thresholds were adjusted to the cultures' activity. The standard deviation used for all Gaussians was 5 ms. Selected episodes extended from -200 ms before centre time to 400 ms after centre time. This was wide enough to capture the whole burst in all measurements. In adherence to earlier work, we call the Gaussian smoothed array-wide firing rate signal a burst profile, and the electrode-specific firing rate signals phase profiles.

Before further analysis, we calculated averages of the profiles over 5 minute bins. This reduced variability and computational load. We treated these averaged profiles as if they were individual profiles. Distances between profiles were calculated using the following formula:

$$d_{i,j} = \frac{\sum \left(profile_j - profile_i \right)^2}{\sum \left(profile_i \right)^2} \tag{4.6}$$

Where $profile_j$ is the 601-element vector describing either a burst profile or a phase profile. We assessed changes made by theta stimulations by grouping before-before distances and after-after distances, and comparing these to before-after distances. For clarity of presentation, the distances in figure 4.7 have renormalized such that the average distance before intervention is unity.

4.3 Results

Theta stimulation

Figure 4.2 gives an overview of theta rhythm stimulation, combined with tetani applied at 90˚ (top panels) and 270˚ (lower panels). The target average rate of stimulation was 10 Hz, modulated with a frequency of 4 Hz and a frequency deviation Δf of 8 Hz. The left panels show that the actual average stimulation rate and frequency swing were slightly smaller than the target values. This is due to the probabilistic nature of triggering stimuli. It can also be seen that activity lags stimulation by some 19 degrees. The observed lag corresponds to the typical response time of the culture to stimuli. As a consequence, a peak in the activity can be seen at 90˚ of the observed activity rhythm, whereas the tetani were delivered at

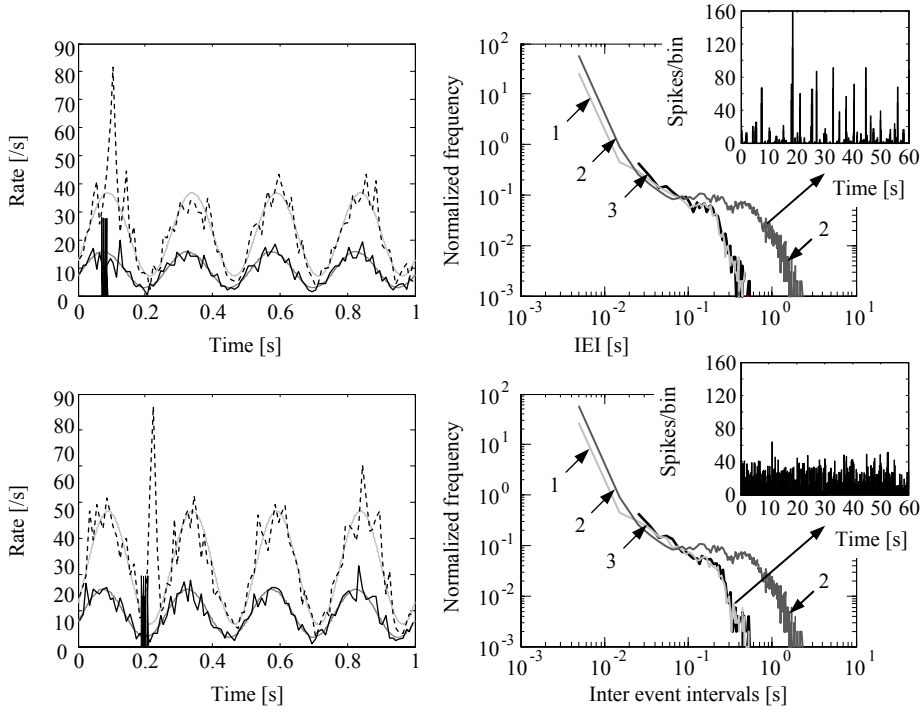

Figure 4.2. Theta stimulation and activity. Top left panel: Histograms of stimuli (black) and activity (dashed) clearly show 4 Hz modulation (bin width 10ms). Tetani (black) were delivered at 90˚ of theta stimulation. Activity lags stimulation by approximately 19˚ and was scaled by a factor 0.2 for clarity. Sinusoidal fits on both histograms are also drawn. Top right panel: Inter-event interval distributions. Curves 1 and 2 show inter-spike interval distributions during theta stimulation and during spontaneous measurements, respectively. Curve 3 shows the inter-stimulus interval during theta stimulation. The inset shows the congregate spike rate, in bins of 0.25 s, for 1 minute of spontaneous activity. Lower panels: The same graphs for 270˚ tetani. The inset shows the congregate spike rate, in bins of 0.25 s, for 1 minute of activity during theta stimulation.

71˚ of the activity rhythm. The black line in the right panels shows that the inter *stimulus* intervals are approximately exponentially distributed (straight line in log-log plot) with a refractory period of 0.02 seconds (the step time in the stimulation algorithm) and an increase at typical inter stimulus intervals (0.1 – 0.25) due to 4 Hz modulation. The inter *spike* interval distribution of observed activity during theta strongly resembles theta stimulation (light gray line). In contrast, the inter spike intervals of spontaneous activity are broader distributed, with the longer lags (*e.g.* > 0.5 s) corresponding to the relatively quiet times between bursts (dark gray lines). Note that for intervals smaller than 0.02 s, the distribution during theta is about 4 times lower than the spontaneous distribution, indicating less bursting. The insets show that activity increased during theta, but that very high peaks (associated with bursts) were reduced.

Post stimulus histograms

An example of changes that may be induced in PSTH's is shown in figure 4.3. In this case there were 22 electrodes that had a PSTH-area that was above threshold

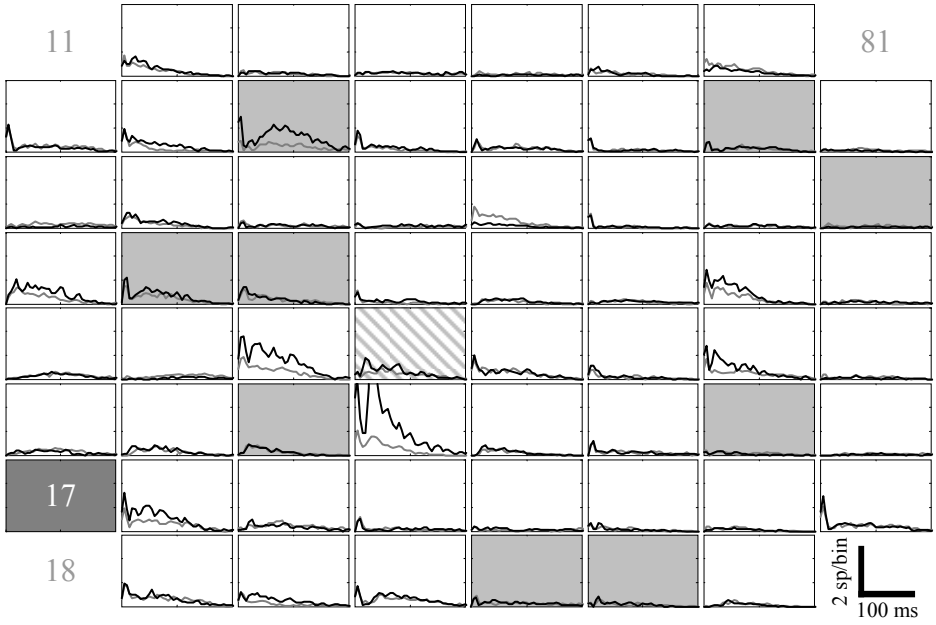

Figure 4.3. Example of PSTH changes. PSTH's in response to stimulation at electrode 17 are shown, before 90˚ theta stimulation in gray, and afterwards in black. Theta rhythm stimulation was applied to the shaded electrodes and tetani to electrode 45 (hatched). In this particular case, there was a general tendency towards increased PSTH areas. The bin width used is 5 ms.

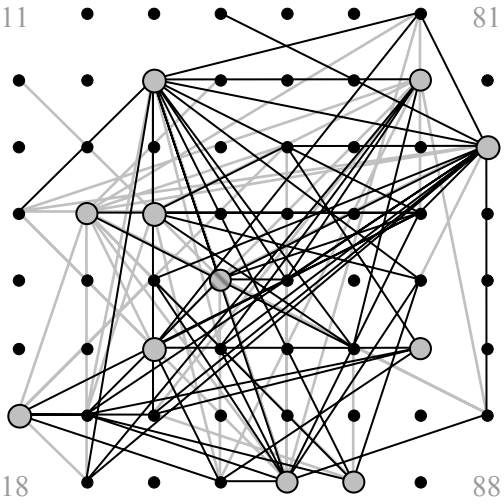

Figure 4.4. Connectivity map. Connections between stimulation electrodes (large gray) and measurement electrodes (small black) were drawn if the PSTH-area changed by more than 20%. Potentiated connections are drawn in black, while gray lines denote connections that decreased in strength. Most electrodes have a mix of potentiated and depressed connections, indicating pathway-specific changes in the network.

(>10 spikes on average). Out of these, the area of 13 PSTH's increased by more than 20% and only 2 decreased by more than 20%. Many electrodes only show activity in the first 10 ms. Such early responses include the direct responses; antidromic action-potentials resulting from direct activation of an axon and thus not involving any synapses [25]. Activity measured later than 10 ms after stimulus do involve synaptic transfers and are usually part of activity patterns that resemble network bursts.

An example of the changes in connectivity that were observed after application of tetani at 90˚ (at electrode 45) is shown in figure 4.4. In this plot a line between a stimulation electrode and another electrode indicates that the PSTH-area of that electrode changed by more than 20%. This experiment is representative in that most electrodes have a mix of weakened (decrease in PSTH-area) and strengthened connections. An overview of the changes in PSTH-area of all individual electrodes that were observed for the 3 different theta stimulation settings and control experiments, are shown in figure 4.5. Only when tetani were delivered at 90˚ of theta stimulation, did the PSTH-areas increase from those observed when no theta stimulation was applied (*i.e.* control). The two other settings of theta stimulation (180˚ and 270˚) resulted in a modest decrease in overall PSTH areas, but no appreciable differences between the two were observed.

The overall change in PSTH area was towards a decrease in PSTH-area. This is best seen by dividing the area of the curve showing over 20% increase by the area of the curve showing more than 20% decrease (equation 5). This ratio is 0.63 when no stimulation was applied. For tetani applied at 180˚ and 270˚ of theta, the ratios were both 0.44, while for tetani applied at 90˚ the ratio was 1.84. Given that no difference was found between 180 and 270 degree tetani, the small decrease in PSTH found with these settings may be attributed to theta stimulation in general.

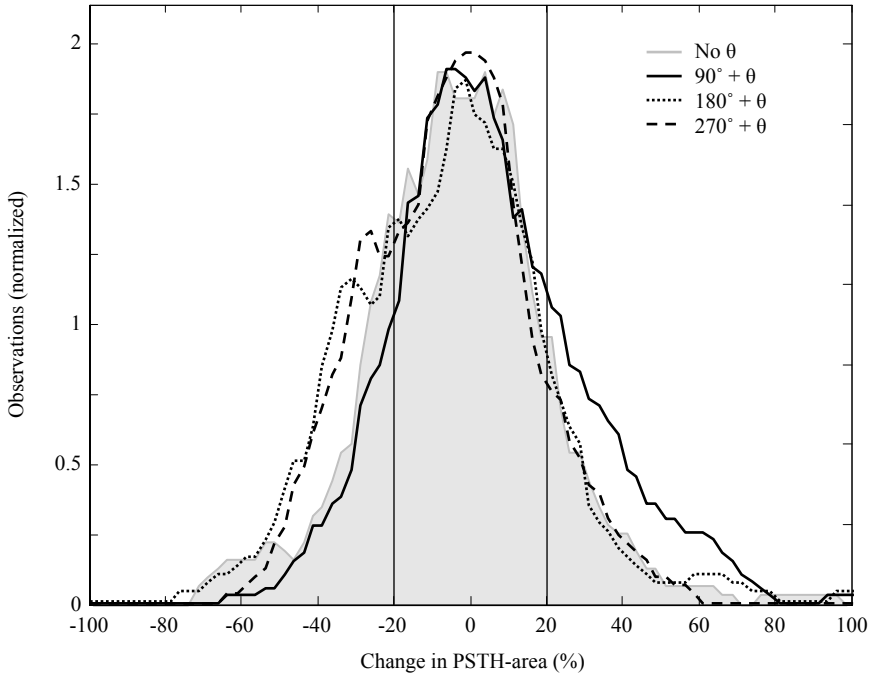

Figure 4.5. Aggregate results for changes in PSTH-area. With no theta stimulation, the shaded curve is found. With tetani applied at 90˚ of theta, a shift towards increases in PSTH-area was found (average change: -3.0% and +5.7% respectively). Slight decreases in PSTH-area were found for tetani applied at 180˚ or 270˚ of theta (average change: -5.5% and -5.6%).

Burst analysis

Figure 4.6 shows an example of phase profiles. It can be seen that there are differences between contributing electrodes. For example, electrode 13 is usually early to fire, whereas electrode 86 contributes mainly to the late phase of bursts. After theta stimulation with tetani applied at 90˚, we found many changes in profile shapes. The general tendency is towards broader profiles with higher peaks, indicating that in this example at least, bursts have become more intense after

intervention. Figures 4.3 and 4.6 are both taken from the same experiment. Figure 4.7 shows aggregate results of distances between profiles. For burst profiles, tetani applied at 90˚ of theta differed significantly from both no-theta and single pulses applied at 180˚. In contrast, tetani applied at 270˚ did not result in significant differences from either no-theta or single pulses at 180˚. For pulses at 180˚ and tetani at 270˚, the mean increase in distance was slightly lower than without theta, but these differences were not significant. For phase profiles, a relatively large increase was observed in mean distance for pulses applied at 180˚. This can occur when changes in phase profiles negate each other when summed, and may indicate that there was a balanced mix of potentiated and depressed phase profiles. Due to this, the only significant change was found between no theta and tetani at 90˚. Note that the spontaneous recordings are also separated by two probe sessions (see methods) in addition to the interventions.

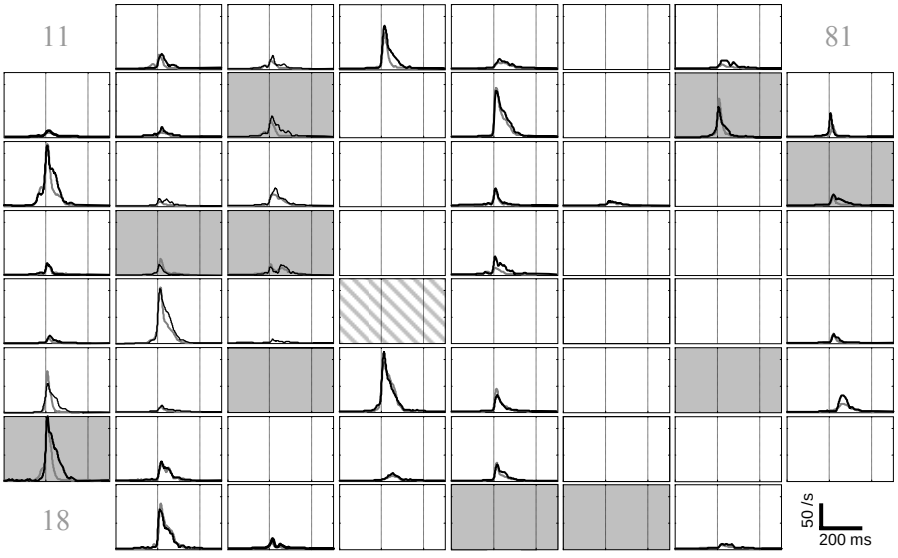

Figure 4.6. Examples of phase profiles before (gray) and after (black) theta stimulation with tetani at 90˚. The profiles are averages of the last 10 minutes of spontaneous recording before theta, and the first 10 minutes after. Spontaneous recordings from the same theta experiment as in figure 3 were used.

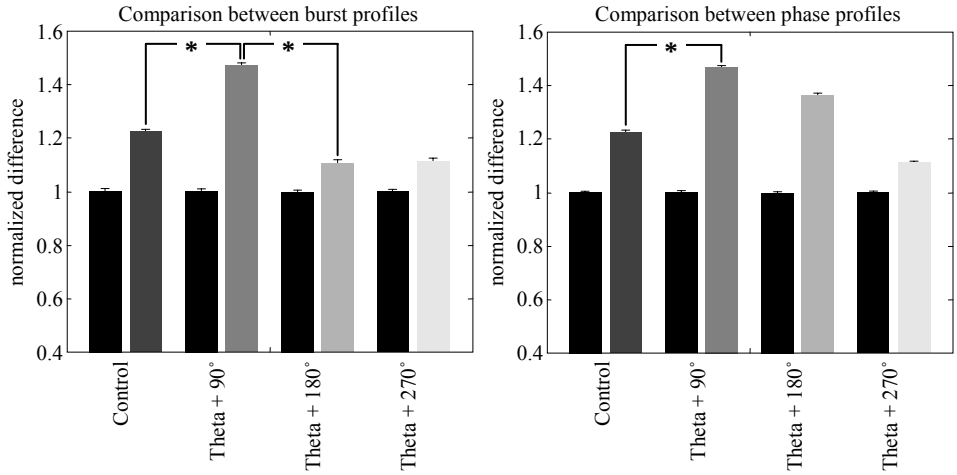

Figure 4.7. Comparison of change in distance between burst profiles (left) and phase profiles (right) for different settings of theta stimulation. Error bars denote standard error of mean; *: $p<0.05$, one-sided Student's *t*-test.

1.4 Discussion

In this study, we investigated whether rhythmic activity in culture would result in similar phase-dependent plasticity as has been demonstrated in hippocampus [19, 20]. Modulated RBS was successful at decreasing the percentage of small inter-spike intervals that would normally be found in network bursts. These small ISI's are most likely to induce spike-timing dependent synaptic plasticity (STDP). The changes in ISI-distribution indicated that bursting was significantly reduced.

The PSTH analysis showed a general decrease in responsiveness for no-theta controls. Applying theta stimulation appeared to decrease PSTH-areas even further (Note that 180˚-setting was single pulse and was not expected to have an effect). However, when tetani were applied at 90˚ an increase in overall PSTH-area was observed. The decrease in PSTH-area by tetani applied at 270˚ may have been obscured by the decrease of PSTH-area during 180˚ single pulse controls but for both settings, a depression of PSTH-area was found. Therefore, with these data we are unable to ascertain the origin of the depressed PSTH-area's. However, the increase in PSTH-areas after 90˚ tetani were applied indicate that successful induction of LTP may have been achieved. These experiments do not show the duration of the PSTH-changes for periods longer than 1 hour. Therefore, we can only hint at the successful induction of LTP.

The limited success of the algorithm at reducing PSTH areas can be explained on several levels. 1) Limited sensitivity of PSTH area to LTD. When two neurons are monosynaptically connected, and this connection was potentiated, we also expect to see an increase in PSTH-area. This idea can be expanded to PSTH's between electrodes, even though they are not necessarily monosynaptically connected. We also applied a threshold PSTH-area of 10 spikes in the first 200 ms after stimulus and expect that this was enough to observe both depression and potentiation. Other settings of this threshold to 5 or 15 spikes did not reveal marked changes in the results. Figure 4.4 shows a mix of changes in connectivity which alludes to (pathway-) specific changes and sensitivity to both potentiation and depression. 2) LTD was not induced, or its effect negated before observation. Possibly, the average synaptic efficacy in dissociated cultures is relatively low, rendering it very difficult to decrease efficacy further. Futhermore, Huerta and Lisman found that naive synapses were not depressed, but the previously potentiated could be depotentiated. Due to the randomized order in which we applied phase-locked tetani, a mix of naive synapses and potentiated synapses may have existed, which limited the effect of LTD. On the other hand, other groups did find LTD, not just depotentiation [19, 21]. Burst analysis shows similar results to those obtained by PSTH's, with only tetani applied at 90˚ of theta showing an increase in distances significantly larger than control. These findings confirm that burst analysis can be valuable tool when describing the 'state' of a network.

Overall, tetani applied at 90˚ of theta can be said to have a definite effect whereas the effect of other settings remains uncertain. This may suggest that the background firing rate at the moment of applying tetani is paramount to the effect. In this view, the theta rhythm modulation serves to suppress bursts and modulate the efficacy of tetani. However, stimuli were generated in a probabilistic manner, such that the stimulation rate at the moment of delivering tetani was highly variable. In fact, a gap of 40 ms between the last theta stimulus and the start of tetani exists because of setup limitations. It is therefore likely that the differences in effects of applying tetani at particular phases are due to rhythmic changes in network excitability. Wagenaar *et al* previously combined RBS (fixed aggregate frequency of 50 Hz, cyclic electrode switching) with tetanic stimulation (20 trains, 20 pulses/train, 20 Hz, 2 s between trains) but found no significant changes in responses to test stimuli [26, 27]. This supports the view that the rhythm is important, not just the background stimulation rate at the time of tetanus delivery.

Although only a definitive increase (potentiation) of PSTH-areas could be attributed to tetani at 90˚, in the other cases we found a decrease of PSTH-area. With theta modulated stochastic RBS then, control over potentiation and depotentiation/depression may be possible.

1.5 References

1. Stegenga, J., J. Le Feber, E. Marani, and W.C. Rutten, *Analysis of cultured neuronal networks using intraburst firing characteristics.* IEEE Trans Biomed Eng, 2008. **55**(4): p. 1382-90.
2. van Pelt, J., P.S. Wolters, M.A. Corner, W.L. Rutten, and G.J. Ramakers, *Long-term characterization of firing dynamics of spontaneous bursts in cultured neural networks.* IEEE Trans Biomed Eng, 2004. **51**(11): p. 2051-62.
3. Wagenaar, D.A., R. Madhavan, J. Pine, and S.M. Potter, *Controlling bursting in cortical cultures with closed-loop multi-electrode stimulation.* J Neurosci, 2005. **25**(3): p. 680-8.
4. Ben-Ari, Y., *Developing networks play a similar melody.* Trends Neurosci, 2001. **24**(6): p. 353-60.
5. Buzsaki, G. and A. Draguhn, *Neuronal oscillations in cortical networks.* Science, 2004. **304**(5679): p. 1926-9.
6. Leinekugel, X., R. Khazipov, R. Cannon, H. Hirase, Y. Ben-Ari, and G. Buzsaki, *Correlated bursts of activity in the neonatal hippocampus in vivo.* Science, 2002. **296**(5575): p. 2049-52.
7. Meister, M., R.O. Wong, D.A. Baylor, and C.J. Shatz, *Synchronous bursts of action potentials in ganglion cells of the developing mammalian retina.* Science, 1991. **252**(5008): p. 939-43.
8. Corner, M.A., J. van Pelt, P.S. Wolters, R.E. Baker, and R.H. Nuytinck, *Physiological effects of sustained blockade of excitatory synaptic transmission on spontaneously active developing neuronal networks--an inquiry into the reciprocal linkage between intrinsic biorhythms and neuroplasticity in early ontogeny.* Neurosci Biobehav Rev, 2002. **26**(2): p. 127-85.
9. Maeda, E., H.P. Robinson, and A. Kawana, *The mechanisms of generation and propagation of synchronized bursting in developing networks of cortical neurons.* J Neurosci, 1995. **15**(10): p. 6834-45.
10. Bakkum, D.J., Z.C. Chao, and S.M. Potter, *Spatio-temporal electrical stimuli shape behavior of an embodied cortical network in a goal-directed learning task.* J Neural Eng, 2008. **5**(3): p. 310-323.
11. Chao, Z.C., D.J. Bakkum, and S.M. Potter, *Shaping embodied neural networks for adaptive goal-directed behavior.* PLoS Comput Biol, 2008. **4**(3): p. e1000042.
12. Chao, Z.C., D.J. Bakkum, D.A. Wagenaar, and S.M. Potter, *Effects of random external background stimulation on network synaptic stability after tetanization.* neuroinformatics, 2005: p. 263-280.
13. Dravid, S.M. and T.F. Murray, *Spontaneous synchronized calcium oscillations in neocortical neurons in the presence of physiological [Mg(2+)]: involvement of AMPA/kainate and metabotropic glutamate receptors.* Brain Res, 2004. **1006**(1): p. 8-17.
14. Harsch, A. and H.P. Robinson, *Postsynaptic variability of firing in rat cortical neurons: the roles of input synchronization and synaptic NMDA receptor conductance.* J Neurosci, 2000. **20**(16): p. 6181-92.
15. Brovelli, A., M. Ding, A. Ledberg, Y. Chen, R. Nakamura, and S.L. Bressler, *Beta oscillations in a large-scale sensorimotor cortical network: directional influences revealed by Granger causality.* Proc Natl Acad Sci U S A, 2004. **101**(26): p. 9849-54.
16. Chrobak, J.J. and G. Buzsaki, *Gamma oscillations in the entorhinal cortex of the freely behaving rat.* J Neurosci, 1998. **18**(1): p. 388-98.
17. Hasselmo, M.E., C. Bodelon, and B.P. Wyble, *A proposed function for hippocampal theta rhythm: separate phases of encoding and retrieval enhance reversal of prior learning.* Neural Comput, 2002. **14**(4): p. 793-817.
18. Geinisman, Y., *Structural synaptic modifications associated with hippocampal LTP and behavioral learning.* Cereb Cortex, 2000. **10**(10): p. 952-62.
19. Holscher, C., R. Anwyl, and M.J. Rowan, *Stimulation on the positive phase of hippocampal theta rhythm induces long-term potentiation that can Be depotentiated by stimulation on the negative phase in area CA1 in vivo.* J Neurosci, 1997. **17**(16): p. 6470-7.
20. Huerta, P.T. and J.E. Lisman, *Bidirectional synaptic plasticity induced by a single burst during cholinergic theta oscillation in CA1 in vitro.* Neuron, 1995. **15**(5): p. 1053-63.

21. Hyman, J.M., B.P. Wyble, V. Goyal, C.A. Rossi, and M.E. Hasselmo, *Stimulation in hippocampal region CA1 in behaving rats yields long-term potentiation when delivered to the peak of theta and long-term depression when delivered to the trough.* J Neurosci, 2003. **23**(37): p. 11725-31.
22. Paulsen, O. and T.J. Sejnowski, *Natural patterns of activity and long-term synaptic plasticity.* Curr Opin Neurobiol, 2000. **10**(2): p. 172-9.
23. Wagenaar, D.A., T.B. DeMarse, and S.M. Potter. *MeaBench: A toolset for multi-electrode data acquisition and online analysis*. in *2nd international IEEE EMBS conference on neural engineering*. 2005. Arlington, VA.
24. Chiappalone, M., P. Massobrio, and S. Martinoia, *Network plasticity in cortical assemblies.* Eur J Neurosci, 2008. **28**(1): p. 221-37.
25. Bakkum, D.J., Z.C. Chao, and S.M. Potter, *Long-term activity-dependent plasticity of action potential propagation delay and amplitude in cortical networks.* PLoS ONE, 2008. **3**(5): p. e2088.
26. Wagenaar, D.A., J. Pine, and S.M. Potter, *Searching for plasticity in dissociated cortical cultures on multi-electrode arrays.* Journal of negative results in biomedicine, 2006. **5**(16).
27. Wagenaar, D.A., J. Pine, and S.M. Potter, *Searching for plasticity in dissociated cortical cultures on multi-electrode arrays.* Journal of negative results in biomedicine, 2007. **6**(3).

Chapter 5,

The effect of learning on bursting

Abstract

We have studied the effect that learning a new stimulus-response (SR) relationship had within a neuronal network cultured on a multi electrode array. For training, we applied repetitive focal electrical stimuli delivered at a low rate (<1 /s). Stimulation was withdrawn when a desired SR success ratio was achieved. It has been shown elsewhere, and we verified that, this training algorithm (named Conditional Repetitive Stimulation, CRS) can be used to strengthen an initially weak SR. So far, it remained unclear what the role of the rest of the network during learning was. We therefore studied the effect of CRS on spontaneously occurring network bursts. To this end, we made profiles of the firing rates within network bursts. We have shown earlier that these profiles change shape on a time base of several hours during spontaneous development. We show here that profiles of summed activity, called burst profiles, changed shape at an increased rate during CRS. This suggests that the whole network was involved in making the changes necessary to incorporate the desired SR relationship. However, a local (path-specific) component to learning was also found by analyzing profiles of single electrode activity, phase profiles. Phase profiles that were not part of the SR relationship changed far less during CRS than the phase profiles of the electrodes that were part of the SR relationship. Finally, the manner in which phase profiles changed shape varied and could not be linked to the SR relationship.

Stegenga J., le Feber J., Marani E. and Rutten W.L.C.

(Accepted for publication, IEEE Trans. Biomed. Eng., September 22nd, 2008)

5.1 Introduction

Altering the processing of information by (electrical) stimulation in cultured neuronal networks on MEAs is something that many groups have struggled with, or still do [1-7]. This may have as much to do with the inherent difficulty of observing changes as with the multitude of culturing and maintenance methods. Apart from inducing changes, where some activity-related measure is changed by stimulation, we ultimately want to be able to predict and control these changes.
The Conditional Repetitive Stimulation (CRS) protocol, introduced by Shahaf *et al* [8], strengthened one electrode's responsiveness to stimuli at another electrode while the global network response remained largely unchanged. This kind of control has not been reported by other algorithms applicable to dissociated cultures. Shahaf *et al* only reported on the difference between series of test stimuli before and after the experiment. Li *et al* [9] recently used the CRS algorithm to study the contribution of the various glutamate receptors on learning dynamics. They found that AMPA receptors were primarily involved in altering temporal patterns, while NMDA receptors were mostly responsible for altering spatial patterns.
We investigated the changes made within the network in order to accommodate the desired stimulus-response (SR) relationship. These could be local (*i.e.* pathway-specific), involving only the stimulus and evaluation sites, or global, involving many sites. Purely pathway-specific interactions would make the CRS expandable to more SR-relationships. We evaluated network activity by calculating the relationship of each electrode to spontaneously elicited network-wide synchronous events; bursts. These are short (50ms to 1s) intervals in which most neurons fire several action potentials, which develop spontaneously in cultured networks and persist throughout the cultures' lifetime [10-15]. Since action potentials within (single neuron) bursts are transmitted reliably by otherwise unreliable synaptic pathways [16], the network connectivity is reflected well by the spatio-temporal structure of network bursts. We previously analyzed the natural development of bursts *in vitro* through profiles of the instantaneous firing rate during bursts [17]. This revealed that both burst profiles (based on activity summed across all electrodes) and phase profiles (electrode specific profiles) changed with an average time-base of several hours. Furthermore, we showed that phase profiles changed at different rates, indicating a dependency on local interactions as well as global interactions.
The incorporation of a new SR relationship is probably the result of interactions between many neurons. The latency at which the SR is observed (up to 100ms) and the fact that many neurons are active at that time (a network burst is triggered by the stimulus) support this. When training is successful, we expect that it is the triggered network burst that has changed such that the desired SR relationship is incorporated. Analysis of bursts may reveal the spatial extent of the changes, if any, caused by CRS training.

5.2 Materials and methods

Culturing

Cortices were taken from newborn Wistar rats. The cells were dissociated mechanically by trituration and chemically by trypsin. The centers of multi electrode arrays (MEAs) were coated with poly-ethyl-imine (PEI), after which a drop of medium was applied. The plating concentration was 1 million cells per ml, which resulted in a monolayer of cells with a density of ~2500 cells per mm^2 at 2 days *in vitro*. Cultures were stored in an incubator with 5% CO_2 to air mixture, and near 100% humidity at 37˚C. Cultures were refreshed twice a week with R12 culturing medium [18], supplemented with 5% bovine serum. The same medium was also used during measurements. R12 is a minimum essential medium for culturing neurons, but with added bovine serum the glial cells multiplied at a low rate. Pilot experiments indicate that the cultures were more active when bovine serum was added, probably due to better functioning of the glial cells (data not shown). Culture ages ranged from 10 to 55 days *in vitro*, with 9 out of a total of 12 experiments performed in the mature phase (≥21 DIV).

Setup

We use MEAs and measurement setup (1060BC preamplifier and STG1002 stimulus generator) manufactured by MultiChannel Systems (Reutlingen, Germany). The MEAs had 60 electrodes which were either 10 or 30 um in diameter, which were spaced either 100 or 200 um apart, respectively. During measurements the temperature at the bottom of the MEA was kept at 36˚C, and a humidified and heated stream of air with 5% CO_2 was blown over the setup. Cultures were sealed with a semi-permeable membrane.

Measurements were controlled entirely by custom LabView (National Instruments**,** Austin, TX) programs. Spikes were detected whenever the signal crossed a threshold of 5.5 times the root-mean-square noise level, and were validated online using a scheme adopted from Wagenaar *et al* [19]. In this algorithm, a putative spike is accepted when it is the highest amplitude of either polarity in a window of ±1 ms. In addition, no spikes of the same polarity and having an amplitude ≥50% as the putative spike may exist in the same window. No spike sorting was attempted in this study, for several reasons. First, the shape of the extracellular potential may change within network bursts. Second, both the CRS algorithm and the profile analysis method work well with signals from neural assemblies. Finally, the selection criteria for the evaluation electrodes all but excluded multi-unit activity.

CRS algorithm

The Conditional Repetitive Stimulation (CRS) algorithm was introduced by Shahaf *et al* [8]. It was their observation that stimuli applied at a low rate (0.3–1 Hz, such that bursts could be triggered) to a single electrode caused changes in functional connectivity within the network. The responses to the stimuli were monitored and when a desired response appeared often enough (*responsiveness*), the stimuli were stopped. A single response was defined as one or more spikes detected on a single evaluation electrode within a certain window after stimulus onset (e.g. from 40-60 ms). The responsiveness was calculated as the moving average of the last ten responses. The target responsiveness was set at two out of ten, where the initial responsiveness was about one out of ten. When the target responsiveness was achieved, or after 10 minutes of stimulation, the stimuli were withdrawn. The stimuli were resumed after a pause of 5 minutes. The number of stimuli required to elicit the desired response was used as a measure for how well the new SR relationship was learned. Our procedure was as follows (figure 5.1). 1) Whenever possible, a long period (>6 hours) of spontaneous activity was measured before test-stimuli were applied. These spontaneous measurements were used assess normal developmental changes in the absence of stimuli. 2) The culture was probed with stimuli of varying amplitude (4-20 uA, biphasic, 200 us/phase, negative phase first) at a rate of 0.2 /s. The post stimulus histograms of array-wide activity (awPSTH) were visually examined to select a small set of stimulus electrodes. 3) A second series of test stimuli was applied to each candidate stimulus electrode. At this point, the stimulation rate was adjusted such that the ratio of evoked bursts to stimuli was maximized. The stimulation rate was usually 1.5 – 3 times higher than the typical spontaneous inter burst interval (IBI). The IBI distribution is given in figure 5.2. Inter stimulus intervals consequently varied between 1.5 and 5 seconds. The minimum stimulation rate was set at 0.1 per second and the ratio at which bursts were evoked had to be above 0.8 in order to continue. 4) A third series of test stimuli was applied at the chosen stimulus electrode and chosen rate. PSTH's of each electrode were calculated, and the evaluation electrode and response

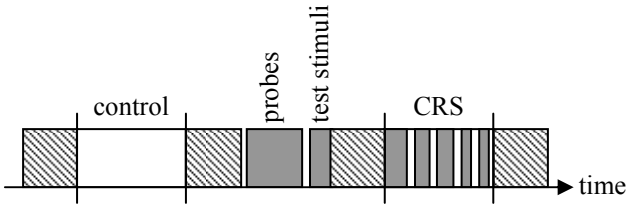

Figure 5.1. Timeline of a measurement. Control experiments of equal length as CRS experiments were used for comparing rates of change during spontaneous development with those during CRS. Control and CRS experiments were preceded and followed by 1 hour measurements of spontaneous activity to compare the effects of CRS with spontaneous development (hatched). Control and CRS experiments were less than 8 hours apart. Preparation for a CRS experiment consisted of selecting a stimulus electrode (probes) and selecting an evaluation electrode/window (test stimuli). Shaded boxes designate periods of stimulation.

window had to be chosen. The criterion was that the area of PSTH within the response window was 0.1. Multiple spikes can be triggered by a single stimulus, so this method may have overestimated the responsiveness. However, for electrodes with this low responsiveness this was not problematic. Unlike Shahaf *et al*, who used a fixed evaluation window (*i.e.* 40-60 ms), we varied the response window such that the peak in the post stimulus histogram of the evaluation electrode was within it. Window widths varied between 20 and 50 ms, with the earliest starting at 10 ms after stimulus and the latest ending at 100 ms. This was done because (1) the network wide response varied between cultures and between ages, and (2) it required connection strength rather than latency to change. 5) Between the test series and the start of CRS-training, an hour of spontaneous activity was measured (figure 5.1). 6) Start of the CRS experiment. A learning experiment was stopped when a stable fast responsiveness was reached, or when the network wide response (*i.e* number of spikes within 300 ms after stimulus) to stimuli became lower than 80% of its initial value. The initial value was calculated by taking the average of

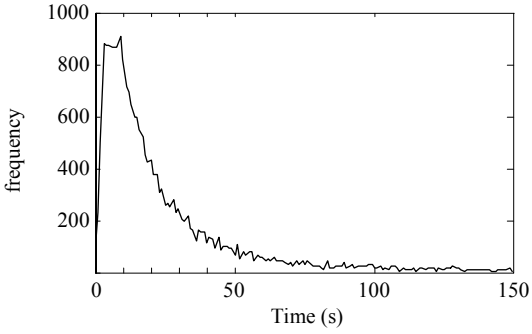

Figure 5.2. Distribution of inter burst intervals. Data from spontaneous measurements before and after all CRS experiments were used. The distribution peaks near 6 s, while the average IBI is 25 s. The bin size used to create the figure is 1 s.

the first 5 iterations of the CRS algorithm and the exact criterion was applied offline. Since a (permanent) degradation in network response resulted in CRS not reaching its goal within 10 minutes, these experiments (4 in total) were ended by the experimenter a few iterations after degradation had set in. Testing for stability of the awPSTH during CRS was not attempted because of variability as iterations of the protocol may comprise of as few as 3 stimuli. Shahaf *et al* already stated that the network response (i.e. triggered network burst) should be stable throughout the experiment, but did not quantify this. 7) After the learning experiment was concluded, spontaneous activity was once again recorded.

Next to the learning curve, which consists of the number stimuli required to reach the desired responsiveness, we calculated: (1) the average network (i.e. on all electrodes) response, calculated by counting the average number of spikes in 500 ms following a stimulus, (2) the average network response within the desired window and, (3) the average evaluation electrode response within the desired

window. All responses were normalised to the value in the first iteration (CRS) or to the average of the first 5 minutes (spontaneous) to enable comparison between experiments.

Profile analysis

Profiles of the within-burst firing rate were calculated from spontaneous activity measured before, during and after CRS experiments (figure 5.1). The procedure has been described earlier [17]. Examples of burst and phase profiles can be found in figure 5.3. The analysis consists of four steps: burst detection, burst profile calculation, phase profile calculation, and profile averaging. First, bursts were detected by dividing the summed activity in 100 ms bins and applying a threshold. The threshold was set at 2 times the number of electrodes that showed action potential activity (*i.e.* an average firing rate > 0.1 spikes/s). Second, burst profiles were calculated by convolving the spike times (summed over all electrodes) in a burst with a Gaussian. The standard deviations were between 5 and 15 ms, depending on activity. Smooth burst profiles near the main peak were necessary for further processing. The profile was calculated from 200 ms before the main peak in the burst profile, to 600 ms after the peak. Third, 60 phase profiles were calculated by convolving the spike times within the above defined window of each individual electrode with a Gaussian with the same SD as used for the burst profile. Fourth, we aligned burst profiles to their main peak and made 5-minute averages. This was done because there may be very few spikes elicited by some electrodes in a single burst. Averaging reduced the variability of phase profiles. An alternative would be to use Gaussians with a large standard deviation, but doing so would lose timing information. We treated the resulting average profiles as if they were profiles from individual bursts.

We used the root-mean-square (RMS) value of the difference between two profiles to quantify change. We normalized the RMS value to the area of the profile (*i.e.* the number of spikes).

$$D_i = \frac{RMS\left(p_i - p_{ref}\right)}{RMS\left(p_{ref}\right)} \tag{5.1}$$

$$RMS\left(x\right) = sqrt\left(\frac{1}{N}\sum_{n=1}^{N} x_n^2\right) \tag{5.2}$$

Where D_i is the normalized distance between profile p_i and a reference profile p_{ref} and each profile consists of N samples. The width of the profiles was 600 ms, containing N=601 data points. This distance measure is sensitive to changes in profile shape and to changes in overall firing rate and was applied to both burst and phase profiles. The rate of change of D during CRS experiments was calculated using the 5 minutes of spontaneous activity between iterations. The reference profile that we used within CRS was the average profile during the first 5 minute

pause. For control measurements we used the average profile during the first 5 minutes as a reference. When one of the spontaneous measurements before the CRS experiment was of equal length (or longer) than the CRS experiment (*N=4*), the change in profiles during the experiment was directly compared to the change over an equal length of time of spontaneous activity. Significance of changes was determined using two sided Student's *t*-tests. The significance of slopes was tested using the following data:

$$a_i = \frac{y_i - b}{x_i} \tag{5.3}$$

Where b is the intercept calculated by normal linear regression and (x_i, y_i) are the original datapoints.

5.3 Results

Learning experiments

Figure 5.3A shows the average learning curve of 12 experiments performed on 9 different cultures. The averaged curve has a negative slope, indicating successful learning. Individual learning curves (figure 5.3E) could be quite erratic, and were qualitatively described by fast initial learning, followed by a relapse starting somewhere between the 10^{th} and 20^{th} iteration before a stable (low) value was reached. During the experiment, the array wide number of spikes elicited by stimulation increased slightly, as seen in figure 5.3B and 5.3C. Since the experiments were of various lengths, the last two data points are averages of only 2 experiments, which may account for the discrepancy between these values and the general trend. In contrast, the number of spikes elicited on the evaluation electrode within the response window (figure 3D), increased fast during the first 3 iterations, stabilized around a value of 2.2 and then increased once more. The examples in figure 5.3D to 5.3F show that during the relapse, in these examples between iteration 13 to 28, the response on the evaluation electrode momentarily reached pre-learning levels, while the array wide response did not change during this period.

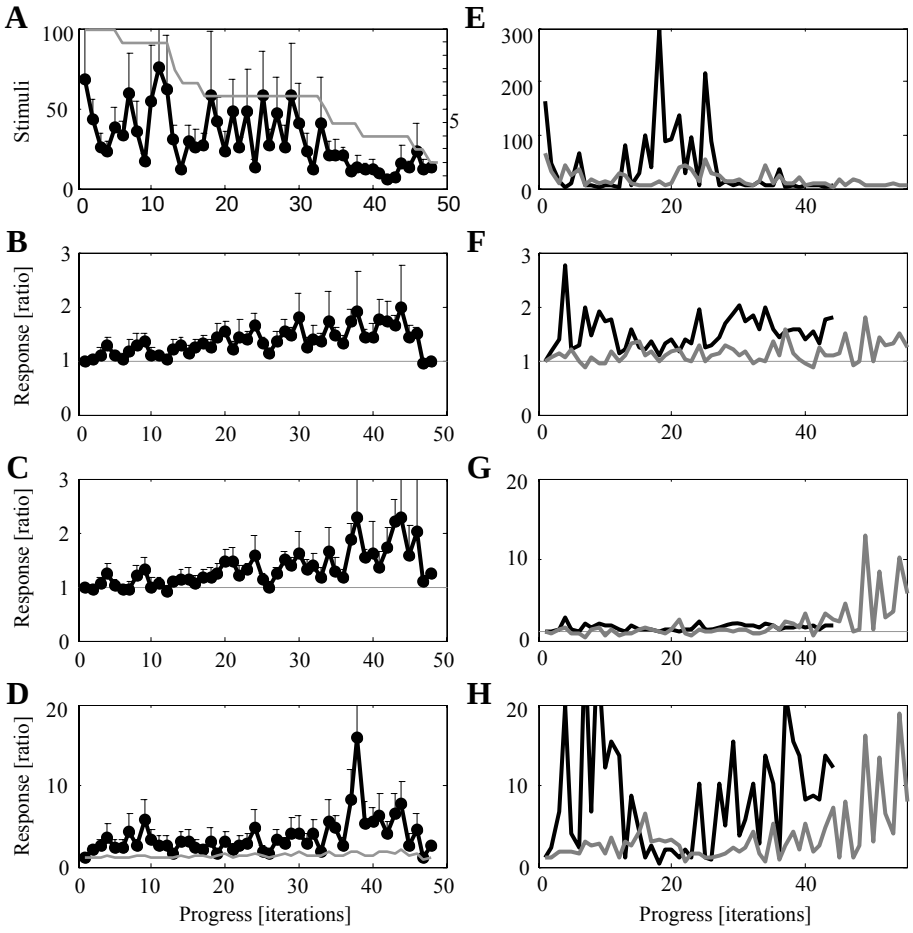

Figure 5.3. A) Average learning curve. The number of stimuli required to elicit the desired response decreased. Slope: -0.749 ± 0.157 per iteration (mean ± standard error), Kendall's τ: -0.450 (p<0.001). Curves show mean + standard error. The right y-axis and the gray line show the number of experiments that the curves are based on. B) Development of the array wide response. Slope: 0.010 ± 0.002, Kendall's τ: 0.466 (p<0.001). Individual curves were scaled to the response in the first iteration before averaging. C) Development of the array wide response within evaluation windows. Evaluation windows differ between experiments. Slope: 0.017 ± 0.003, Kendall's τ: 0.546 (p<0.001). D) Normalized response on the evaluation electrode. This response consists of spikes on the evaluation electrode within the evaluation window, again normalized to the value in the first iteration. Slope: 0.068 ± 0.023, Kendall's τ: 0.282 (p=0.004). In gray, the normalized array wide response is reproduced. E, F, G and H) The same curves for two example experiments.

Profiles

Profiles of spontaneous bursts before and after learning were compared with measurements separated by the same amount of time as the learning protocol (control). These were taken either before or after learning. Figure 5.4 shows an example of a learning experiment and controls taken before learning. During the control measurement the burst profile remained unchanged and 9 out of 25 phase

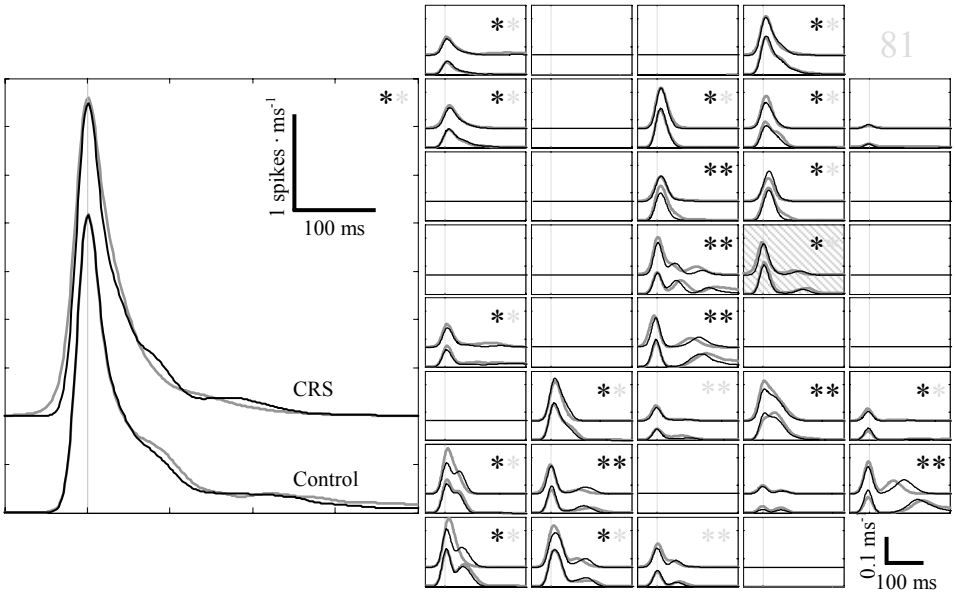

Figure 5.4. Left panel: Example of changes in burst profiles immediately before and after CRS (top two traces, black equals before, gray after). The lower two traces are immediately before and after an equal period of spontaneous development. All curves are 45 minute averages. Right panels: Phase profiles of the most active part of the MEA in the same experiment, shown in the same layout as the electrodes. The hatched plot is at the location of the stimulus electrode (*i.e.* 74), evaluation was at electrode 73. Significantly changed profiles are denoted by black asterisks, left for CRS and right for control.

profiles were changed. During learning, 20 out of 25 phase profiles changed significantly and this resulted in the significant change of the burst profile as well. The right panels in figure 5.4 also illustrate the complexity that phase profiles can have; most notably a 2nd or even 3rd phase of firing. In the 4 experiments in which controls were possible, all burst profiles changed during CRS compared to 2 spontaneous burst profiles changes (Student's *t*-test; $p \leq 0.01$). For phase profiles, 57% changed during CRS, while 46% changed spontaneously. On average, there were 13 active electrodes per culture in these experiments.

The distances between burst profiles are shown in figure 5.5. Variability in the burst profiles is represented by a baseline (the average value in the first hour) of about 0.2. The sensitivity of the profile method to profile changes is given by the baseline. Of greater importance is the presence of a positive slope, which indicates a progressive change from the initial profile. An increase in distance can be observed in the CRS experiments after 150 minutes, which roughly corresponds to the 22nd iteration. Even though the standard errors are high, a positive slope (0.036 per hour) can be seen during the CRS protocol. During spontaneous measurements a positive slope of only 0.012 per hour, is less visible. Calculations of Kendall's τ correlation coefficient show a clear positive correlation during CRS and a smaller correlation during spontaneous development.

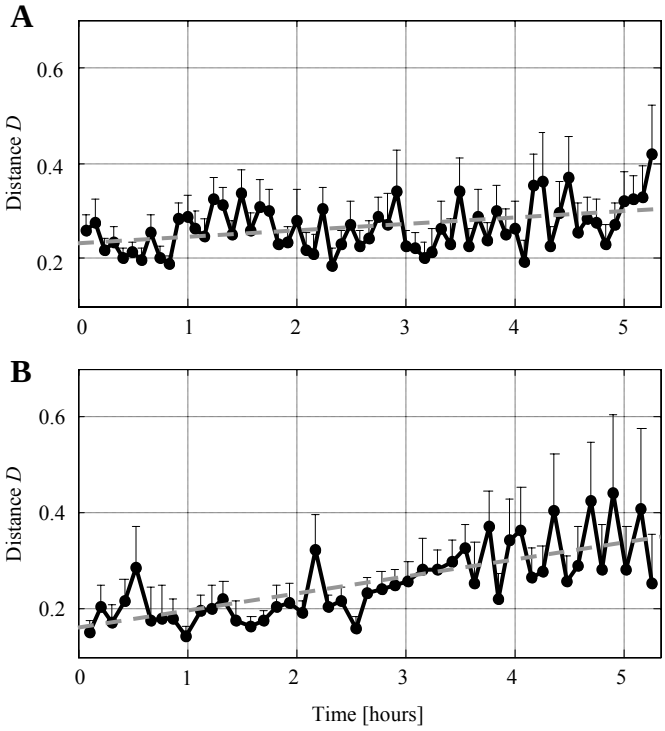

Figure 5.5. Development of distance D of change of burst profiles. A) Development of D of burst profiles in control experiments (N=4). Slope: 0.012 ± 0.004 per hour, Kendall's τ: 0.220 (p=0.011). Graphs show mean + standard error. B) Development of D of burst profiles during CRS (N=12). The first 5 minute pause, which is after the first stimulation round, was taken as a reference. Slope: 0.036 ± 0.005 per hour (mean ± standard error), Kendall's τ: 0.585 (p<0.001). The difference between the two slopes was significant (p=0.0015).

The distances between phase profiles are shown in figure 5.6. Again, a baseline can be seen around 0.34 during spontaneous measurements (top panel) and 0.41 during CRS (lower panels). These baselines are higher than their burst profile counterparts in figure 5.5, indicating the higher variability of phase profiles and thus also a decreased sensitivity to changes. In this case, the calculated slopes for spontaneous development and electrodes not used by CRS are comparable, while the slope for electrodes used for evaluation show a much higher slope. Kendall's τ correlation coefficients show that phase profiles on electrodes not used by CRS are stronger correlated (with time) than phase profiles during spontaneous development. Phase profiles on electrodes used for CRS have the highest correlation coefficient (0.021 per hour). Next to the rate of change, a change was also seen between profiles immediately before and after CRS (figure 5.7). The average duration of CRS, 5 hours, was longer than the typical time-base of spontaneous change, which is several hours [17]. Therefore, a change was observed during control measurements in which no stimulation was applied. However, figure 5.6 shows that the rate of change of burst profiles during CRS exceeded the spontaneous rate. The phase profiles showed the same, in that all phase profiles showed a small but significant

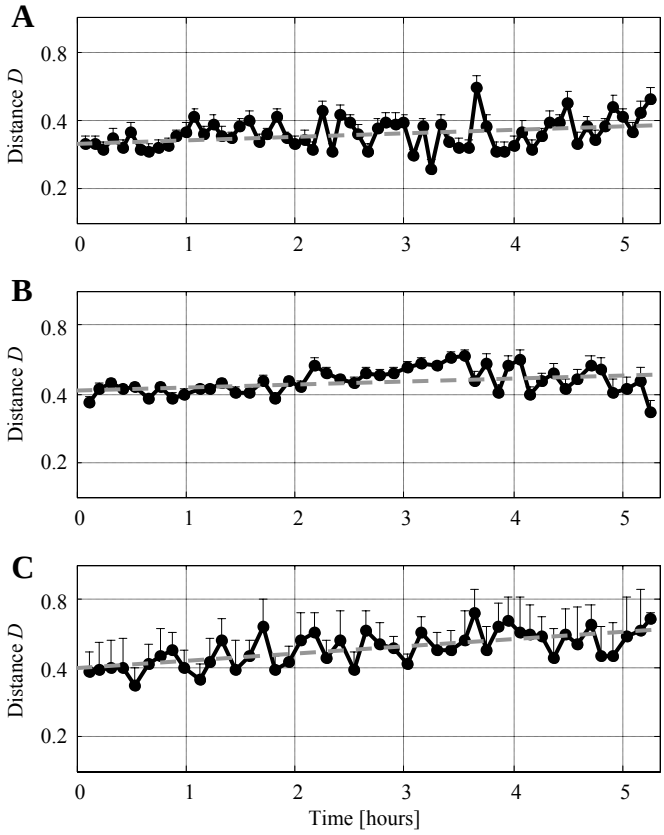

Figure 5.6. Development of distance *D* of phase profiles. A) Development of phase profiles during control (*N*=4). Slope: 0.009 ± 0.004 per hour, Kendall's τ: 0.203 (p=0.019). B) Development of phase profiles on all electrodes except those used for evaluation during CRS (*N*=12). Slope: 0.008 ± 0.003 per hour, Kendall's τ: 0.283 (p=0.005). C) Change of the phase profiles of evaluation electrodes during CRS (*N*=12). Slope: 0.021 ± 0.004 per hour, Kendall's τ: 0.473 (p<0.001). Graphs show mean + standard error. The difference between curves A and B was not significant (p=0.6161), while curve C differed significantly from both A and B (p=0.0203, p=0.0069).

increase in rate of change during CRS. The increase was considerably larger on evaluation electrodes than on other electrodes, indicating a pathway specific component in training using CRS.

How then did the phase profiles change? Phase profiles from four CRS experiments are shown in figure 5.8. A decrease in peak firing rate was observed in most cases, but also shifts in the position of the main peak and in some cases an increasing second phase were observed. The decrease in firing rate of phase profiles was often accompanied with a decrease in firing rate of burst profiles. We have observed such changes during spontaneous activity as well, albeit that it is rare to observe an increase in second phase spontaneously. It should be noted that out of the 8 cases in which the stimulation electrode was also spontaneously active, there were 6 cases in which phase profiles on the evaluation electrode increased in size relative to phase profiles on the stimulation electrode. Therefore, a decrease in

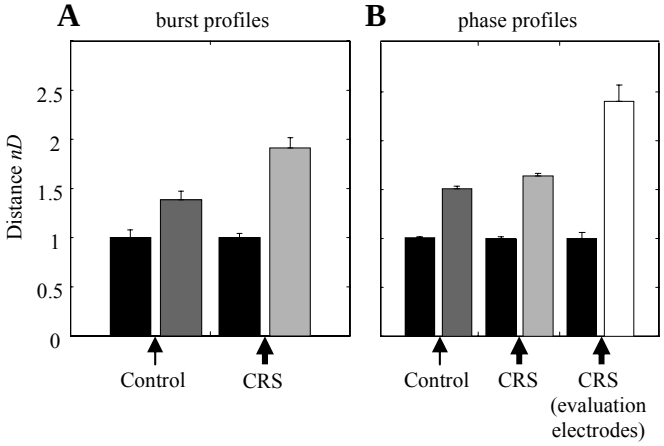

Figure 5.7. A) Changes between burst profiles immediately before and immediately after control (small arrow) and CRS experiments (bold arrows). Distances (*D*) were renormalized to the average distance in the 'before' groups (black bars). Bars show mean + standard error of mean. B) Changes between phase profiles. All means were statistically different (all $p<0.005$, student *t* test).

size of a phase profile on evaluation electrode may reflect an overall decrease in activity and does not exclude strengthening of the relationship between stimulus and evaluation electrode.

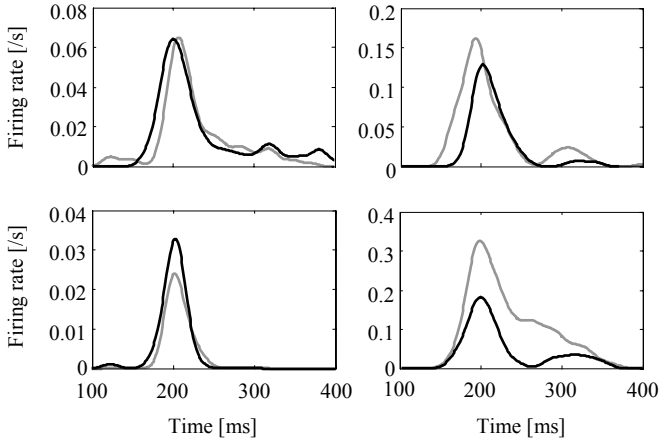

Figure 5.8. Four examples illustrate the types of changes between phase profiles at the start of CRS (black) and at the end (gray). We observed shifts of the main peak in 3 cases, an increase in peak firing rate in 4 cases, a decrease in peak firing rate in 6 cases and an increase in 2nd phase amplitude in 5 cases.

5.4 Discussion

CRS protocol

The selection procedure before starting the learning experiment itself was critical for the success of the experiment. For instance, the CRS paradigm was designed to enhance connectivity strength of initially low-strength connections, but not to a very high responsiveness (from 1/10 to 2/10). Using CRS to increase responsiveness from ~3/20 to 3/12, or from 1/10 to 3/10 was never successful (data not shown). This limits the general usefulness of CRS. Next to cultures that did not have a stable network response at inter stimulus intervals smaller than 10 s, we also had to discontinue experiments (4 out of 12) because the network wide response to stimuli (*i.e.* awPSTH) deteriorated during the course of an experiment. Such deterioration in awPSTH was seen when spontaneous bursts started occurring in between stimuli, which also increased the variability of the response. Whether all this was due to changes in the entire network or locally at the stimulus site, is subject of further investigation. When observing 80% criterion, the awPSTH-area steadily increased (figure 5.3B). However, the (relative) increase of PSTH-area on the evaluation electrode (figure 5.3D) was far greater.

In a number (*i.e.* 14) of cases we found that the criterion was reached very quickly in the first iterations of CRS, despite our efforts to select an evaluation electrode with a low responsiveness. Changes that may have occurred during the test stimuli or during the spontaneous activity that separated test stimuli from the start of CRS may be the cause of this. These experiments were aborted, as there was no further learning possible. Shahaf *et al* did not report on the number of cultures that did not fulfill the boundary conditions, but in our investigation only 9 out of 22 (otherwise active and easy to stimulate) cultures met the prerequisites [8]. Initial learning curves (first 10 iterations) resembled the examples given by Shahaf *et al*. Further iterations of the CRS protocol often showed a period with a relapse in learning, something that was not reported earlier. Consequently, a stable low value was reached much later. We found it necessary to adjust the evaluation window to a value that corresponded to a latency at which activity was elicited. The larger differences in latency that we found may be due to the fact that we used MEAs with two different electrode spacings or due to a larger spread in culture age (10-55 DIV). However, more subtle differences in preparation and maintenance cannot be excluded. Despite the erratic learning rates we found that the cultures that met all the prerequisites were trainable. One possibility to reduce variability in responses, which may result in smoother learning curves, is to create a pool of evaluation neurons [20]. However, it is not known what impact this may have on learning.

Profile change

The rate at which both burst and phase profiles (of evaluation electrodes) changed during CRS stimulation was higher than during spontaneous development. However, phase profiles on electrodes that were not used during CRS changed at a rate comparable to spontaneous development (judged by slope). Since the burst profiles dìd change, and a burst profile is essentially a summation of phase profiles, this result was unexpected. It is possible however, because the changes in phase profiles are normalized to the area of the profile (*i.e.* the activity of the electrode), while the influence of electrodes on the burst profile is activity dependent. Therefore, the results indicate that highly active sites changed more rapidly. Also, given the relatively large rate of change of burst profiles, it is likely that a number of phase profiles changed in the same general direction. Such convergent changes are commonly seen during spontaneous development, only on a larger timescale. From this point of view, the stimulation accelerated, but did not alter the normal development.

In contradiction to this view, we observed that phase profile on electrodes used for evaluation during CRS changed at a very high rate. This result is surprising because the phase profiles on evaluation electrodes were always small (low spiking activity), and large phase profiles generally had a higher rate of change. This cannot be explained merely by a speeding up of normal development. Instead, by withdrawing stimuli when the desired response is achieved, the changes occurring on the evaluation electrodes were 'cultivated', while changes on other electrodes may go back and forth and negate each other. The CRS algorithm thus relies on accelerating changes by means of stimuli (*i.e.* induction of exploratory behavior [8]), and preserving these changes on the evaluation electrodes.

The coupling between phase profiles on evaluation electrodes and SR relationships is complex. A phase profile shows one electrodes' contribution to network collective bursts, while an SR-relationship involves two electrodes. It is through the fact that stimulation elicits bursts, that the two are coupled. The complexity of this coupling is probably also the reason why no correlation between the stimulation-evaluation electrode pair and the changes in phase profiles could be found. Comparing phase profiles immediately before CRS to phase profiles immediately after CRS showed a small increase in number of phase profile changes and also an increase in distance *D*.

The results suggest that the whole network was involved during training in a lesser degree, and that stimulation and evaluation electrodes were particularly involved. Assuming that a change in phase profile (site-specific) is related to the change in responsiveness (pathway-specific), it is not clear how changes in the phase profiles of evaluation electrodes depend on changes in other phase profiles or even burst profiles. Since only one SR relationship is controlled, it may simply be that the rest of the network incorporates this change in a way that requires the least modifications. Conversely, it may also be that changes throughout the whole of

network are driving the SR relationship toward a higher efficacy. Whatever the case, expanding the CRS algorithm to multiple SR relationships will not be straightforward, partly due to global network interactions and partly due to the selection criteria for trainable SR relationships.

5.5 References

1. Chiappalone, M., P. Massobrio, and S. Martinoia, *Network plasticity in cortical assemblies.* Eur J Neurosci, 2008. **28**(1): p. 221-37.
2. Jimbo, Y., T. Tateno, and H.P.C. Robinson, *Simultaneous induction of pathway specific potetiation and depression in networks of cortical neurons.* Biophys J, 1999. **76**(2): p. 670-678.
3. Madhavan, R., Z.C. Chao, and S.M. Potter, *Plasticity of recurring spatiotemporal activity patterns in cortical networks.* Phys Biol, 2007. **4**(3): p. 181-93.
4. Maeda, E., et al., *Modification of parallel activity elicited by propagating bursts in developing networks of rat cortical neurones.* Eur J Neurosci, 1998. **10**(2): p. 488-96.
5. Marom, S. and D. Eytan, *Learning in ex-vivo developing networks of cortical neurons.* Prog Brain Res, 2005. **147**: p. 189-99.
6. Ruaro, M.E., P. Bonifazi, and V. Torre, *Toward the neurocomputer: image processing and pattern recognition with neuronal cultures.* IEEE Trans Biomed Eng, 2005. **52**(3): p. 371-83.
7. Wagenaar, D.A., J. Pine, and S.M. Potter, *Searching for plasticity in dissociated cortical cultures on multi-electrode arrays.* Journal of negative results in biomedicine, 2006. **5**(16).
8. Shahaf, G. and S. Marom, *Learning in networks of cortical neurons.* J Neurosci, 2001. **21**(22): p. 8782-8.
9. Li, Y., et al., *Characterization of synchronized bursts in cultured hippocampal neuronal networks with learning training on microelectrode arrays.* Biosens Bioelectron, 2007. **22**(12): p. 2976-82.
10. Chiappalone, M., et al., *Dissociated cortical networks show spontaneously correlated activity patterns during in vitro development.* Brain Res, 2006. **1093**(1): p. 41-53.
11. Kamioka, H., et al., *Spontaneous periodic synchronized bursting during formation of mature patterns of connections in cortical cultures.* Neurosci Lett, 1996. **206**(2-3): p. 109-12.
12. Maeda, E., H.P. Robinson, and A. Kawana, *The mechanisms of generation and propagation of synchronized bursting in developing networks of cortical neurons.* J Neurosci, 1995. **15**(10): p. 6834-45.
13. Van Pelt, J., et al., *Longterm stability and developmental changes in spontaneous network burst firing patterns in dissociated rat cerebral cortex cell cultures on multielectrode arrays.* Neurosci Lett, 2004. **361**(1-3): p. 86-9.
14. van Pelt, J., et al., *Long-term characterization of firing dynamics of spontaneous bursts in cultured neural networks.* IEEE Trans Biomed Eng, 2004. **51**(11): p. 2051-62.
15. Wagenaar, D.A., J. Pine, and S.M. Potter, *An extremely rich repertoire of bursting patterns during the development of cortical cultures.* BMC Neurosci, 2006. **7**: p. 11.
16. Lisman, J.E., *Bursts as a unit of neural information: making unreliable synapses reliable.* Trends Neurosci, 1997. **20**(1): p. 38-43.
17. Stegenga, J., et al., *Analysis of cultured neuronal networks using intraburst firing characteristics.* IEEE Trans Biomed Eng, 2008. **55**(4): p. 1382-90.
18. Romijn, H.J., F. van Huizen, and P.S. Wolters, *Towards an improved serum-free, chemically defined medium for long-term culturing of cerebral cortex tissue.* Neurosci Biobehav Rev, 1984. **8**(3): p. 301-34.

19. Wagenaar, D.A., T.B. DeMarse, and S.M. Potter. *MeaBench: A toolset for multi-electrode data acquisition and online analysis*. in *2nd international IEEE EMBS conference on neural engineering*. 2005. Arlington, VA.
20. Bonifazi, P., M.E. Ruaro, and V. Torre, *Statistical properties of information processing in neuronal networks.* Eur J Neurosci, 2005. **22**(11): p. 2953-64.

Chapter 6,

Discussion

6.1 Analysis of culture state

Many different approaches exist for the analysis of action potential firing patterns in neural networks. Depending on the application, one may be preferred over the other. This diversity is greatest when characterizing the state of neural networks during development. Since bursts have always been the most prominent form of activity in cultures of dissociated neurons, many parameters have been devised which make use of bursts. The time between bursts, burst duration, number of action potentials per burst, the recruitment rate during bursts have been used to characterize the global state of the network. Given the many unknowns in culture, such as its connectivity, these statistical global parameters were a logical starting point. The global state can be of interest when studying the effect of bath-applied drugs, developmental changes etc. However, these parameters have proved to be not detailed enough to observe the relatively small changes in network activity patterns that may be induced by electrical stimulation (chapter 3, [1, 2]).
In chapter 2 we introduced burst analysis by burst and phase profiles in an attempt to extract more information about the network. We showed that under certain conditions, a definite relationship exists between phase profiles and functional connectivity. Despite this relationship, the two analyses are far from interchangeable. A major difference may lie in the assumptions of stationarity of the time series. Some groups have clustered bursts that are similar in intra-burst firing characteristics and found that similar bursts were not elicited in temporal proximity [3-6]. This suggests that bursts should be considered by themselves and that a time-average of many bursts may obscure valuable information. Many algorithms that calculate some form of functional connectivity ignore bursts and may thus be less than optimal.
Time-averages (5 minute bins) of burst and phase profiles were used throughout this thesis, because classification did not reveal distinct burst types in mixed temporal order. For our objective of analyzing developmental changes and demonstrating the usefulness of profile analysis this may not be a problem. However, from literature it has been suggested that the presence of distinct burst types may form a substrate for memory [5]. It is certainly true that in the presence of multiple burst types, a positive result may be found even when only one burst type is changed or its occurrence ratio altered [6]. Nevertheless, we found changed burst profiles in chapters 4 and 5. Despite earlier positive results, many groups

have struggled to observe changes using the stimulation protocols described in chapter 3 as well.

Another way to assess the network state is to use responses to probe stimuli. These have the advantage of being repeatable, circumventing some of the variability that is inherent to spontaneous activity [1, 2, 7-12]. We have also used PSTH's to determine the effect of stimulation (Chapters 4 and 5) and also to provide feedback on the cultures' performance (Chapter 5). In these experiments, PSTHs were determined using a straightforward scheme; applying stimuli at a low rate such that bursts were evoked and spontaneous bursts were minimized.
A refinement of this approach has recently been proposed such that PSTH's are stabilized. A considerable part of the variation in PSTH's can be attributed to the network state at the time of stimulus. In particular, (spontaneous) bursts occurring just before stimulus have a detrimental effect on PSTH area and shape [13]. Conditioning of the network state by applying a short period (~1 s, dependent on spontaneous activity) of random background stimulation (RBS) before the actual probe stimulus, stabilizes PSTH's [14]. In the latter study no repetitions were required to establish a PSTH stabile enough to base decisions on. In chapter 4, we repeated the probe several (>15) times such that we could increase stability of PSTH's by averaging.
It is still a matter of debate whether RBS, or indeed the probe sequences used to calculate PSTH's, result in changes within the network. The risk of such changes may appear small in lieu of the many difficulties we encountered in attempting to change network behavior using tetanic stimulation in chapter 3. However, under certain circumstances (*i.e.* high $[Mg^{2+}]$) the mere triggering of bursts by stimuli may be enough to induce changes [10]. In more general culturing conditions, several studies have shown a long-term effect of low rate, single pulse stimulation [15, 16]. Analysis of spontaneously occurring bursts therefore has a definite advantage over other methods in long term studies.

6.2 Plasticity, learning and memory in dissociated cultures

Plasticity mechanisms have mostly been studied by changes in cell-cell (*i.e.* synaptic) interactions, either in intact brain structures and all activity that goes with it, or by isolating two connected neurons from the network. In these cases, the structure of the network is known to some extent, and the activity is either natural in appearance or controlled by the experimenter. The opposite is true for cultures of dissociated neurons. Here, the structure is random and activity takes the form of network wide bursts. Both complicate the study of information processing and storage.

The network connectivity *in vivo* is far from random. While it's impossible that all connections are programmed in the genetic code, brain areas are very specifically interconnected on a broader scale. The flexibility of neurons and synapses compensate for what cannot (or should not) be genetically determined. Dissociated cultures do not retain connectivity on any scale, nor can it learn through experience, as it is disconnected from the outside world. Synaptic connections in dissociated cultures are thus initiated at random. Throughout the lifetime of the culture, network connectivity is reinforced by spontaneous action potentials that are thought to be randomly generated by stochastic membrane fluctuations. Without external intervention, this results in bursts of action potentials, the role of which is discussed later.

We should therefore not be surprised that the resulting network does not have all beneficial properties that an intact brain (region) has. However, as simple as the dissociated cultures may be, models of such networks (artificial neural networks) suggest that the computational properties of such networks are significant. Recent work suggests that primitive pattern recognition may be possible in culture [17]. We have shown that bursts were plastic in that the spatiotemporal structure was dependent on maturation (Chapter 2) and could also be changed by stimulation (Chapters 4 and 5). However, the time-scale of these changes was quite large (tens of minutes to hours) and not relevant for fast processing in organisms. In studies on hippocampal slices, a single 4 pulse train applied at the correct phase the natural theta rhythm can change EPSPs significantly and long-term (several hours) [18-20]. Such mechanisms would allow single trial learning on biologically relevant time-scales.

So far, the timescale of experiments in cultures has been largely determined by network burst rate [6, 8, 9, 11, 21, 22]. Burst suppression by RBS may result in a more natural 'operating point' for the cells in the network and may be also faster input-output processing. However, RBS has some practical drawbacks. Extracelullar electrical stimulation results in artifacts on the stimulating electrodes (200 ms to 1 s, depending on electrode-medium impedance), and also on other measuring electrodes (~2 ms) because relatively large amplitudes are required. Other means of stimulation are now being investigated. Promising methods are:

- Local chemical stimulation. New MEA's are being designed which allow very small amount of chemicals to be released locally. It remains to be seen if the speed of application and diffusion are fast enough to induce biological rhythms [23].
- Light/laser stimulation. Neurons can further be directly stimulated thermally by laser [24], or can be made sensitive to light by transfection of neurons with channelrhodopsin [25]. The latter method effectively creates sensory neurons, such that stimulation is also more natural.

Combining these stimulation techniques with multi-electrode arrays may be beneficial for analyzing information processing in cultures under more natural conditions.

6.3 Bursts; blessing or curse?

In the intact brain, bursts are seen in early development where they are thought to control neural outgrowth [26]. However, when sensory neurons become active, this type of bursting ceases. Bursts in culture are similarly important for the creation of a new neural network from dissociated neuronal cells, in the absence of sensory input. This is confirmed in several studies where bursting is suppressed during network development [27-31]. Therefore, bursts have at least one definite purpose; the creation and maintenance of network connectivity. Since neurons need to be active to be viable, bursts may even be important for overall culture health. Perhaps as a result of the previous, burst and phase profile analysis yields information on the physiological and computational structure of a network. We used this information in Chapter 2, where gross developmental changes were tentatively coupled to changes in bursts and the spatio-temporal structure of bursts to functional connectivity.
However, bursting in mature networks is often likened to epileptic seizures [26-28, 32-36]. As such, bursts are not regarded as providing very good conditions under which information processing is possible. When a culture is bursting, neurons operate in two extremes; very low input or very high input. In chapters 3 and 4 we have seen that when neurons are prevented from operating in these extremes, the culture as a whole is more sensitive to stimuli. Therefore, when the goal is to study plasticity and memory, bursts are best regarded as a necessary evil. They are useful for guiding outgrowth and maintaining initial connectivity but do not provide a good platform to do further studies.

6.4 Outlook

It appears that cultures of neurons may retain some basic information processing abilities. We have demonstrated that learning is possible and that it changes the network in terms of spontaneous firing characteristics (Chapter 5). The process however was slow, with experiments lasting several hours. However, an effort to induce plasticity in otherwise spontaneously active cultures was unsuccessful, even though we used quite strong stimuli (Chapter 3). We attributed this to the bursting

activity, which may overwhelm plasticity mechanisms. One remedy is to bring the overall activity in a network to a more natural state of dispersed activity. We expanded on this idea by applying dispersed stimuli with a rhythmic component in the theta-band (Chapter 4). In this state, the cultures were sensitive to short trains (tetani) of 4 pulses at 200 Hz. This general increase of sensitivity to external manipulation by putting networks in a more natural state make cultured networks again a viable platform for studying learning dynamics.

There is still a long way to go before cultured networks can be used to perform tasks such as face recognition. Currently, the training is slow and only applicable for relationships that initially have very specific parameters. It is likely that in the future the outgrowth will be controlled and that continuous external stimuli will be applied in order to enable a culture to perform a specific task. Spontaneous bursts may be allowed to initially wire the network, but will soon be replaced by external stimuli. Burst analysis in cultures may then focus more on the topic of epileptic seizures than on information processing.

6.5 References

1. Wagenaar, D.A., J. Pine, and S.M. Potter, *Searching for plasticity in dissociated cortical cultures on multi-electrode arrays.* Journal of negative results in biomedicine, 2006. **5**(16).
2. Wagenaar, D.A., J. Pine, and S.M. Potter, *Searching for plasticity in dissociated cortical cultures on multi-electrode arrays.* Journal of negative results in biomedicine, 2007. **6**(3).
3. Baruchi, I. and E. Ben-Jacob, *Functional holography of recorded neuronal networks activity.* Neuroinformatics, 2004. **2**(3): p. 333-52.
4. Baruchi, I., et al., *Functional holography analysis: simplifying the complexity of dynamical networks.* Chaos, 2006. **16**(1): p. 015112.
5. Beggs, J.M. and D. Plenz, *Neuronal avalanches are diverse and precise activity patterns that are stable for many hours in cortical slice cultures.* J Neurosci, 2004. **24**(22): p. 5216-29.
6. Madhavan, R., Z.C. Chao, and S.M. Potter, *Plasticity of recurring spatiotemporal activity patterns in cortical networks.* Phys Biol, 2007. **4**(3): p. 181-93.
7. Chiappalone, M., P. Massobrio, and S. Martinoia, *Network plasticity in cortical assemblies.* Eur J Neurosci, 2008. **28**(1): p. 221-37.
8. Jimbo, Y., H.P. Robinson, and A. Kawana, *Strengthening of synchronized activity by tetanic stimulation in cortical cultures: application of planar electrode arrays.* IEEE Trans Biomed Eng, 1998. **45**(11): p. 1297-304.
9. Jimbo, Y., T. Tateno, and H.P.C. Robinson, *Simultaneous induction of pathway specific potetiation and depression in networks of cortical neurons.* Biophys J, 1999. **76**(2): p. 670-678.
10. Maeda, E., et al., *Modification of parallel activity elicited by propagating bursts in developing networks of rat cortical neurones.* Eur J Neurosci, 1998. **10**(2): p. 488-96.
11. Shahaf, G. and S. Marom, *Learning in networks of cortical neurons.* J Neurosci, 2001. **21**(22): p. 8782-8.
12. Tateno, T. and Y. Jimbo, *Activity-dependent enhancement in the reliability of correlated spike timings in cultured cortical neurons.* Biol Cybern, 1999. **80**(1): p. 45-55.
13. Weihberger, O., et al. *Network-state dependent stimulation efficacy and interaction with bursting activity in neuronal networks in vitro*. in *6th international meeting on substrate-integrated micro electrode arrays*. 2008. Reutlingen, Germany: BIOPRO Baden-Würtemberg GmbH.

14. Bakkum, D.J., Z.C. Chao, and S.M. Potter, *Spatio-temporal electrical stimuli shape behavior of an embodied cortical network in a goal-directed learning task.* J Neural Eng, 2008. **5**(3): p. 310-323.
15. Bologna, L.L., et al. *Constant low frequency stimulation shows long-term response changes in in-vitro cortical cultures during development*. in *6th international meeting on substrate-integrated micro electrode arrays*. 2008. Reutlingen, Germany: BIOPRO Baden-Würtemberg GmbH.
16. Vajda, I., et al., *Low-frequency stimulation induces stable transitions in stereotypical activity in cortical networks.* Biophys J, 2008. **94**(12): p. 5028-39.
17. Ruaro, M.E., P. Bonifazi, and V. Torre, *Toward the neurocomputer: image processing and pattern recognition with neuronal cultures.* IEEE Trans Biomed Eng, 2005. **52**(3): p. 371-83.
18. Holscher, C., R. Anwyl, and M.J. Rowan, *Stimulation on the positive phase of hippocampal theta rhythm induces long-term potentiation that can Be depotentiated by stimulation on the negative phase in area CA1 in vivo.* J Neurosci, 1997. **17**(16): p. 6470-7.
19. Huerta, P.T. and J.E. Lisman, *Bidirectional synaptic plasticity induced by a single burst during cholinergic theta oscillation in CA1 in vitro.* Neuron, 1995. **15**(5): p. 1053-63.
20. Hyman, J.M., et al., *Stimulation in hippocampal region CA1 in behaving rats yields long-term potentiation when delivered to the peak of theta and long-term depression when delivered to the trough.* J Neurosci, 2003. **23**(37): p. 11725-31.
21. Chao, Z.C., D.J. Bakkum, and S.M. Potter, *Shaping embodied neural networks for adaptive goal-directed behavior.* PLoS Comput Biol, 2008. **4**(3): p. e1000042.
22. Li, Y., et al., *Characterization of synchronized bursts in cultured hippocampal neuronal networks with learning training on microelectrode arrays.* Biosens Bioelectron, 2007. **22**(12): p. 2976-82.
23. Zibek, S., et al. *Chemical stimulation of cells - microsystem, experiment & modelling*. in *6th international meeting on substrate-integrated micro electrode arrays*. 2008. Reutlingen, Germany.
24. Kang, G. and Y. Nam. *In vitro neuronal activity change induced by thermal effects of near-infrared laser stimulation*. in *6th international meeting on substrate-integrated micro electrode arrays*. 2008. Reutlingen, Germany.
25. Hofmann, B., et al. *Analysis of light-induced activity in defined neural networks*. in *6th international meeting on substrate-integrated micro electrode arrays*. 2008. Reutlingen, Germany: BIOPRO Baden-Würtemberg GmbH.
26. Ben-Ari, Y., *Developing networks play a similar melody.* Trends Neurosci, 2001. **24**(6): p. 353-60.
27. Corner, M.A., R.E. Baker, and J. van Pelt, *Homeostatically regulated spontaneous neuronal discharges protect developing cerebral cortex networks from becoming hyperactive following prolonged blockade of excitatory synaptic receptors.* Brain Res, 2006. **1106**(1): p. 40-5.
28. Corner, M.A., et al., *Physiological effects of sustained blockade of excitatory synaptic transmission on spontaneously active developing neuronal networks--an inquiry into the reciprocal linkage between intrinsic biorhythms and neuroplasticity in early ontogeny.* Neurosci Biobehav Rev, 2002. **26**(2): p. 127-85.
29. Van Ooyen, A., *Competition in neurite outgrowth and the development of nerve connections.* Prog Brain Res, 2005. **147**: p. 81-99.
30. van Ooyen, A. and J. van Pelt, *Activity-dependent neurite outgrowth and neural network development.* Prog Brain Res, 1994. **102**: p. 245-59.
31. Van Ooyen, A., J. Van Pelt, and M.A. Corner, *Implications of activity dependent neurite outgrowth for neuronal morphology and network development.* J Theor Biol, 1995. **172**(1): p. 63-82.
32. Ben-Ari, Y., *Cell death and synaptic reorganizations produced by seizures.* Epilepsia, 2001. **42 Suppl 3**: p. 5-7.
33. Buzsaki, G. and A. Draguhn, *Neuronal oscillations in cortical networks.* Science, 2004. **304**(5679): p. 1926-9.
34. Leinekugel, X., et al., *Correlated bursts of activity in the neonatal hippocampus in vivo.* Science, 2002. **296**(5575): p. 2049-52.
35. van Oss, C. and A. van Ooyen, *Effects of inhibition on neural network development through activity-dependent neurite outgrowth.* J Theor Biol, 1997. **185**(2): p. 263-80.
36. Watanabe, S., et al., *Development of low magnesium-induced spontaneous synchronized bursting and GABAergic modulation in cultured rat neocortical neurons.* Neurosci Lett, 1996. **210**(1): p. 41-4.

Summary

Investigations into synaptic plasticity have been done by measuring pairs of neurons in brain regions where the connections are known. Measuring a great number of cells accurately has been technically impossible until recently. Multi-electrode arrays are glass plates with a number of electrodes (typically 60) that allow the extracellular recording of action-potential activity of many neurons in parallel. However, the network has to essentially consist of a single layer as the neurons need to be close to the electrodes, but also need sufficient access to substances in the supporting medium. One possibility was to re-grow networks from dissociated neurons taken from very young animals. The networks become spontaneously active after about one week, when synaptic connections have been made. The type of activity that dominates throughout the lifetime of cultures consists of short (50 ms to 1 s) periods in which most neurons are active, separated by periods of very low activity by few neurons. This pattern is called bursting.

In **chapter 2** we show that the activity during bursts is not random. Instead, calculations of the instantaneous firing rate of each recorded neuron during bursts (profiles) have shapes which are highly neuron-specific. Furthermore, the profile shapes are preserved across consecutive bursts. This stability in bursts was maintained on a time-base of several hours. We conjecture that the specific spatio-temporal structure of bursts reflects the synaptic connectivity of the network. Support for this comes from studies of the physical structure of cultures, which develops at a similar timescale. We also show that under certain conditions, a mathematical relationship exists between profiles and functional connectivity calculated by cross-correlations between electrode-pairs. In comparison to cross-correlation analysis which describes N^2 relationships (N is the number of electrodes), profile analysis only describes N relationships. Profile analysis provides a balance between global statistical analysis and localized detailed analysis. Since the presented analysis is also based on spontaneous activity, it does not influence normal development of a culture. This is contrary to the widely used method of applying probe stimulus pulses to ascertain the network state.

The stability of profiles was the motivation for using profiles to analyze a number of interventions that had been shown in literature to produce changes in network

firing patterns. In **chapter 3**, we apply interventions consisting of single stimuli (single electrode single pulse; SESP), stimulus pairs (PESP), trains of stimuli (SEPT) and paired trains of stimuli (PEPT). Trains consist of 10 pulses applied at a rate of 20 per second. When applied in pairs, the stimuli on the secondary electrode lag those of the leading electrode by 10 ms. We compare the average difference in shape between burst profiles measured before and after the interventions with the difference found by spontaneous development (CTRL). For burst profiles this produces mixed results, with an increase in difference for PESP and SEPT but a decrease for SESP and PEPT. Comparing phase profiles with control shows that only SESP and PESP produce changes in shape larger than spontaneously. On electrodes used for stimulation, we observe stronger effects than on non-stimulated electrodes. The mixed results and small effects of the various interventions are attributed mainly to bursting of cultures. All interventions that we applied triggered activity that resembles network bursts which, we suggest channel activity into spontaneous patterns.

In **chapter 4** we present a new method to make cultures more susceptible to interventions. Using stimuli applied randomly to 10-13 electrodes we established rhythmic activity (4 Hz) in the network without network bursts. Next, short trains of 4 stimuli were applied at the peak or trough of the rhythm. From literature it is known that applying stimuli locked to the local theta rhythm (peaks in EEG between 4-12 Hz) in hippocampus can cause long-term potentiation or depression, depending on the phase of theta. We analyze the differences in post stimulus histograms before and after intervention, as well as differences in spontaneous bursts before and after intervention. When stimulus trains are applied at the peak of rhythmic activity in culture, an increase in post stimulus histogram area is observed. With the same settings, burst and phase profiles also show a significant difference from control. For stimulus trains applied at the trough of theta, the post stimulus histogram area decreases but a similar decrease is also observed during controls. Also, burst and phase profiles do not change shape more than control measurements when stimuli are applied at the through of the rhythm. The experiments show that rhythms can be induced in cultures. Reduction of bursts alone makes cultures more susceptible to external stimuli. In addition, differential signaling occurs at different phases of the rhythm. This shows for the first time the importance of natural activity patterns in general and rhythmic activity in particular.

With the use of feedback of performance in a culture, we show in **chapter 5** that single pulses can be used to alter input-output relationships and also profiles of spontaneous bursts. Through feedback, an initially random change can be cultivated such that it becomes part of the normal repertoire of activity patterns in a culture. We choose an electrode for stimulation which triggers bursts and an electrode for evaluation of performance which elicits very few spikes in response to stimulation. We then apply stimuli until the evaluation electrode measures an action-potential in a certain window (e.g. 10 to 50 ms) after stimulus in 2 out of the 10 last stimuli. The number of stimuli that are given before this criterion is fulfilled is recorded, and stimuli are stopped for 5 minutes. We show that when stimuli are resumed, on average, fewer stimuli are needed to reach the criterion.
Again, we calculate burst profiles and phase profiles before, during and after learning. The time-base of change of burst and phase profiles is increased during learning compared to the spontaneous time-base. Consequently, a burst and phase profiles change significantly more during learning than over an equal period of spontaneous development.

A new method of analysis in cultured neuronal networks is developed and is applied in several experiments designed to change network firing patterns through external electrical stimulation. We show that bursts consolidate existing network state, making it hard to influence network connectivity. This resistance to change can be overcome by applying external stimulation to reach a natural state without bursts, or by cultivating small changes through feedback.

Samenvatting

Onderzoek naar synaptische plasticiteit heft zich geconcentreerd op het meten van neuronenparen in hersengebieden waarvan de connecties bekend zijn. Het accuraat meten van een groot aantal cellen was tot voor kort onpraktisch. Multi elektrode arrays zijn glasplaatjes met daarin een 60-tal elektroden, die het mogelijk maken om van veel neuronen tegelijkertijd extracellulair de aktiepotentialen te meten. Om dit mogelijk te maken moeten de neuronen vlakbij de elektroden liggen, en toegang tot voedingsstoffen in het medium hebben. Daarom worden netwerken op MEA's 2-dimensionaal gemaakt/gehouden. Dit kan worden bereikt door gedissocieerde neuronen uit zeer jonge proefdieren te zaaien op het MEA oppervlak en die te laten uitgroeien tot nieuwe netwerken. Na ongeveer een week zijn de synaptische verbindingen in dergelijke netwerken zodanig volgroeid dat spontaan gegenereerde actiepotentialen kunnen worden doorgegeven naar andere neuronen. Metingen van activiteit geven weer dat de activiteit in deze culturen getypeerd word door korte periodes (50 ms tot 1 s) waarin zeer veel neuronen één of meerdere aktiepotentialen vuren, afgewisseld met periodes waarin slechts enkele neuronen vuren. Dit patroon van activiteit wordt 'bursting' genoemd en domineert gedurende de hele levensduur van culturen.

In **hoofdstuk 2** laten we zien dat de activiteit binnen een burst verre van willekeurig is. Wanneer we de instantane vuurfrequenties van individuele neuronen berekenen (zgn. profielen) zien we dat de vorm van hiervan neuronspecifiek is. Tevens laten we zien deze specifieke vorm bewaard wordt gedurende opeenvolgende bursts. De profielen waren stabiel over een tijdsduur van enkele uren. We hypothetiseren dat de specifieke spatio-temporele structuur van bursts de synaptische connectiviteit weergeeft. Ondersteunend bewijs komt voort uit onderzoek naar de fysieke uitgroei van neuronen in cultuur, waaruit is gebleken dat deze op dezelfde tijdsschaal verandert. We laten ook zien dat er onder bepaalde omstandigheden een wiskundig verband bestaat tussen profielen en functionele connectiviteit die berekend wordt d.m.v. kruiscorrelaties tussen elektrodeparen. In vergelijking met kruiscorrelaties waarin N^2 relaties worden berekend (met N het aantal actieve elektroden), zijn er 'slechts' N profielen. Analyse van profielen vormt een balans tussen globale statistische analyse en de zeer gedetailleerde analyse van elektrodeparen. Een teveel aan detail kan averechts werken aangezien

er meer data nodig is voor een vergelijkbare stabiliteit. De analyse zoals wij die presenteren maakt ook geen gebruik van test stimuli, zoals wel gebruikelijk in veel ander methoden om het netwerk te karakteriseren. Dit kan een voordeel zijn aangezien uit literatuur steeds meer blijkt dat stimuli de normale ontwikkeling van netwerken beïnvloeden.

De stabiliteit van profielen was de aanleiding om verschillende interventies, waarvan uit literatuur bekend is dat ze veranderingen in vuurpatronen teweeg brengen, te gaan analyseren met profielen. In **hoofdstuk 3**, beschrijven we het effect op profielen van 4 verschillende interventies, te weten: enkele pulsen op één elektrode (SESP), enkele pulsen op een elektrodepaar (PESP), pulstreinen op één elektrode (SEPT) en pulstreinen op elektrodeparen (PEPT). Pulstreinen bestaan uit 10 pulsen toegediend op een frequentie van 20 Hz. Bij stimulatie op twee elektrodes word de pulsen op de tweede elektrode 10 ms later toegediend. We vergelijken de veranderingen die we vinden tussen profielen voor en na interventie met de veranderingen die we vinden zonder interventie (CTRL). Voor burstprofielen zijn de resultaten niet eenduidig; Verschillen tussen burstprofielen worden groter dan CTRL voor PESP en SEPT, terwijl ze kleiner worden voor SESP en PEPT. Voor faseprofielen zien we dat alleen SESP en PESP interventies resulteren in vormveranderingen die groter zijn dan CTRL. Algemeen blijkt dat de faseprofielen van elektroden die gebruikt zijn voor stimulatie sterker veranderen dan faseprofielen op niet-gestimuleerde elektroden. Als voornaamste oorzaak van het gebrek aan eenduidige resultaten dragen we het burst-gedrag van het netwerk aan. Alle interventies die we toepassen veroorzaken activiteit die lijkt op bursts. Deze bursts kunnen de geïnduceerde activiteit sturen naar al bestaande (spontane) patronen.

In **hoofdstuk 4** demonstreren we een nieuwe manier om culturen gevoeliger te maken voor interventies van buitenaf. Door in willekeurige volgorde 10 tot 13 elektroden te stimuleren kunnen we ritmische activiteit (4 Hz) zonder bursts bewerkstelligen. Vervolgens dienen we korte maar hoogfrequente stimulustreinen (4 pulsen; 200 Hz) toe op de piek of dal van het ritme. Uit de literatuur is gebleken dat stimulatie op bepaalde fases van het theta ritme (piek in het EEG tussen 4 en 12 Hz) in hippocampus, resulteert in lange-termijn potentiatie of lange-termijn depressie van synaptische verbindingen, afhankelijk van de fase waarop ze toegediend worden. We analyseren de veranderingen met behulp van post stimulus

histogrammen, die vlak voor en meteen na de interventie worden bepaald, maar daarnaast ook met behulp van veranderingen in burst- en faseprofielen. Wanneer in onze culturen treinen worden toegediend op de top van het ritme, zien we dat het oppervlak van PSTH's groter wordt. Tevens zien we ook dat de burst- en faseprofielen significant meer veranderen ten opzichte van spontane veranderingen en veranderingen ten gevolge van ritmische stimulatie zonder stimulustreinen. Voor stimuli die in het dal van het (theta) ritme worden aangeboden zien we een daling in PSTH-oppervlak, maar een dergelijke daling wordt ook gevonden bij ritmische stimulatie zonder stimulustreinen. Tegelijkertijd is de verandering in burst- en fase profielen niet groter dan spontane veranderingen. De experimenten laten zien dat neuronenculturen ritmische activiteit kunnen vertonen. Voorgaand onderzoek heeft al aangetoond dat culturen zonder bursts beter van buitenaf zijn te beïnvloeden. Ons onderzoek voegt daaraan toe dat verschillende plasticiteitmechanismes worden geactiveerd, afhankelijk van de fase van het ritme waarop ze toegediend worden. Dit benadrukt het belang van natuurlijke activiteitspatronen in het algemeen, en in het bijzonder de mogelijkheden van ritmische activiteit.

Door een koppeling te maken tussen stimuli en de prestatie van het netwerk, laten we in **hoofdstuk 5** zien dat losstaande pulsen (dus geen treintjes) ook veranderingen in een netwerk teweeg kunnen brengen. Door terugkoppeling is het mogelijk om kleine, willekeurige veranderingen die de prestatie verbeteren te cultiveren zodat deze uiteindelijk deel uit zullen maken van het normale repertoire van activiteitspatronen. Om dit te bereiken kiezen we een elektrode waarop stimuli een burst van activiteit veroorzaken, en een elektrode die zeer weinig actiepotentialen registreert na stimuli op voorgaande elektrode. Vervolgens dienen we stimuli toe, totdat we na 2 van de laatste 10 stimuli een actiepotentiaal meten op de evaluatie elektrode in een bepaald tijdvak na stimuli (bijv. 10 tot 50 ms). Het aantal stimuli dat nodig is om dit criterium te bereiken wordt bewaard, en de stimuli 5 minuten opgeschort. We laten zien dat wanneer de stimuli worden hervat, er gemiddeld minder stimuli nodig zijn om de het criterium te bereiken.
Wederom berekenen we burst- en faseprofielen voor, tijdens en na training. Gedurende de training veranderen de burst- en faseprofielen sneller dan gedurende spontane activiteit. Het gevolg is dat burst- en faseprofielen significant meer veranderen tijdens training dan over een gelijke periode spontane activiteit.

Een nieuwe analysemethode voor de activiteit in neuronale netwerken word beschreven en toegepast in verschillende experimenten die ontworpen zijn om netwerk activiteit te veranderen door externe elektrische stimulatie. We laten zien dat bursts de spontane activiteitspatronen consolideren, wat het moeilijk maakt om het netwerk te beïnvloeden. Deze weerstand tot verandering kan worden overkomen door (1) natuurlijke activiteitspatronen aan te brengen (door elektrische stimulatie), en (2) door kleine veranderingen te versterken met behulp van terugkoppeling.

Dankwoord

Na 4+ jaren ploeteren is ligt nu dan toch het proefschrift voor u. Er zijn momenten geweest waarop het leek dat het nooit zover zou komen, maar blijkbaar is het waar wanneer men zegt: “3/4 van het werk van een promovendus word in het laatste jaar gedaan”. Een goed moment om de mensen te bedanken die de afgelopen jaren deel uit hebben gemaakt van mijn werk- en leefomgeving.

Als eerste wil ik mijn beide promotoren bedanken. Wim, jij was er altijd om mij weer op scherp te zetten wanneer de experimenten weer eens tegenvielen. Je ervaring en pragmatische aanpak zijn van grote invloed geweest voor het tot een einde brengen van dit traject. Enrico, jij hebt altijd een positieve kijk op de dingen en behield het overzicht op momenten waarop het nodig was. Toen ik net begon heb je mij de beginselen van de neurofysiologie uit moeten leggen, aangezien ik tijdens mijn opleiding niet had voorzien ooit deze tak van wetenschap te gaan beoefenen. Tegen het eind van deze dit traject weet ik er iets meer van, maar besef ik vooral hoeveel er nog niet bekend is. Joost, hoewel je geen officiële functie als begeleider had, kwam ik met ideeën en problemen toch altijd het eerst bij jou. De openheid en ontspannenheid waarmee jij te werk gaat zal daar zeker mee te maken hebben (gehad). De discussies die wij regelmatig hebben gehad, hebben mij zeker op weg geholpen zo niet geïnspireerd om de dingen weer eens vanuit een compleet ander perspectief te gaan bekijken.

Esther, jij bent mijn vaste kamergenote geweest tijdens mijn hele promotie, eerst in Hogekamp 6262 en later ook in Zuidhorst 210. De praktische kanten van onderzoeken, van informatie verzamelen tot het schrijven van artikelen (in Word) heb ik mede dankzij jou onder de knie gekregen. De eerste maand bij elkaar op de kamer was wel even aftasten, maar toen we erachter kwamen dat we naar hetzelfde concert (Red Hot Chili Peppers) gingen klikte het. Onze kamer was/is dan ook een van de weinige waar de radio gewoon aanstaat. Je bent een fijne collega en vriendin en mede dankzij jou is mijn tijd als promovendus naast leerzaam ook vooral leuk geweest. Inmiddels ben jij zelf ook bijna klaar en kunnen jij, Guido en ik binnenkort op een terrasje met een La Chouffe terugkijken op de ‘goede oude tijd’.

Remy, dit project zou nooit zijn geslaagd zonder jouw hulp. Niet alleen omdat jij het prepareren en onderhoud van kweken verzorgde, maar ook omdat we tussen het labwerk door, in de relatieve privacy van het lab, konden we altijd enorm 'openhartige gesprekken' konden voeren. Je gevoel voor humor en je optimisme hebben me door menige dip geholpen. Door je bijna verontrustende voorkeur voor (munt)ballen kwam je ook regelmatig bij onze kamer 'buurten', en konden we uiteraard meteen de laatste nieuwtjes uitwisselen.
En dat is een mooi bruggetje naar Daphne; Sinds we jou hebben mogen begroeten als kamergenote is het uitwisselen van nieuwtjes tot kunst verheven. Je energie (niet zo hard rennen) en spontaniteit hebben verfrissend gewerkt tijdens een periode dat je beide kamergenoten bij tijd en wijle geen puf meer hadden.
Ed, jij was soms wel de belichaming van het gezegde "hoe ouder hoe gekker", en iedere dag kwam je dan ook langs om de vier-uur moppen van Veronica te vertellen (en natuurlijk twee muntballen). Als vaste waarde tijdens de koffiepauze hebben we veel met elkaar gelachen. En toch, op zondagavond kon ik je wel schieten (virtueel wel te verstaan).

Ik heb een groot deel van mijn promotie ook gespeeld in het zaalvoetbalteam van BSS/BW, waar ik met mijn beperkte voetbaltalent mijn best deed om het doel schoon te houden. Met toenemend succes kwam ook een toenemende professionaliteit, zodat we nu zelfs shirtjes hebben. Maar het plezier van het voetballen ging altijd voorop, en da's maar goed ook met het debacle van het afgelopen kersttoernooi nog vers in het geheugen. Jongens, al was ik de laatste tijd niet vaak meer van de partij, ik heb altijd met veel plezier in het team gespeeld en hoop het in de toekomst ook weer regelmatig te gaan doen.
Wat ik verder ook altijd leuk heb gevonden was het pubquizzen, woensdagavond in de Irish pub. Als invaller bij het vaste groepje van Esther, de Four Roses, mocht ik mijn feitjeskennis laten zien. Later is het idee van de pubquiz ook aangeslagen bij andere collega's en nu gaan we regelmatig quizzen met een groepje enthousiastelingen. Dat mijn/onze feitjeskennis niet zo groot is, blijkt wel dat we nooit boven de middenmoot uitsteken. Maar gelukkig is het altijd wel enorm gezellig, tijdens èn na de quiz. Met name nababbelen met Colleen of Suzanne heb ik leuk gevonden. Soms wel iets te leuk, want ook via MSN heb ik vooral veel afleiding van/aan jou gehad, Suzanne.

Rest mij nog de rest van de afdeling te bedanken voor hun collegialiteit de afgelopen jaren, in het bijzonder wil ik Meyke en Martin. De sfeer tijdens koffiepauzes en dergelijke was altijd goed en we hebben veel gelachen. Tot slot wil ik uiteraard mijn ouders en beide zussen bedanken. Jullie hebben mij, weliswaar van afstand, altijd gesteund wanneer dat nodig was.

Iedereen van harte bedankt voor jullie directe of minder directe bijdrage aan mijn werk de afgelopen jaren.

Curriculum vitae

Jan Stegenga was born on april 19th 1979 in Wijckel, The Netherlands. In 1996 he received his HAVO diploma at the Bogerman College in Sneek. He started his study to become an electrical engineer at the Noordelijke Hogeschool Leeuwarden in the same year. In 2000 he finished this study with the design and working prototype of a 1 kW hybrid DC-power supply in which a passive (bridge converter) and an active (switched converter) supplied power in parallel. He went on to study electrical engineering at the University of Twente, Enschede, The Netherlands. In 2004 he received his MSc-title on the project entitled: 'Landmine detection using nuclear quadrupole responses'. His project dealt with the accurate classification of NQR measurements, which detect the explosive itself rather than its encasing and typically have very low signal to noise ratio. During his master studies, he studied the design of artificial neural networks to be used as predictors of chaotic time-series under the supervision of Dr. Ariën van der Wal. This sparked his interest in biological information processing.

Since 2004, he has been working as a PhD-student at the Biomedical Signals and Systems group, also at the University of Twente. Under the supervision of professors Wim Rutten and Enrico Marani, he has studied the action-potential behavior of neuronal cultures *in vitro*.

List of publications

Journal articles

In preparation and submitted:

- Stegenga J., le Feber J., Marani E., Rutten, W.L.C., *The effect of learning on bursting*, IEEE Transactions on BioMedical Engineering, *accepted for publication (DOI:* 10.1109/TBME.2008.2006856*)*
- Stegenga J., Marani E., Rutten, W.L.C., *Robustness of bursts in electrically stimulated neuronal networks*, Journal of Neural Engineering, *submitted*
- Stegenga J., leFeber J., Marani E., Rutten, W.L.C., *Theta rhythm stimulation in cultured networks*, European Journal of Neuroscience, *submitted*
- Gritsun T., Stegenga J., le Feber J., Rutten W.L.C., *Network bursts in cortical cultures are best simulated using pacemaker neurons and adaptive synapses*, Biological Cybernetics, *submitted*
- le Feber J., Stegenga J., *Do external stimuli, applied to train cultured cortical networks, disturb the balance between activity and connectivity?*, in preparation

Published:

- Stegenga J., le Feber J., Marani E., Rutten, W.L.C. (2008) *Analysis of cultured neuronal networks using intraburst firing characteristics.* IEEE transactions on biomedical engineering, 55 (4). pp. 1382-1390
- le Feber J., Rutten W.L.C., Stegenga J., Wolters P.S., Ramakers G.J., van Pelt J. (2007) *Conditional firing probabilities in cultured neuronal networks: a stable underlying structure in widely varying spontaneous activity patterns.* Journal of Neural Engineering, 4. pp. 54-67

Conference contributions

- Stegenga J., le Feber J., Marani E., Rutten, W.L.C. (2008) *Changes in bursting during learning*, In: proceedings of the 30th Annual International Conference of the IEEE Engineering in Medicine and Biology Society IEEE-EMBS, 20-25 August 2008, Vancouver, Canada. pp. 4968-4971.
- le Feber J., Stegenga J., Rutten, W.L.C. (2008) *Do external stimuli, applied to train cultured cortical networks, disturb the balance between activity and*

connectivity? In: proceedings of the 30th Annual International Conference of the IEEE Engineering in Medicine and Biology Society IEEE-EMBS, 20-25 August 2008, Vancouver, Canada. pp. 5081-5084.

- Stegenga J., le Feber J., Marani E., Rutten, W.L.C. (2008) *Changes in bursting caused by learning.* In: Proceedings of the 6th international meeting on substrate-integrated micro electrode arrays, July 8-11, 2008, Reutlingen, Germany. pp. 87-88. BIOPRO Baden-Wuerttemberg GmbH, Stuttgart, Germany
- le Feber J., Stegenga J., Rutten, W.L.C. (2008) *Learning in live neuronal cultures: a training protocol eveluated.* In: Proceedings of the 6th international meeting on substrate-integrated micro electrode arrays, July 8-11, 2008, Reutlingen, Germany. pp. 65-66. BIOPRO Baden-Wuerttemberg GmbH, Stuttgart, Germany
- Gritsun, T., Stegenga J., le Feber J., Rutten, W.L.C. (2008) *Explaining burst profiles using models with realistic parameters and plastic synapses.* In: Proceedings of the 6th international meeting on substrate-integrated micro electrode arrays, July 8-11, 2008, Reutlingen, Germany. pp. 26-28. BIOPRO Baden-Wuerttemberg GmbH, Stuttgart, Germany
- Marani E., Heida T., Stegenga J., le Feber J., Usunoff K.G. (2007) *Culturing and modeling for parameters in Deep Brain Stimulation.* In: The Trakia Journal of Sciences, 1-3 June 2007, XVIII National Congress of the Bulgarian Anatomical Society. pp. 4-4. The Trakia Journal of Sciences 5 (1, suppl. 2, 2007). The Trakia University
- Stegenga J., Rutten W.L.C.,Marani, E. (2007) *Intra-burst firing characteristics as network state parameters*, In: 1st Dutch conference on BioMedical Engineering, 18-19 january, Egmond aan Zee, The Netherlands
- le Feber J., Rutten W.L.C., Stegenga J., van Pelt J. (2006) *Strengthening and weakening of relationships in cortical cultures: latency dependent?* In: Proceedings of the 1st IEEE/ EMBS Benelux Symposium, 7-8 dec 2006, Brussels, Belgium. pp. 179-182
- Stegenga J., le Feber J., Rutten W.L.C., Marani E. (2006) *Intra-burst firing characteristics as network state parameters.* In: Conference proceedings of the 5th international meeting on substrate-integrated micro electrode arrays, 4-7 july 2006, Reutlingen, Germany. pp. 64-66. BioPro Baden-Wuertenberg GmbH

- le Feber J., Rutten W.L.C., Stegenga J., Wolters P.S., Ramakers G.J., van Pelt J. (2006) *Cultured cortical networks described by conditional firing probabilities*. In: 5th international meeting on substrate-integrated micro electrode arrays, 4-7 july 2006, Reutlingen, Germany. pp. 67-70. BIOPRO Baden-Wuerttemberg GmbH, Stuttgart, Germany
- Stegenga J., Rutten W.L.C., Marani, E. (2005) *The effectiveness of PCA-like algorithms versus ad-hoc features in spike sorting*, KNAW Man-Machine Interactions: Interfaces between the brain and the out-side world, 25 January 2005, Amsterdam, The Netherlands